

**NASA
Reference
Publication
1213**

1989

The Cassini Mission:
Infrared and Microwave
Spectroscopic Measurements

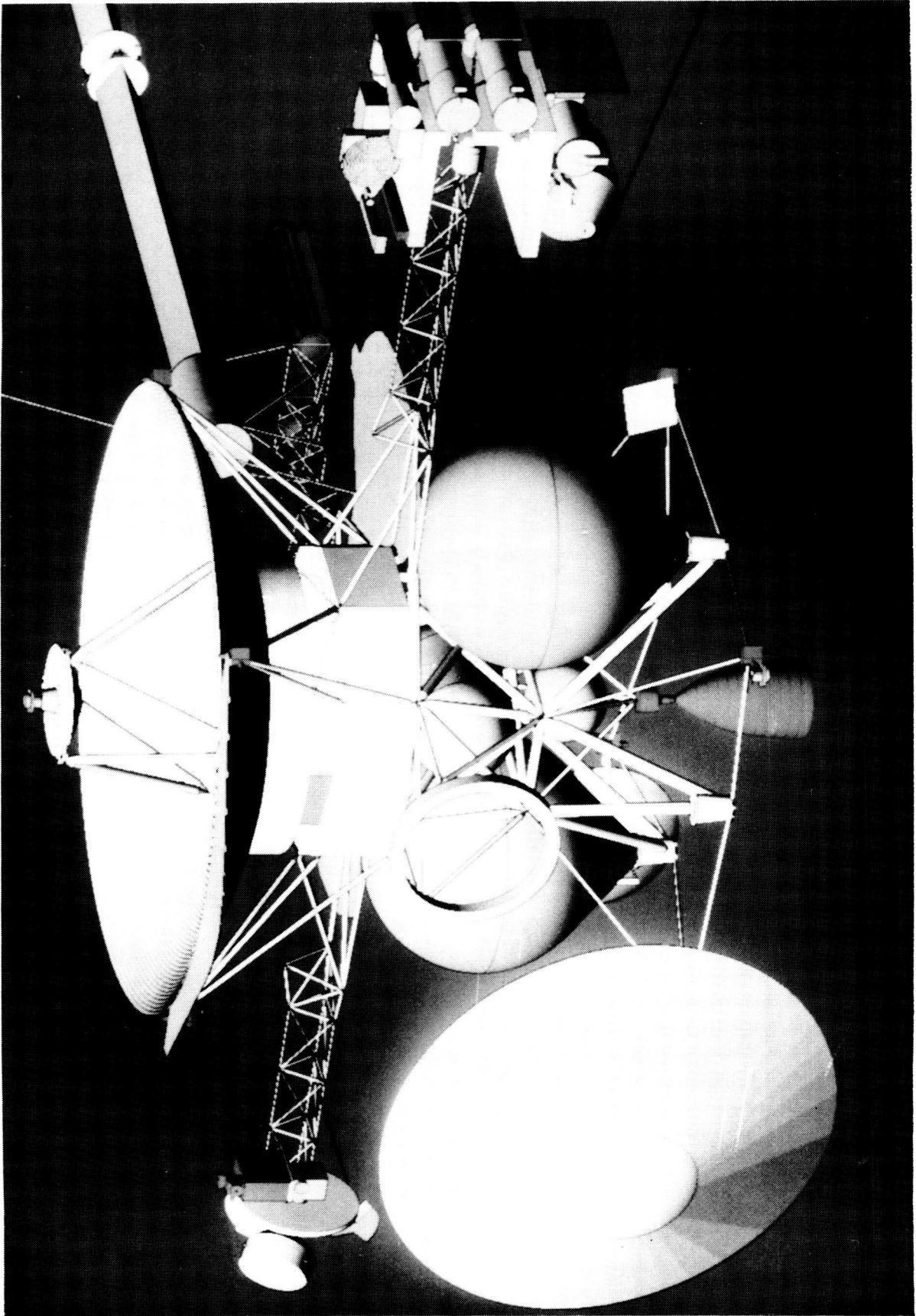
V. G. Kunde
*Goddard Space Flight Center
Greenbelt, Maryland*



National Aeronautics
and Space Administration

Scientific and Technical
Information Division

ORIGINAL PAGE IS
OF POOR QUALITY



Mariner Mark II spacecraft configuration for the Cassini mission. The scan platform with ultraviolet, imaging, and infrared instruments is located in the far right-hand side of the figure.

THE CASSINI MISSION INFRARED AND MICROWAVE SPECTROSCOPIC MEASUREMENTS

TABLE OF CONTENTS

<u>Section</u>	<u>Page</u>
Foreword	iv
1 Introduction.	1
2 Instrument Descriptions	2
2.1 Microwave Spectrometer and Radiometers (MSAR).	2
2.2 Composite Infrared Spectrometer (CIRS)	2
2.3 Cassini Stratospheric Sounder (CSS).....	5
2.4 Cassini Visible and Near IR Mapping Spectrometer (C-VIMS)	5
2.5 Descent Imager/Spectral Radiometer (DISR)	6
2.6 Probe Infrared Laser Spectrometer (PIRLS).....	7
3 Infrared and Microwave Science Objectives	8
3.1 Fundamental Objectives Addressed By Infrared and Microwave	8
3.2 Specific Goals Addressed by Infrared and Microwave	13
3.2.1 Saturn.....	13
3.2.1.1 Thermal Structure and Dynamics	13
3.2.1.2 Chemical Composition	15
3.2.1.3 Cloud/Haze Composition and Structure	18
3.2.1.4 Science Summary of Individual Instruments	19
3.2.2 Titan.....	20
3.2.2.1 Thermal Structure and Dynamics	20
3.2.2.2 Chemical Composition	24
3.2.2.3 Cloud/Haze Composition and Structure	30
3.2.2.4 Thermal Balance.....	31
3.2.2.5 Surface	32
3.2.2.6 Science Summary of Individual Instruments	33
Appendix A MSAR Background Information and Figures.....	37
Appendix B CIRS Background Information and Figures	55
Appendix C CSS Background Information and Figures	97
Appendix D C-VIMS Background Information and Figures	107
Appendix E DISR Background Information and Figures	113
Appendix F PIRLS Background Information and Figures	123

FOREWORD

This document was prepared in part from contributions presented at three Cassini Infrared Spectroscopic Workshops held in Tucson, Arizona (March 1987), Paris, France (July 1987), and Darmstadt, FRG (March 1988). The characteristics presented here for the instruments are preliminary and therefore subject to some changes in the future. We hope that the science objectives presented here will appear attractive enough to our colleagues of the planetary science community that they will actively support the Cassini mission.

Virgil Kunde

Goddard Space Flight Center

Régis Courtin

Meudon Observatory

CONTRIBUTORS

B. Bézard, DESPA, Obs. Meudon, France

G. Bjoraker, NASA/GSFC, Greenbelt, MD

A. Boischot, DASOP, Obs. Meudon, France

S. Calcutt, U. of Oxford, Oxford, England

R. Carlson, JPL, Pasadena, CA

T. Clancy, LASP, U. of Colorado, Boulder, CO

M. Combes, DESPA, Obs. Meudon, France

A. Coustenis, DESPA, Obs. Meudon, France

M. Flasar, NASA/GSFC, Greenbelt, MD

D. Gautier, DESPA, Obs. Meudon, France

D. Hunten, U. of Arizona, Tucson, AZ

1. INTRODUCTION

Observations from the infrared spectrometer on the Voyager spacecraft have contributed extensively to our knowledge of the gaseous composition of Saturn and Titan, and of the thermal structure and dynamics of Saturn. These results have demonstrated the power of remote sensing infrared spectroscopy for answering fundamental questions on the atmospheres of Saturn and Titan, and, in turn have raised new questions. The potential for significant future advances in addressing these new questions on composition and structure with infrared instrumentation, ranging from the near infrared to the microwave region, on the Saturn orbiter and the Titan probe is great.

This document describes 1) the fundamental scientific objectives for Saturn and Titan which can be addressed by infrared and microwave instrumentation, 2) the instrument requirements and the accompanying instruments, and, 3) the synergism resulting from the comprehensive coverage of the total infrared and microwave spectrum by the complement of individual instruments. The baseline consists of four instruments on the orbiter and two on the Titan probe. The orbiter infrared instruments are: 1) a microwave spectrometer and radiometer for determination of composition and roughness of Titan's surface and sounding of Saturn's deep atmosphere, 2) a far to mid-infrared spectrometer for tropospheric and stratospheric thermal structure, gas and aerosol distributions in the Saturn and Titan atmospheres, 3) a pressure modulation gas correlation spectrometer for high altitude resolution of the thermal structure, aerosol, C_2H_2 , and C_2H_6 distributions in Saturn's and Titan's stratospheres, and 4) a near infrared grating spectrometer for cloud structure in the tropospheres of Saturn and Titan. The two Titan probe infrared instruments are: 1) a near infrared instrument to provide images and near-infrared spectra during the probe decent, and 2) a tunable diode laser infrared absorption spectrometer and nephelometer for in situ sensing of gas and cloud particles.

Three IR Spectroscopic Workshops have been held to define the infrared science objectives, define the resulting instrument requirements, define the minimum number of baseline instruments, and review the developmental state of these instruments. These workshops were held in Tucson, Arizona (LPL) in March 1987, in Paris, France (Meudon Obs.) in July 1987, and in Darmstadt, FRG, in March 1988.

2. INSTRUMENT DESCRIPTIONS

A brief description of the instrument characteristics for the potential baseline infrared and microwave instruments is given in Table 2.1 for the Saturn orbiter and Table 2.2 for the Titan probe. Additional information for each instrument is presented in the Appendices.

2.1 MICROWAVE SPECTROMETER AND RADIOMETERS (MSAR)

Two radio instruments are designed to measure, either spectroscopically or radiometrically, radiation at various wavelength intervals in the range from about 2.2 to 230 GHz (wavelengths of 13 cm to 1.3 mm). Radiometry at 13 and 3.5 cm is proposed to probe the deep atmosphere of Saturn and the sub-surface of Titan. This experiment requires shared use of either the 4-meter communications antenna or the probe relay antenna. A second instrument is designed to measure polarimetry of Saturn's rings and Titan's surface at 2 cm, and to limb sound Titan's atmosphere up to altitudes above 400 km at 1-3 mm wavelengths. This instrument requires a dedicated 30-cm antenna on the science platform.

The combined radio experiments are capable of sounding temperature/ NH_3 abundance in the atmosphere of Saturn down to 12 bars total pressure; near-surface properties of the solid body of Titan, rings and other satellites; and tropospheric-stratospheric variability of emission by CO (from which atmospheric temperature can be derived), HCN, and HC_3N for Titan and to utilize the N_2 absorption to study the Titan troposphere.

2.2 COMPOSITE INFRARED SPECTROMETER (CIRS)

The CIRS will use a dual interferometer configuration; one will cover the far infrared ($10\text{-}700\text{ cm}^{-1}$), and the other the middle infrared ($700\text{-}1325\text{ cm}^{-1}$). The spectral resolution will be 0.25 cm^{-1} unapodized. Both interferometers share a 50-cm Cassegrain telescope. The far infrared interferometer (FIRS) will use a 1×5 thermal detector array, either thermopiles or pyroelectrics, with each detector having a 4.3×13.9 mrad field of view. The middle infrared interferometer will use two 1×43 HgCdTe arrays, cooled to 70-90 K, with each detector having a $.1\times 3$ mrad field of view. The CIRS will observe Saturn in the limb mode with a maximum altitude resolution of 50 km, and Titan in the limb mode with a maximum altitude resolution of 10 km.

The far infrared interferometer will sound deep in the troposphere of Titan (down to the surface) as well as deep in the atmosphere of Saturn. The mid-infrared interferometer will be able to sound the stratospheres of both Saturn and Titan. The major scientific objectives of this instrument are: determining the tropospheric and stratospheric temperature and aerosol structure of Saturn and Titan; determining the mixing ratios and spatial distributions of trace gases in both atmospheres (many organic molecules for Titan and PH_3 , NH_3 for Saturn); constraining properties of NH_3 ice clouds in Saturn's atmosphere as well as determining the bulk composition of Saturn's atmosphere. Surface temperature properties of the smaller icy satellites can be determined, as well as the emissivity of the rings.

TABLE 2.1 Proposed Orbiter Instrument Characteristics

Instrument	MSAR	CIRS	CSS	C-VIMS
Wavelength	1.3+1.7+2.6 mm 2.0+3.5+13.0 cm	7.5-1000 μm	7.8-8.1 μm 11.8-12.6 μm 13.1-14.5 μm	.4-5.2 μm
Frequency range	230+177+115 GHz 15+8.5+2.3 GHz	10-1325 cm^{-1}	1240-1290 cm^{-1} 790- 850 cm^{-1} 690- 760 cm^{-1}	1923-25000 cm^{-1}
Spectral resolution	600 MHz/500-1000 resolution points	0.25 cm^{-1} unapodized	Doppler line width (10^{-3} cm^{-1})	3% at .4 μm
Individual detector field-of-view	0.3°-1.4° (diff.limited)	.25°/.0057° (4.3/0.1 mr)	0.0004x0.057° (0.07x1.00mr)	.023° (.4 μr)
Number of pixels or detectors	6	5/43	45	192 InSb, Si 128 InSb
Integration time	10 sec	25 sec	10	
Mass	16 kg	23 kg	15 kg	

TABLE 2.2 Proposed Probe Instruments

Instrument	DISR	PIRLS
Wavelength range	a) Descent Imager 0.50-0.60 μm 0.60-0.70 μm 0.72-0.84 μm b) Spectrometer 0.5-1.0 and 1.0-2.0 μm	a) Gas composition 5-10 diode lasers 3-20 μm b) Nephelometry 2 diodes at 0.78 μm
Frequency range	5000-20000 cm^{-1}	3-20 μm , 0.7-0.9 μm
Spectral resolution	0.005 μm (0.4 to 1 μm) 0.05 μm (1-2 μm)	.0001 cm^{-1}
Field-of-view	0.2°/pixel (in imager) 4x4°/pixel (downward viewing spectrometer) 1/2 of upward hemisphere (upward viewing spectrometer)	Deployed reflector, 20 cm away
Number of pixels or detectors	a) 1/2 of 512x512 CCD for images, spectra at $\lambda < 1 \mu\text{m}$ (images are 3x200x200, spectra are 2x10x200) b) 2x40 HgCdTe for spectra at $\lambda > 1 \mu\text{m}$	2 detectors per laser, HgCdTe and InSb
Integration time	10 msec (for CCD)	300 msec
Mass	6 kg	5.4 kg

2.3 CASSINI STRATOSPHERIC SOUNDER (CSS)

The CSS employs both filter and pressure modulation radiometry (PMR) to sense thermal emission from the stratospheres of Saturn and Titan. The CSS will use a telescope with a 30-cm diameter primary, designed to make observations of the limb of Saturn at orbital distances within $10 R_s$. The vertical field-of-view for limb scanning will be $67 \mu\text{rad}$ which will yield a vertical resolution better than one-half the atmospheric scale height (30 km for Saturn and 17 km for Titan) at a range of $7.5 R_s$ from Saturn and $34 R_s$ from Titan. At Titan's closest approach, the altitude resolution will be ~ 5 km. The spectral bandpass of both the pressure modulated and wideband signal components of each PMR channel in the CSS will be defined by narrowband multilayer filters which lie in the $7\text{--}15 \mu\text{m}$ spectral region. Comparison of the modulated and mean signals allows differentiation between gaseous and aerosol emission and, hence, determination of vertical profiles of aerosol opacity. The instrument will carry three pressure modulators with coincident fields-of-view for measurements of pressure, and temperature (using CH_4), along with the abundances of two selected species. Candidate gases currently are C_2H_2 , C_2H_6 , and HCN . Linear or two-dimensional HgCdTe detector arrays will be used. The CSS focal plane assembly (including bandpass filters, condensing optics and detectors) will be cooled to below 80 K, and the remaining optics, including the pressure modulators, will be maintained below 200 K.

The CSS will provide high vertical resolution, global and temporal mapping of profiles of temperature, important chemical species and aerosols for the Saturn and Titan stratospheres.

2.4 CASSINI VISIBLE AND NEAR INFRARED MAPPING SPECTROMETER (C-VIMS)

A Visible and Near-Infrared Mapping Spectrometer (VIMS) has icy satellite surface science as its prime scientific objective. However, it also has the capability for atmospheric science measurements of Saturn and Titan. This instrument would be similar to the Mars Observer (MO) and Comet Rendezvous/Asteroid Flyby (CRAF) VIMS Experiments which are derivatives of the Galileo Near Infrared Mapping Spectrometer. The C-VIMS instrument will consist of an imaging telescope, a triple-blazed diffraction grating spectrometer, and a 320-element linear array detector oriented along the plane-of-dispersion in the focal plane of the spectrometer. The telescope is a 26-cm diameter "Cassegrain" with a two-axis "wobbling" secondary to provide spectral imaging in two spatial dimensions. Thus, Cassini VIMS behaves as a framing camera, but with 320 contiguous spectral channels. Each pixel of the instrument is 0.4 rad on a side, and each "frame" of the instrument contains $64 \times 64 (=4096)$ pixels, providing coverage over an angular area of roughly $26 \mu\text{rad} \times 26 \mu\text{rad}$. Discrete motion of the spacecraft scan platform allows one to mosaic adjacent frames. The spectral range of VIMS is $0.4\text{--}5.2$ microns; i.e., from the near-ultraviolet to the mid-infrared. In the second order of the grating ($0.4\text{--}2.40$ microns) there are 192 detector elements, Si and InSb, each with a triangular response of 0.011 microns (FWHM). Between 2.4 and 5.2 microns, 128 InSb detector elements provide spectral data at 0.022 micron resolution (FWHM).

The atmospheric science objectives include: 1) cloud studies, such as vertical structure, morphology, and temporal variations. For Saturn, spatially resolved spectral images of the sunlit disc at multiple phase angles can be used to determine vertical structure as well as for investigating microphysical properties such as particle size and mass loading. Similar studies can be performed for Titan, along with limb scans for improved vertical characterization, and, 2) atmospheric composition and spatial/temporal variability.

2.5 DESCENT IMAGER/SPECTRAL RADIOMETER (DISR)

This instrument is located on the Titan entry probe. The DISR makes two types of measurements; spectra of upward and downward solar fluxes, and images of the clouds and the ground. A CCD detector is used to record both three-color images, and upward and downward solar flux spectra at wavelengths between 0.4 to 1 micron. Two separate HgCdTe linear array detectors are used for solar flux spectra between 1 and 2 microns. The spectral resolution is 0.005 μm for wavelengths less than 1 micron, and 0.05 μm at longer wavelengths. The CCD is used to record the variation in intensity across the solar aureole for measurements of the size of haze particles above the probe. The solar aureole data and the upward and downward solar flux spectra are recorded at vertical resolutions of a few km or better throughout the descent. In the last 30 minutes of the descent, the probe data rate will be sufficiently high to permit telemetry of images of the cloud tops and Titan's surface in addition to the flux spectra and aureole measurements. The field-of-view of the images will be large (40 degrees) to maximize areal coverage. As the probe nears the surface, successive images obtained at lower altitudes will have increasing spatial resolution to a maximum resolution of the order of 1 m in the last images obtained at altitudes of less than 1 km. Images can be collected simultaneously in three colors. As the ground is approached, the ratio of the upward to downward spectral fluxes gives the reflection spectrum of the ground. If the probe survives landing, a flash lamp will be used to permit reflection spectra of the ground throughout the region from 0.4 to 2 microns (including spectral regions where the incident sunlight has been strongly attenuated by methane bands) to obtain information on the surface composition.

The DISR instrument addresses science in four general areas: 1) the profile of the absorption of solar energy from instrument deployment (some 160 km altitude) to the surface at wavelengths from about 0.4 to 2 microns for studies of the thermal balance and radiative drives for atmospheric dynamics; 2) parameters concerning the vertical structure and nature of the photochemical haze and condensation clouds throughout this vertical region of Titan's atmosphere. The extinction optical depth, single scattering phase function, mean particle size, local number density, single scattering albedo, and refractive index are determined as functions of altitude and wavelength. Information on the morphology of the clouds is also obtained in the images looking down on the clouds from above as well as looking up at them from below; 3) information on the morphology and composition of the surface. The surface composition is constrained by measurements of the spectral reflectivity from 0.4 to 2 microns at ten locations in a strip across the center of each image; and, 4) absorption

features as the probe falls beneath the diffusing haze. These spectra can be used to determine the vertical profile of the mixing ratio of methane throughout the descent.

2.6 PROBE INFRARED LASER SPECTROMETER (PIRLS)

The Probe Infrared Laser Spectrometer (PIRLS) instrument is a tunable diode laser infrared absorption spectrometer and nephelometer designed for the in-situ sensing of Titan's atmosphere on the Titan Probe. The PIRLS instrument uses up to ten narrow-bandwidth (0.0001 cm^{-1}) tunable diode lasers operating at 82 K at selected mid-infrared wavelengths in the region of 3-20 μm . For the absorption measurements, these sources would be directed over an open pathlength defined by a small reflector located about 20 cm away.

Because of the high sensitivity of diode laser harmonic (derivative) detection methods which allow peak absorptances lower than 0.01% to be measured for atmospheric pressures expected on Titan (up to 1.5 bar), volume mixing ratios of 10^{-9} should be measurable for several species of interest. Vertical profiles of the concentrations of molecules such as CH_4 , CO , CO_2 , HCN , C_2H_2 , C_2N_2 , C_3H_4 , C_3H_8 , HC_3N , C_4H_2 , etc. will be determined simultaneously with a vertical resolution of less than a scale height from 200 km down to the surface. Search for stratospheric NH_3 and H_2O at high sensitivity could also be implemented. For appropriate species present in relatively large concentrations, isotopic ratios such as $^{13}\text{C}/^{12}\text{C}$ and D/H could be determined.

As a nephelometer, the vertical extent of the cloud structure, its physical properties such as the particle size distribution and number density can also be measured using shorter wavelength diode laser sources at 0.78 μm and 0.83 μm returned from the same deployed reflector. As a single particle device, the vertical profile of the particle size distributions from entry down to the surface will be made with a vertical resolution of 100 m. With 32 size classes, particles in the range 0.2-50 μm diameter will be measured. Independent simultaneous forward and back scatter measurements will allow computation of the refractive index.

3. INFRARED AND MICROWAVE SCIENCE OBJECTIVES

3.1 FUNDAMENTAL OBJECTIVES ADDRESSED BY INFRARED AND MICROWAVE

A summary of the baseline infrared instruments and their primary measurements is given in Table 3.1. The infrared instruments cover approximately six decades of the spectrum (Fig. 3.1), allowing important new information to be obtained for Saturn's atmosphere, rings, and satellites, and for Titan's atmosphere and surface.

The scientific objectives for the Cassini mission have been defined by a joint ESA/NASA Science Study Team. The fundamental objectives, relating to characterizing Saturn, its rings and icy satellites, and Titan's atmosphere and surface, which can be addressed by the infrared and microwave are:

1. the thermal structure and composition of the atmosphere of Saturn,
2. the atmospheric dynamics and general circulation of the atmosphere of Saturn,
3. the composition of Saturn's rings and icy satellites,
4. the thermal structure and composition of the atmosphere of Titan,
5. the atmospheric dynamics and general circulation of the atmosphere of Titan,
6. chemical evolution and the synthesis of complex organic compounds,
7. the radiation budget of Titan, and
8. the nature of the surface of Titan.

The Cassini infrared and microwave instruments will provide specific information on the above objectives through the following measurement goals:

SATURN

1. GLOBAL MAPPING OF THERMAL STRUCTURE FROM 0.01 MBAR to 12 BAR
2. GLOBAL MAPPING OF H₂ ORTHO-PARA RATIO
3. GLOBAL MAPPING OF TRACE GAS COMPOSITION
 - o TROPOSPHERE - NH₃, PH₃, GeH₄, CO
 - o STRATOSPHERE - C₂H₂, C₂H₆
4. MEASURE ELEMENTAL GAS COMPOSITION AND ISOTOPIC RATIOS - He, D/H, ¹²C/¹³C
5. SEARCH FOR NEW MOLECULES - CO, HCN, HCP, H₂S, H₂Se, HALIDES, H₂O, C₃H₄, C₃H₈, C₂H₄
6. GLOBAL MAPPING OF STRATOSPHERIC AEROSOL STRUCTURE
7. GLOBAL MAPPING OF RADIATION BUDGET
8. GLOBAL MAPPING OF CLOUD/HAZE COMPOSITION AND STRUCTURE
9. MAP COMPOSITION, PARTICLE SIZE, AND THERMAL CHARACTERISTICS OF RINGS
10. MAP COMPOSITION AND THERMAL CHARACTERISTICS OF ICY SATELLITES

TITAN

1. GLOBAL MAPPING OF THERMAL STRUCTURE FROM .01 MBAR to 750 MB
2. GLOBAL MAPPING OF VERTICAL DISTRIBUTIONS OF STRATOSPHERIC TRACE GASES
 - o HYDROCARBONS - C_2H_2 , C_2H_6 , C_2H_4 , C_4H_2 , C_3H_4
 - o NITRILES - HCN, C_2N_2 , HC_3N
 - o O-BEARING - CO, CO_2
3. MEASURE ISOTOPIC RATIOS FOR H, C, O, N
4. SEARCH FOR NEW MOLECULES - H_2O , PREBIOTIC COMPLEX ORGANICS
5. GLOBAL MAPPING OF TROPOSPHERIC AND STRATOSPHERIC CLOUDS/HAZE/AEROSOL COMPOSITION AND STRUCTURE
6. DETERMINE THE HEATING/COOLING RATE FROM 160 KM TO TITAN'S SURFACE
7. GLOBAL MAPPING OF SURFACE TEMPERATURE
8. MAP TITAN'S SURFACE EMISSIVITY
9. MEASURE SURFACE ROUGHNESS ON TITAN
10. SEARCH FOR LIQUIDS ON TITAN'S SURFACE

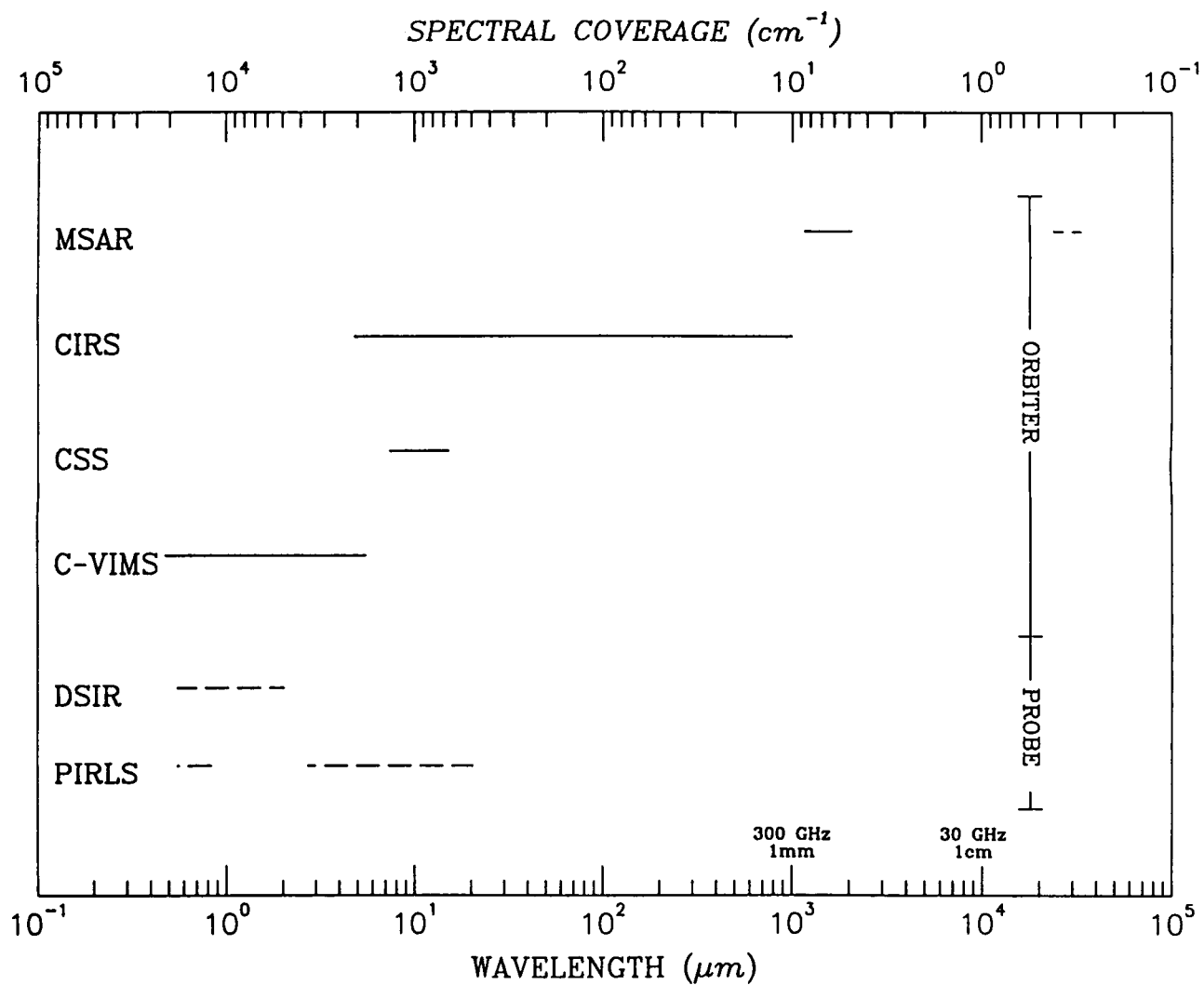


Figure 3.1 Spectral coverage of Cassini infrared and microwave instruments.

TABLE 3.1 Potential Cassini Baseline Infrared and Microwave Instruments

Saturn Orbiter	Science Objectives
MSAR - Microwave Spectrometer	<ul style="list-style-type: none"> o Deep atmosphere of Saturn and Radiometer o Surface composition and roughness of Titan's surface o CO, HCN, HC₃N plus isotopes in Titan's stratosphere and troposphere o Emission and scattering in Saturn's rings
CIRS - Composite Infrared Spectrometer	<ul style="list-style-type: none"> o Tropospheric and stratospheric thermal structure of Saturn and Titan o Tropospheric and stratospheric gas and aerosol structure of Saturn and Titan o Temperature of Titan's surface o Composition, thermal characteristics of icy satellites
CSS - Cassini Stratospheric Sounder	<ul style="list-style-type: none"> o Stratospheric thermal structure of Saturn and Titan with high vertical resolution o C₂H₂, C₂H₆ distributions in stratosphere of Saturn and Titan o Aerosol vertical distribution in stratosphere of Saturn and Titan
C-VIMS - Visible and Near Infrared Mapping Spectrometer	<ul style="list-style-type: none"> o Cloud vertical structure

Titan Probe	Science Objectives
DISR - Descent Imager/Spectral Radiometer	<ul style="list-style-type: none"> o Thermal balance o Clouds and aerosols: vertical distribution, size, optical properties o Surface images and reflection spectrum o Methane abundance profile o In-situ measurements of gas composition and particulates o Vertical profiles of particle size distributions from entry with 100-m resolution o Particle sizes from 0.2 to 50 microns o CH₄ vertical profile o Parts-per-billion sensitivities (10⁻⁹) for several species such as CO, CO₂, HCN, C₂H₂, C₂N₂, C₃H₄, C₃H₈, HC₃N, C₄H₂, etc. o Isotopic ratios ¹²C/¹³C, D/H
PIRLS - Probe Infrared Laser Spectrometer	

3.2 SPECIFIC GOALS ADDRESSED BY INFRARED AND MICROWAVE

3.2.1 SATURN

3.2.1.1 Thermal Structure and Dynamics

Saturn, like Jupiter, has a large internal energy source, rapid rotation, and a pattern of zonal winds near the cloud tops which is symmetric about the equator up to latitudes $\pm 60^\circ$. Seasonal effects in the stratosphere are of much higher amplitude for Saturn than for Jupiter because of Saturn's higher obliquity.

The Voyager IRIS experiment furnished the first global maps of temperature in Saturn's upper troposphere. A north-south hemispheric variation of temperature at the tropopause (~ 150 mbar) was observed, indicating a response by an atmosphere with moderate thermal inertia to the seasonally varying insolation of a planet with an obliquity of 27° . The experiment also observed smaller-scale thermal structure correlated with the meridional variation in the zonal winds inferred from cloud-tracking studies. Application of the thermal wind equation indicated that the winds decay with altitude in the tropopause region. Because of a malfunctioning scan platform on Voyager 2, the spatial resolution obtained in the southern hemisphere was rather coarse.

The altitude coverage of Saturn's thermal structure available from the Cassini infrared instruments is shown in Fig. 3.2. The solid line portion of the temperature profile indicates the altitude range covered by Voyager.

Both CIRS and MSAR will provide information on temperature in Saturn's troposphere. Limb sounding is not feasible at these levels because of the large optical depths in H_2 . However, nadir sounding at closest approach by CIRS will provide a maximum horizontal resolution of 1000 km, or 1° of planetocentric great circle arc on Saturn. The capability exists both for global mapping at moderate spatial resolution ($5\text{--}10^\circ$) as well as localized mapping at high spatial resolution ($<2^\circ$); e.g. the ribbon feature on Saturn at 46° N. As did the Voyager IRIS experiment, CIRS will derive temperatures in the upper troposphere and tropopause region of Saturn through inversion of radiances in the broad S(0) and S(1) lines of molecular hydrogen. An important objective is to observe Saturn's thermal structure during a different season, southern summer for Cassini compared to northern spring for Voyager. If the north-south hemispheric asymmetry in temperature observed by Voyager near the tropopause is attributable to the moderate thermal inertia of the atmosphere, then the meridional profile of temperature should be more nearly symmetric about the equator at the Cassini encounter.

Measurements in the 3.5 and 13 cm channels of the MSAR will sound temperature and NH_3 abundance at 2 and 12 bars, respectively. This range of altitudes is thought to comprise the top of Saturn's convective interior. The 3.5-cm channel has a maximum horizontal spatial resolution of 2500 km and is capable of resolving the zonal wind structure. Observations at this wavelength may bear on the question of how deeply the observed cloud-top wind system extends into Saturn's deep atmosphere. At 13 cm, the resolution is coarser, >9000 km, but

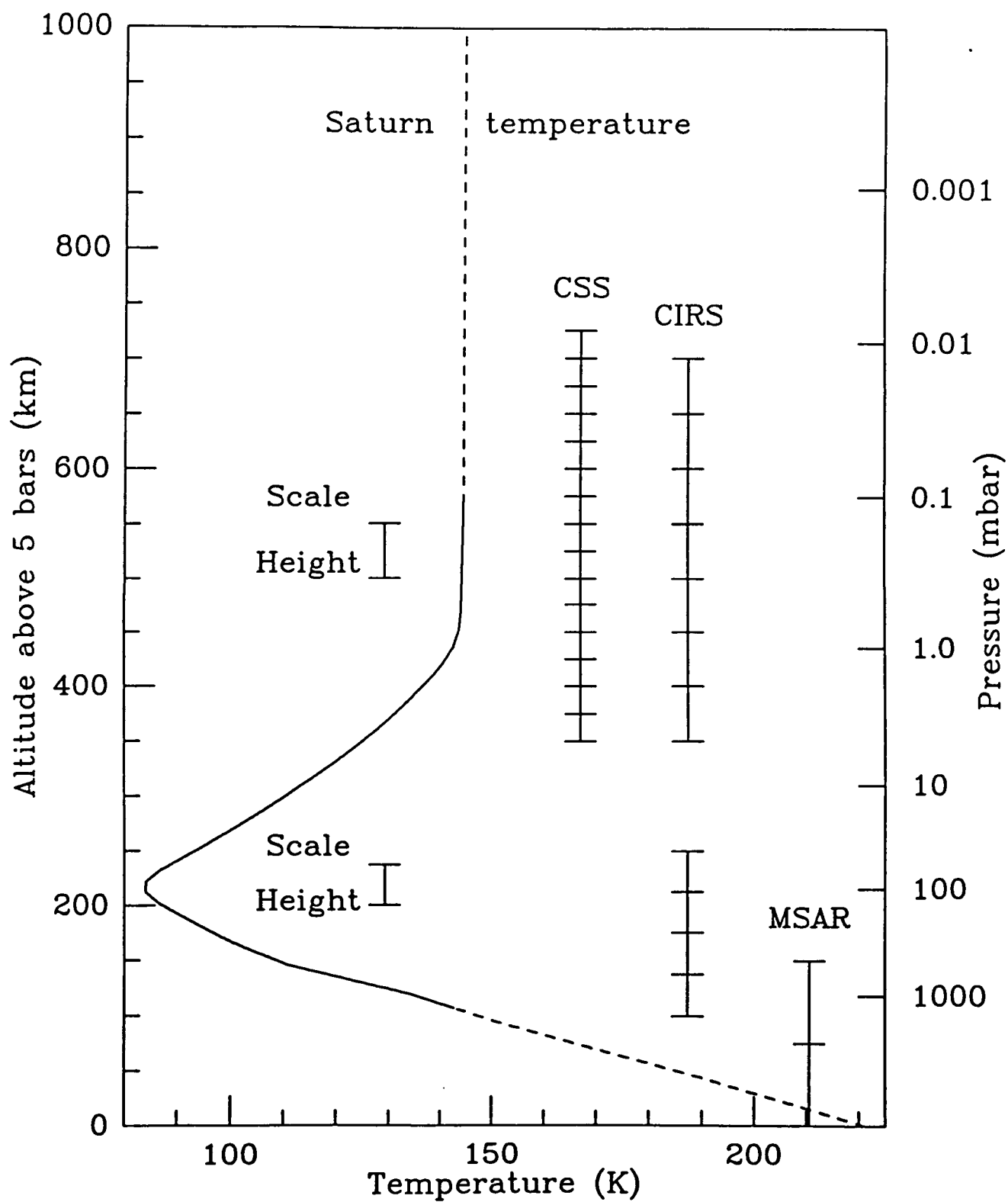


Figure 3.2 Altitude coverage of Saturn temperature profile.

such observations are still capable of resolving planetary scale gradients in temperature and NH_3 , which would pertain to the dynamical redistribution of heat over the globe.

The temperature field of Saturn's stratosphere is expected to show a variety of scientifically interesting phenomena. Ground-based observations reveal extremely strong infrared brightening near the summer pole as a result of the seasonal insolation maximum. Ground-based maps of stratospheric brightness temperatures show a warm band at mid-latitudes in the northern hemisphere, similar to a band in the Jovian atmosphere. Other features similar to those seen in the Jovian atmosphere may also exist, such as a warming of the upper stratosphere by particles precipitating down magnetic field lines near the pole, horizontal planetary waves in the stratosphere, and smaller, more transient features which appear to be independent of tropospheric activity. It is highly desirable to have measurements of the latitudinal temperature gradients at higher altitudes. On the scale of the zonal winds, the derived meridional gradients in temperature can be used to infer the vertical variation of these winds. This will provide insights into the processes that maintain the zonal wind system at these altitudes. For example, Voyager IRIS temperature measurements at the tropopause implied that the jets decay with altitude to a uniform rotation rate that is shorter than the SKR rotation rate. It is important to determine whether this trend continues at higher altitudes. The CSS will retrieve temperature structure over the 350-700 km range with one-half scale height resolution.

3.2.1.2 Chemical Composition

The altitude coverage for chemical composition in Saturn's atmosphere is shown in Fig. 3.3 for the Cassini infrared instruments.

The close passage to Saturn and the simultaneous coverage over a large range of wavenumbers permitted Voyager IRIS to add significantly to our knowledge of the composition of Saturn's atmosphere. For example, the radiances observed between 200 and 400 cm^{-1} indicated that the ratio of helium to hydrogen in Saturn's atmosphere is depleted compared to that measured in Jupiter's atmosphere and to that believed to characterize the sun. Analysis of these data also indicated that, globally, the ortho-states and para-states of molecular hydrogen are approximately in equilibrium in the upper troposphere of Saturn. This is different from Jupiter, for which significant deviations from equilibrium were found, implying that the dynamical and radiative time scales are much longer on Saturn than on Jupiter. The relative abundances of hydrogen molecules in the ortho- and para-states can be mapped with high signal-to-noise from CIRS. Local departures from equilibrium can be indicators of dynamical transports. Derivation of the ratio of ortho- to para-states depends on redundancies occurring in the spectrum: radiances at different wavenumbers have the same brightness temperature. In the analysis of Voyager IRIS observations the relevant wavenumbers were within the S(0) and S(1) lines of molecular hydrogen, and the nominal level of sounding was approximately 400 mbar.

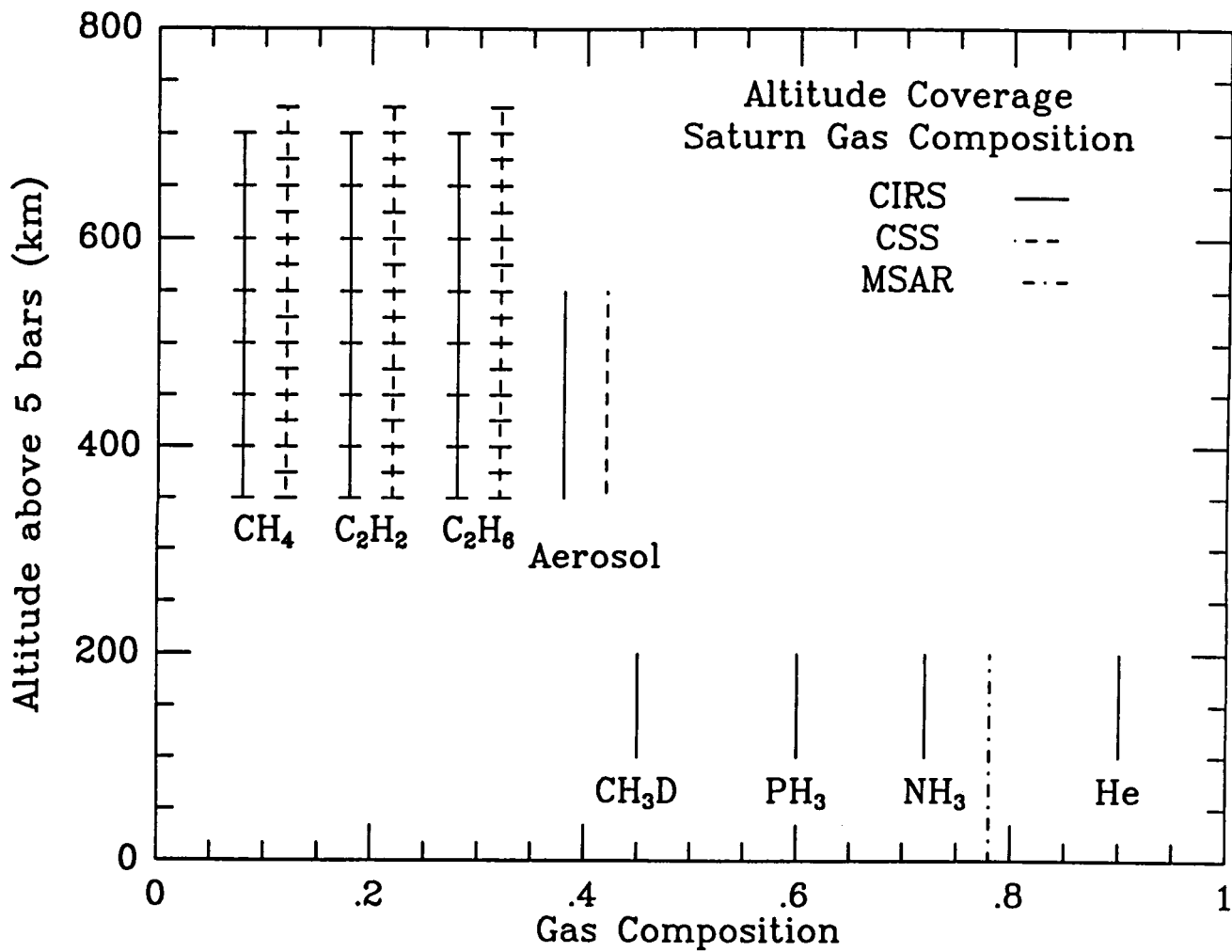


Figure 3.3 Altitude coverage of Saturn gas composition.

With the CIRS, use can be made of redundancies occurring at lower wavenumbers associated with the translation continuum of molecular hydrogen, permitting deeper sounding in the atmosphere. The improved spectral resolution of CIRS over that of IRIS will allow better measurements of the features associated with the dimer $(\text{H}_2)_2$ transitions at the position of the S(0) and S(1) lines. An independent determination of the ortho-para ratio can be obtained from them.

The distributions of NH_3 and PH_3 on Saturn are not very well known. Limited information on the deep tropospheric abundance of NH_3 has been obtained from ground-based microwave measurements as well as Voyager IRIS spectra, but virtually no information is available on its abundance profile above the cloud base ($P < 1.3$ bar). Conflicting results have been obtained in the case of the PH_3 stratospheric distribution through the interpretation of IUE and Voyager IRIS spectra. Measurements of far-infrared rotational lines by CIRS will yield global maps of the tropospheric abundances of these two constituents, thus providing fundamental input for the study of the cloud structure (NH_3) and atmospheric mixing (PH_3). This information will be completed or corroborated in two ways: 1) by global mapping of the temperature/ NH_3 abundance profile with the MSAR instrument operating in the wing of the NH_3 inversion band; and, 2) by the determination of the PH_3 upper tropospheric/stratospheric distribution from CIRS mid-infrared spectra.

Apart from the by-products of photochemical processes, other species are expected to be brought up into the visible atmosphere through disequilibrium mechanisms. Among these species, several are spectroscopically active in the far-infrared, for instance, H_2S , CO , HCl , HF , and HBr . At the level of production which is predicted by the theory, detection of some of these molecules is expected with CIRS. Our understanding of the disequilibrium thermochemical processes taking place in the deep troposphere of Saturn can therefore be tested through such measurements.

Knowledge of the global distribution of photochemically active molecules is the key to understanding the thermal structure, haze production, and vertical transport in the atmosphere of Saturn. The photolysis of CH_4 in the atmosphere produces C_2H_6 and C_2H_2 . In the region of the atmosphere sampled by CIRS and CSS, the abundance of C_2H_6 is controlled by vertical transport. Comparison of abundances inferred from CIRS and CSS observations to those predicted by theoretical models will allow determination of the strength of vertical mixing. Both photochemistry and vertical transport control the abundance of C_2H_2 . Photolysis of C_2H_2 results in the production of polyacetylenes, which are potential aerosols. The observed abundances of C_2H_2 can provide constraints on this production. As on Titan, the hydrocarbons and photochemically produced aerosols contribute to the radiative heating and cooling of the atmosphere. This results in a coupling between photochemistry and dynamics. Global mapping of the hydrocarbons will help elucidate dynamical transport in Saturn's atmosphere.

As on Jupiter, the coupled photochemistry of NH_3 and C_2H_2 is believed to be a source of HCN on Saturn. Because of the low partial pressure of ammonia in Saturn's upper atmosphere, the HCN mixing ratio should be

smaller than on Jupiter. On the other hand, given the higher abundance of PH_3 on Saturn, the coupled photochemistry of PH_3 and C_2H_2 should result in substantial amounts of HCP (and also CH_3PH_2). CIRS will be able to search for both HCN and HCP and other organo-phosphorus compounds.

Hydrogen and CNO isotopes are very useful indicators of the origin and chemical evolution of planetary atmospheres. Furthermore, in the case of deuterium, the Jovian and Saturnian abundances are thought to be characteristic of the deuterium content in the protosolar nebula, thus providing a constraint on the chemical evolution of the Galaxy at the epoch of formation of the solar system. The CIRS instrument will determine at least two isotopic ratios on Saturn, namely $^{12}\text{C}/^{13}\text{C}$ and D/H, from measurements in the CH_4 - ν_4 and CH_3D - ν_6 fundamental bands.

3.2.1.3 Cloud/Haze Composition and Structure

Aerosol and cloud particles in Saturn's atmosphere play important and direct roles in many physical processes, such as determining the Bond albedo and modulating stratospheric temperatures. Furthermore, they influence tropospheric temperatures and circulation through their infrared opacity, latent heat, and absorption and reflection of sunlight. Unfortunately, the physical properties and spatial distribution of such particles in the Saturnian atmosphere are very incompletely known. Large differences in cloud properties as a function of latitude act as forcing mechanisms for atmospheric circulation. Clouds and aerosol particles provide clues to other atmospheric properties such as chemical mixing ratios, and they can serve as tracers for atmospheric processes such as photochemistry and dynamics. A main portion of the cloud near and above the 1-bar level in the atmosphere is probably ammonia ice particles, with other condensate clouds, such as water, deeper in the troposphere. The ammonia cloud layer is probably thicker than in the atmosphere of Jupiter, and particle sizes may become smaller with altitude. Closer to the temperature minimum, near the 100-mbar level, particles of another origin appear likely, and they may be mixed with ammonia cloud particles. These may originate in the stratosphere and could be compositionally related to diphosphine (P_2H_4) or organic photolysis by-products of methane. The stratospheric haze is most optically thick near the poles. Other very strong latitudinal variations of cloud properties are observed. Time-variability is also expected, closely coupled with insolation-forced changes in stratospheric temperatures. For example, acetylene may condense in the stratosphere during the Saturnian winter but not in the summer.

Some properties of atmospheric particles can be elucidated by analysis of reflected visible and ultraviolet solar radiation. Observations at longer wavelengths, however, can provide equally valuable information on particle properties. Observations in the near-infrared region by C-VIMS can take advantage of variations of gaseous opacity which are much larger than in the visible/ultraviolet spectrum to discern vertical particle distributions between 10 bars and 10 mbar. Together with the visible/ultraviolet data, they can constrain particle size by examining the variation of cloud or haze optical thickness as a function of wavelength. High-resolution images

in the infrared can provide information on zonal velocities at altitudes quite different from those sensed at visible/ultraviolet wavelengths. Thermal radiation emerging from “windows” in the gaseous opacity near 5 microns (C-VIMS), 9 microns (CIRS), and 45 microns (CIRS) are sensitive to cloud optical thickness. These spectral regions, together with knowledge of the temperature structure, provide some independent information about atmospheric particles, and they are sensitive to a larger particle size regime. While earth-based measurements show little similarity between the appearance of 5-micron “hot spots” in Jupiter and the 5-micron spatial morphology of Saturn, the higher spatial resolution afforded by spacecraft observations may be able to detect related or similar phenomena (e.g., small “warm spots”). In any case, such observations would be sensitive to thermal radiation emerging from as deep as the 10-bar level in the atmosphere. It is expected that observations at 9 and 45 microns would be sensitive to the ammonia cloud region alone; this can be used to discriminate among various models for particle size for this isolated cloud layer. CSS can measure extinction coefficient profiles for the stratospheric aerosol at several wavelengths from 7-14 μm .

3.2.1.4 Science Summary of Individual Instruments

MSAR

- o Composition and chemistry + condensation clouds
 - High-resolution 3-dimensional study of NH_3 from measurements in the wings of 1.25-cm transition
 - Search for CO and HCN in Saturn’s troposphere
- o Rings
 - Particle size distribution from polarization measurements of scattered emission
- o Satellites
 - Surface and sub-surface brightness temperatures

CIRS

- o Thermal structure and dynamics
 - Retrieval of tropospheric temperatures between the 100- and 1000- mbar levels from nadir measurements in the H_2 - H_2 pressure-induced absorption
 - Retrieval of stratospheric temperatures between the 0.01- and 10-mbar levels from limb measurements in CH_4
- o Composition and chemistry
 - New determination of the He abundance
 - Variations of the ortho-para ratio for hydrogen from measurements of the H_2 features

- Vertical distributions and latitudinal variations of minor constituents: NH_3 , PH_3 , hydrocarbons, etc.?
- Isotopic ratios: $^{12}\text{C}/^{13}\text{C}$, D/H
- Search for disequilibrium species in the deep troposphere: CO, HCN, H_2S , etc. ?
- o Condensation clouds and haze
 - Study of cloud structure from correlations between near- and far-infrared measurements
- o Rings
 - Search for local impurities from their infrared spectral signatures
- o Satellites
 - Surface brightness temperatures

CSS

- o Thermal structure and dynamics
 - Global mapping of stratospheric temperature profiles between the 0.01- and 10- mbar levels on Saturn with high vertical resolution, using limb measurements in CH_4
 - Global mapping of vertical distribution, spatial variation and temporal variation of CH_4 and selected key chemical species in the stratosphere of Saturn (candidates CH_4 , C_2H_2 , C_2H_6 , and HCN)
- o Condensation clouds and haze
 - Global mapping of vertical profiles of aerosol extinction coefficient in the stratosphere of Saturn at several wavelengths from 7-14 μm .

C-VIMS

- o Condensation clouds and haze
 - Global mapping of vertical structure of clouds using phase angle coverage. Particle sizes, mass loading for clouds.
- o Composition and chemistry
 - Global mapping of PH_3

3.2.2 TITAN

3.2.2.1 Thermal Structure and Dynamics

Titan is the second known example, along with Venus, of a cyclostrophically balanced super-rotating atmosphere; but unlike Venus, the system is subject to strong seasonal modulation. For this reason, its atmospheric thermal structure and meteorology are of particular interest. Vertical profiles of atmospheric temperature were provided by the Voyager radio occultation experiment, but only at two equatorial locations

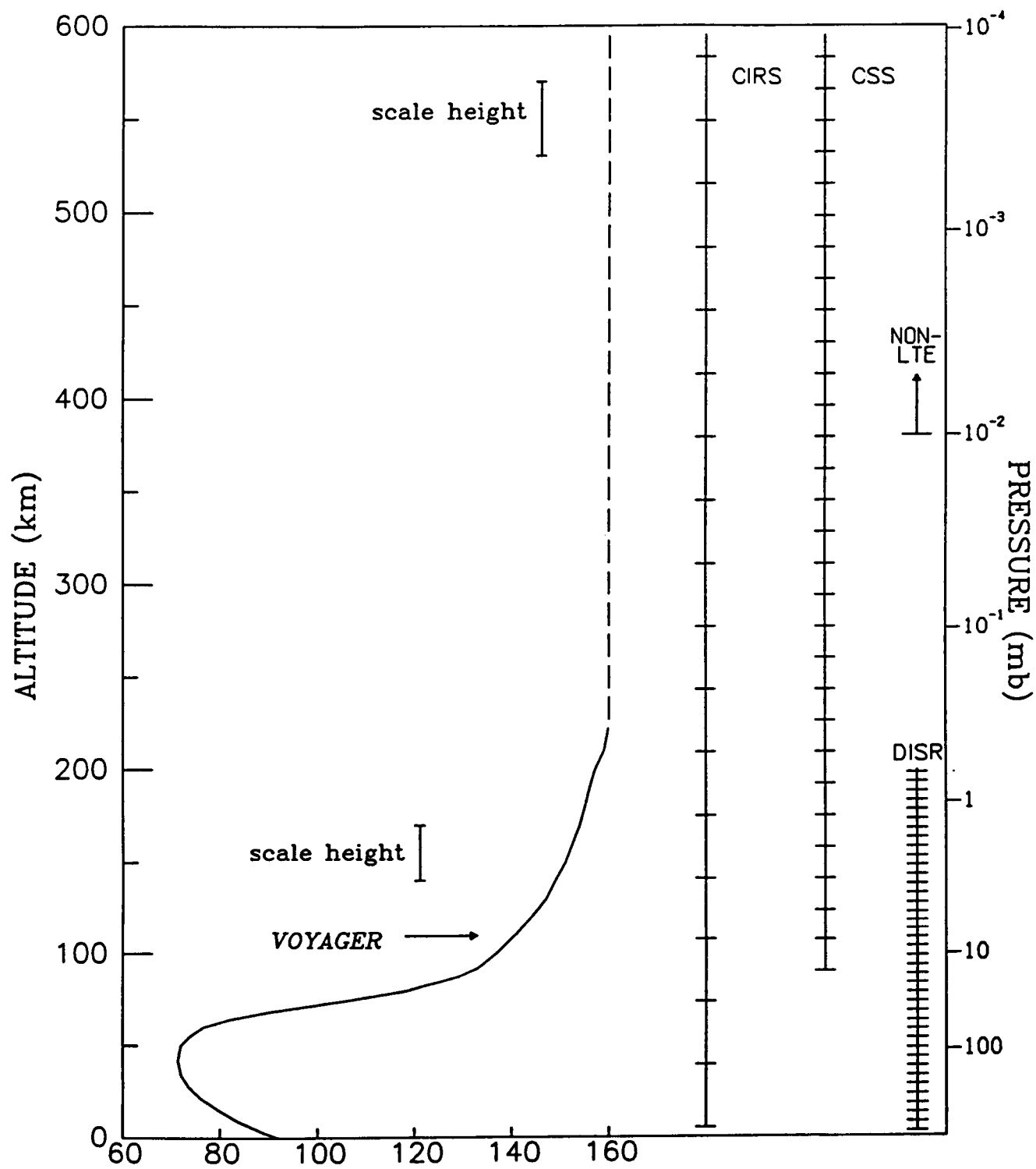


Figure 3.4 Altitude coverage of Titan temperature profile.

on Titan. Maps of atmospheric and surface temperatures were derived from IRIS observations. Observations at three wavenumber intervals were used to infer temperatures at the surface/lower troposphere, at the tropopause, and in the upper stratosphere.

Altitude coverage of the Titan thermal structure by the Cassini infrared instruments is shown in Fig. 3.4. The temperature profile for the lower 200 km, as inferred from the Voyager radio occultation, is indicated by the solid line.

It was difficult to unambiguously retrieve temperatures in the troposphere and lower stratosphere of Titan from Voyager IRIS measurements, because condensates probably account for much of the middle and far infrared opacity, and the spatial distribution of these is not well known. In addition to the complications of the infrared aerosol opacity, radiances at wavenumbers $> 600 \text{ cm}^{-1}$ are extremely sensitive to temperature. This results in the complete insensitivity of measurements at these wavenumbers to the relatively cold upper troposphere and lower stratosphere. The former part of the atmosphere is of interest, because methane clouds are thought to condense there. The latter is of interest, because many of the hydrocarbons present in the stratosphere are expected to condense in this region. It is also the transition region dynamically where the radiative relaxation time becomes comparable to the seasonal forcing time scale. To probe these regions, MSAR and CIRS measurements in the far infrared are required. Fig. 3.5 shows the CIRS contribution functions for spectral intervals in a region dominated by pressure-induced N_2 opacity. Here the contribution to the opacity from aerosols and condensates can be neglected to a first approximation. The uppermost contribution function is for limb-tangent viewing, and indicates that it is possible to sound the lower stratosphere by this approach.

Voyager IRIS measurements of radiance near 1304 cm^{-1} in CH_4 did permit some mapping of stratospheric temperatures near the 1-mbar level, where the contribution of aerosol opacity is probably small. Limb sounding by CIRS and CSS will provide coverage of the stratosphere from 0.01 to 10-mbar with good altitude resolution. Below approximately the 0.01-mbar level, atmospheric temperatures can be retrieved from the assumption of local thermodynamic equilibrium; at higher altitudes this assumption is not valid and more complex modeling is required to derive atmospheric temperature from the source function.

An important question, which limb sounding in the middle-infrared can address, is whether the atmosphere is isothermal above 0.5 mbar or exhibits a more complex vertical structure.

Global mapping of temperature fields in the stratosphere and upper troposphere will elucidate the seasonally changing meridional variation in temperature and, through application of the thermal wind equation, the concomitant change in the zonal winds. Observations of zonal variations (i.e., with longitude) are also an important objective, because they bear on the important question of waves and eddies, which can drive or damp the zonal flows. The improved mapping capabilities afforded by the Cassini orbiter over Voyager, and the improved sensitivity of the Cassini instrumentation offer a better chance of detecting eddies and waves and unraveling the complex question of the origin and maintenance of global cyclostrophic flows. In principle,

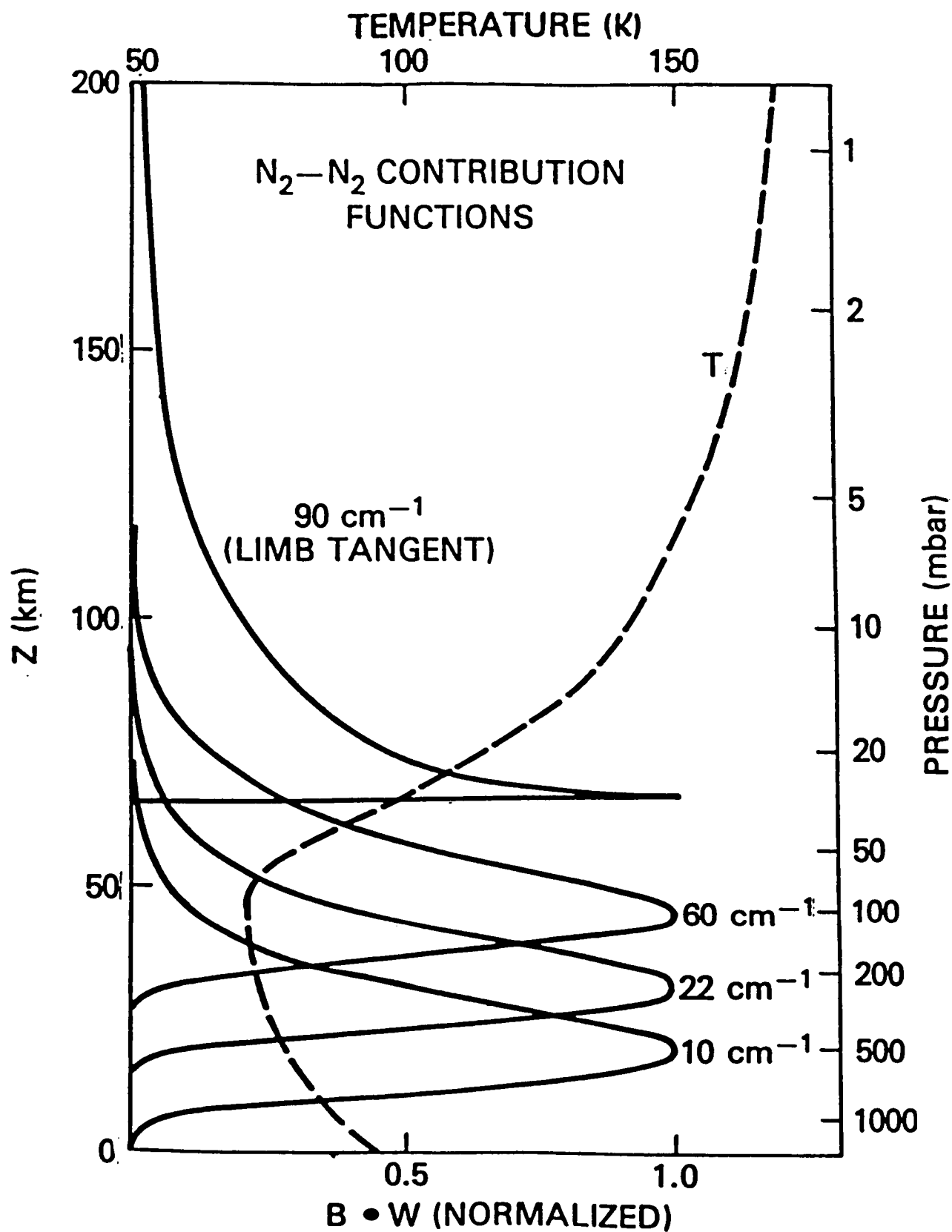


Figure 3.5 CIRS contribution functions for pressure induced N_2 absorption in Titan's troposphere.

the winds can be directly measured using Doppler shifts of microwave lines. These measurements would add some instrumental complexity to MSAR.

3.2.2.2 Chemical Composition

Continuum measurements in the far-infrared by CIRS will provide constraints on CH_4 relative humidity in the troposphere as well as on the H_2 mixing ratio. Detection of the $\text{H}_2\text{-N}_2$ dimer absorption features may also become possible, thereby allowing a determination of the H_2 abundance with increased accuracy.

The photochemically active molecules occurring in Titan's stratosphere are important in understanding the origin and evolution, thermal structure, meteorology, and haze layers of Titan's atmosphere. The irradiation of CH_4 by solar UV and electron impact of N_2 results in the formation of complex organics (C_2H_2 , C_3H_8 , C_4H_2 , C_2H_4 , C_2H_6 , etc.), prebiotic nitriles (HCN , HC_3N , C_2N_2 etc.), and polymers, which condense and ultimately precipitate to the surface of Titan. The oxygen compounds CO_2 and CO have also been identified in Titan's stratosphere.

Because of the large flyby distance of the spacecraft, Voyager IRIS was mostly limited to near nadir observations of Titan. As a result, only limited information could be obtained on the vertical distribution of gases. By limb sounding at much closer distances, MSAR, CIRS, and CSS will obtain detailed vertical profiles of stratospheric gas composition over a wide altitude range (Figs. 3.6 and 3.7). The MSAR measures CO , HCN , and HC_3N ; the CIRS measures many species simultaneously for input to comprehensive atmospheric models; and the CSS measures coincident CH_4 , C_2H_2 and C_2H_6 profiles with altitude resolutions of better than 0.5 scale heights within 4 R_s of Titan.

C_2H_2 and C_2H_6 are two key chemical species important to stratospheric photochemistry and transport; both are measured by CIRS and CSS. The contribution functions indicate good altitude coverage from 600 km down to 90 km (Fig. 3.8). HCN is the most abundant nitrile, is central to the nitrile chemistry, and is found to vary with latitude. The HCN contribution functions for MSAR are shown in Fig. 3.9. Improved vertical profiles of the nitriles will also determine the relative importance of cosmic rays and Saturn's magnetospheric electrons in producing them.

CO is the most abundant oxygen-bearing compound. Recent observations suggest that the stratosphere is depleted in CO relative to the troposphere. The altitude distribution of this important gas will be determined by the MSAR instrument. The MSAR contribution functions for the 1-0 CO line (115 GHz) are shown in Fig. 3.10.

In addition to the monitoring of the known species illustrated in Figs. 3.6 and 3.7, the broadband spectral coverage of CIRS will allow a spectroscopic search to be made for new molecules, for example, H_2O . Photolysis of H_2O can result in the formation of CO and CO_2 , both of which have been detected on Titan. Meteoritic infall has been proposed to be the source of water, but this has yet to be confirmed. Alternatively,

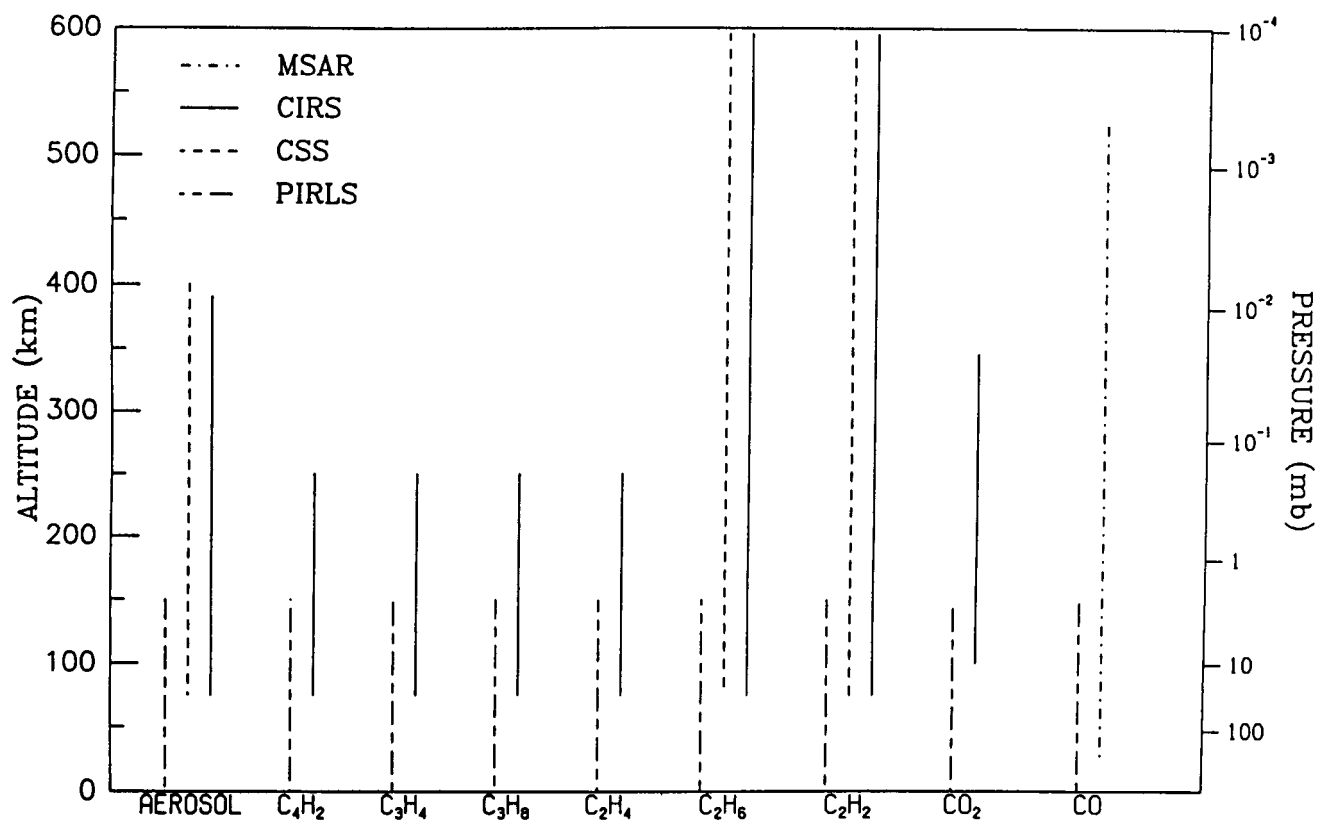


Figure 3.6 Altitude coverage of Titan gas and aerosol composition.

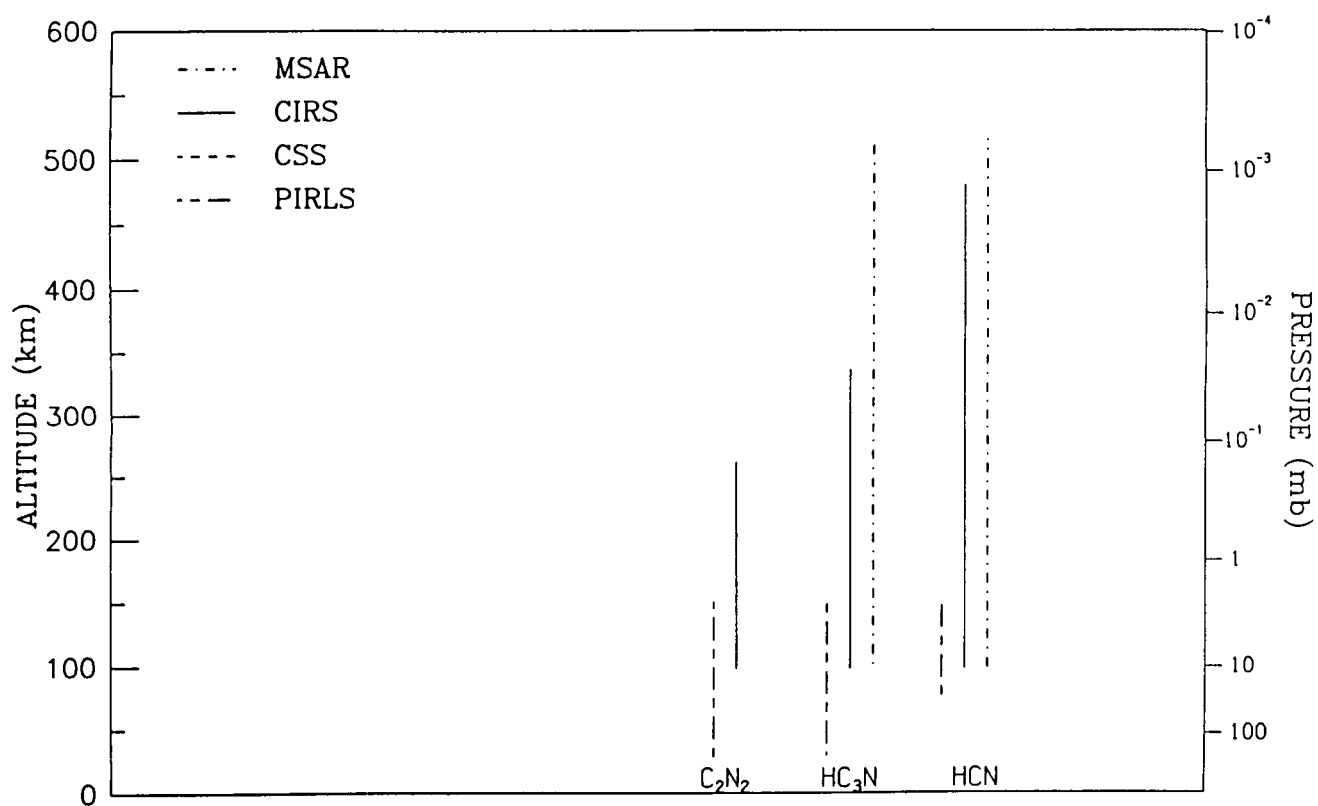


Figure 3.7 Altitude coverage of Titan nitrile gas composition.

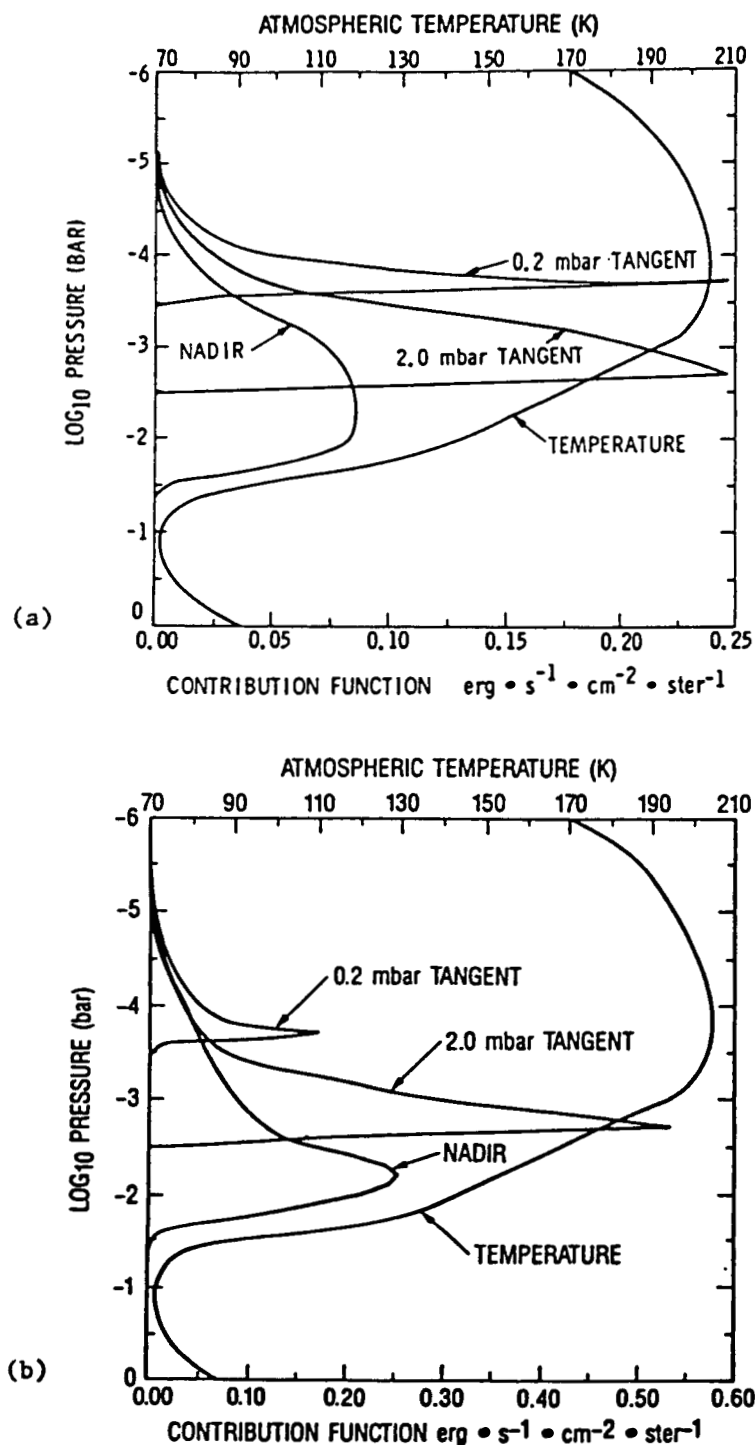


Figure 3.8. CSS contribution functions for nadir and selected limb views of Titan using pressure modulator cells observing (a) Ethane and (b) Acetylene.

- Conditions:
- (a) Ethane mixing ratio $2.0\text{E-}05$, Bandpass $805 - 845 \text{ cm}^{-1}$.
Cell, 5.0 cm , 150 K , $P_{\text{min}}=24\text{mbar}$, $P_{\text{max}}=96\text{mbar}$.
 - (b) Acetylene mixing ratio $2.0\text{E-}06$, Bandpass $730 - 760 \text{ cm}^{-1}$.
Cell, 1.0 cm , 150 K , $P_{\text{min}}=24\text{mbar}$, $P_{\text{max}}=96\text{mbar}$.

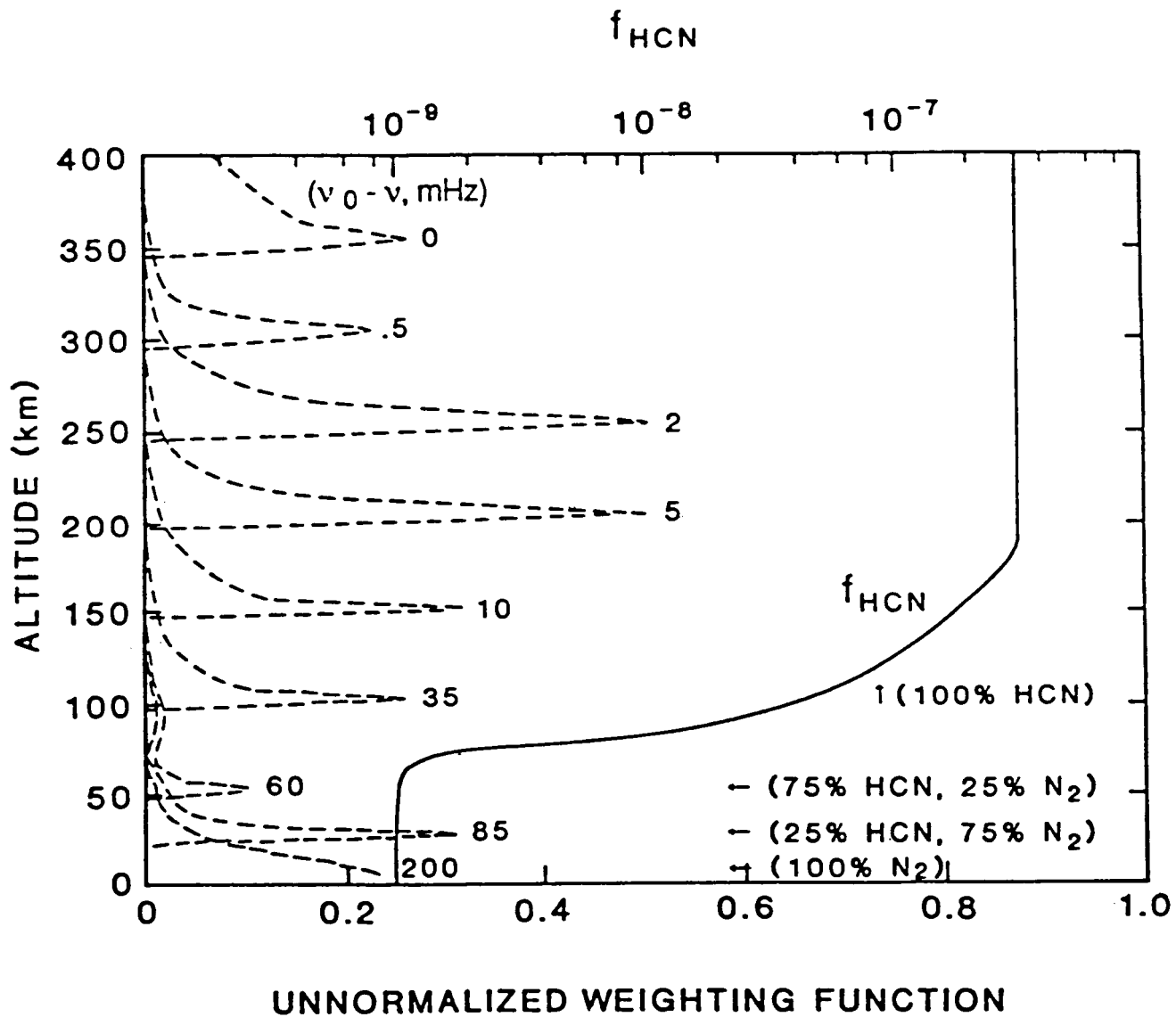


Figure 3.9 MSAR limb weighting functions for HCN in Titan's stratosphere;
 f is the HCN mixing ratio profile.

$$\frac{[\text{CO}]}{[\text{N}_2]} = 6 \times 10^{-6}$$

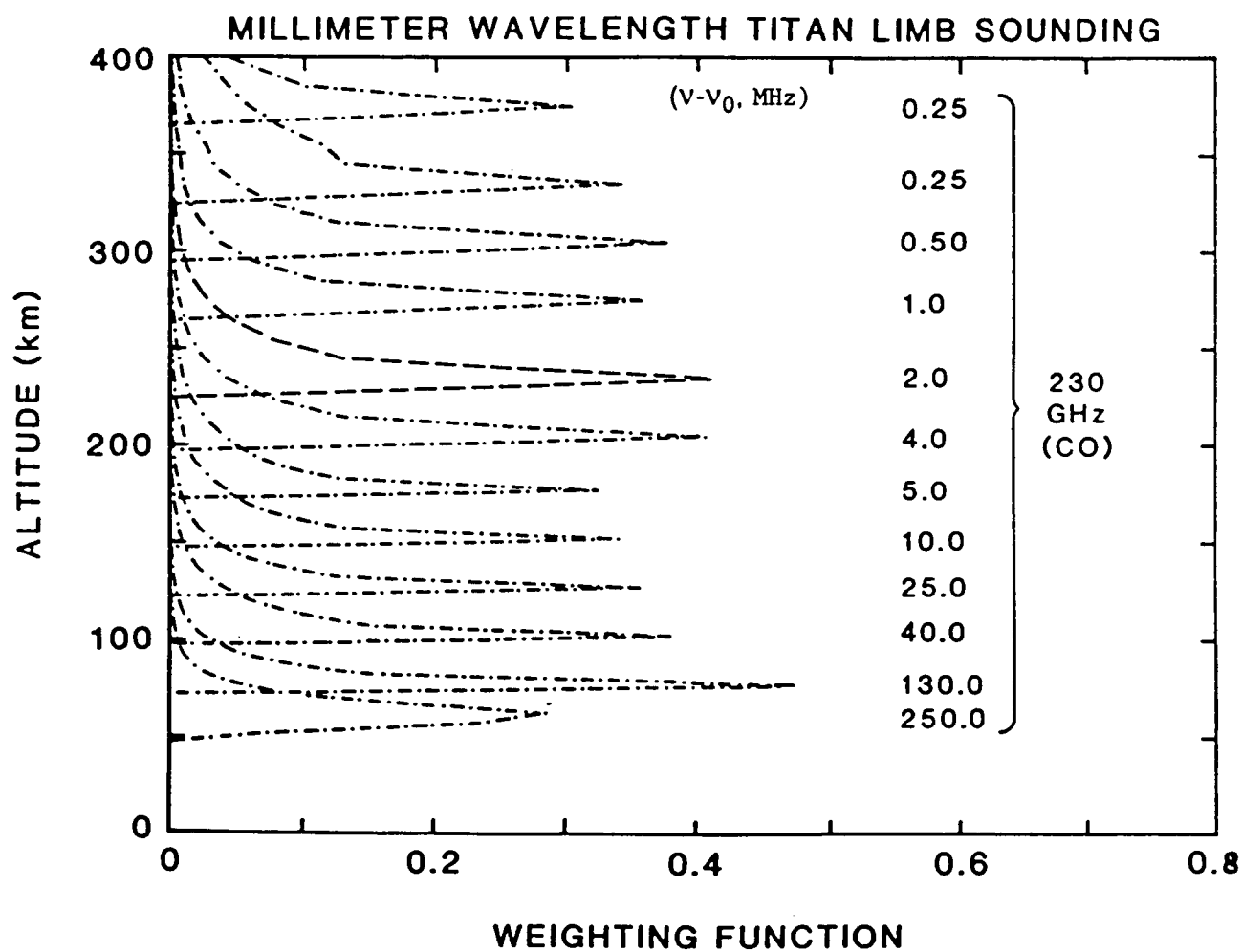


Figure 3.10 MSAR limb weighting functions for CO in Titan's stratosphere.

it has been proposed that the observed CO originates from clathrates at the surface. CO_2 would then be formed from CO and hydrocarbons dissociated high in the atmosphere. The low wavenumber cut-off of 10 cm^{-1} will allow CIRS to search for stratospheric emission of H_2O near 150 cm^{-1} . Detection of H_2O would thus place an important constraint on the source of oxygen in Titan's atmosphere. In addition to H_2O , a search will also be made for complex N-containing organic compounds with vibration bands in the $100\text{--}400\text{ cm}^{-1}$ region.

Global mapping of the hydrocarbons, nitriles, and nitrogen bearing compounds will be diagnostic of the sources and sinks of these molecules, the distribution of radiative heating and cooling attributable to them, and the dynamical circulations that transport them. Because the observations will occur at a different season and level of solar activity than the Voyager observations, they will provide constraints on the relevant lifetimes of these species. The detailed mapping that will be afforded by the repeated close passages of Titan in the Cassini mission will for the first time permit detailed radiative-photochemical-dynamical modeling of Titan's stratosphere.

The two probe instruments will provide composition information for the $0\text{--}160\text{ km}$ altitude region. The PIRLS will provide profiles with a vertical resolution less than a scale height for a number of molecules, including the important species CH_4 , CO, and CO_2 . The DISR will also provide a CH_4 profile.

3.2.2.3 Cloud/Haze Composition and Structure

There are three basic components to Titan's cloud structure. One is a photochemical aerosol spread throughout the stratosphere between altitudes of 40 and 350 km . Its composition is unknown, but polyacetylenes admixed with complex nitrogen-bearing polymers are likely possibilities. A second component consists of combinations of simple nitriles and hydrocarbons between 45 and 100 km . At these altitudes, these compounds have vapor pressures exceeding those required for saturation, and condensation should take place. Finally, condensed methane is thought to exist in the troposphere between 5 and 35 km .

Several aspects of this composite cloud structure will be clarified by the CIRS and CSS. When the spacecraft is close to Titan, the limb sounding mode will permit good vertical resolution of the stratospheric photochemical aerosol in addition to yielding the overall abundance. This will be done as a function of position on the disk as the spacecraft flies repeatedly past Titan. Comparisons with limited data of the same kind from Voyager 1 will permit the study of seasonal effects - the sun was at equinox at the time of the Voyager 1 flyby, and will be near solstice during the Cassini mission.

The C-VIMS will be very useful in investigating the latitudinal variation of albedo, and contrasting it with that observed by Voyager 1. Temperature profiles will be obtained by both the CIRS and radio occultation. Intercomparisons of the latitudinal dependences of aerosol properties, gas abundances, and temperature can then be made, and inferences drawn about stratospheric heating and cooling rates, leading to various chemical and dynamical processes operating in the upper atmosphere.

A few emission features in Voyager 1 spectra have been identified with condensates of C_4N_2 , HC_3N , and possibly H_2O . Analyses of CIRS spectra should greatly enhance our knowledge of condensates in the lower stratosphere. Comparisons of CIRS and Voyager 1 spectra will yield the seasonal dependence of these condensates on latitude.

Finally, a careful mapping of the CIRS spectral continuum between 10 and 500 cm^{-1} will disclose horizontal opacity variations in the troposphere. Both limb and normal viewing spectra will be needed to separate stratospheric and tropospheric effects. The patchiness of tropospheric methane clouds will thus be exposed, leading to the most direct evidence yet for their existence. The amount of cloud cover inferred will be crucial in developing thermal equilibrium models to explain the temperature structure of Titan's atmosphere. CSS can measure aerosol extinction coefficient profiles with high vertical resolution at several wavelength from 7-14 μm .

3.2.2.4 Thermal Balance

The thermal state of Titan's atmosphere is determined by the complex interaction of several physical processes. Solar energy is absorbed by gaseous absorption bands, photochemical haze particles, and the surface. The details of the solar heating depend on the poorly known vertical and horizontal distribution, size, and optical properties of the haze and cloud particles in the atmosphere. The solar heating in each volume element is partially balanced by infrared radiative emission that depends on the temperature and emissivity of the aerosols, condensed cloud particles, and the atmospheric gases. In steady state, the net radiative heating or cooling is balanced by heat carried into or out of the element by mass motions (or other processes such as latent heat effects). If the temperature profile, distribution and optical properties of the particulates, and the gaseous composition were all perfectly known, it would, in principle, be possible to compute the net radiative drives for dynamical motions throughout the atmosphere.

It is known that Titan's stratospheric haze aerosols are very dark at visible wavelengths and absorb sunlight quite efficiently. Because of their small size, these particles are relatively poor emitters at long wavelengths, and so they are important in elevating Titan's stratosphere temperature substantially above its effective temperature (the temperature a black body would have in equilibrium with the amount of sunlight absorbed by Titan). Unfortunately, the distribution and optical properties of haze aerosols and the temperature profile are not well known through Titan's stratosphere. Variations with latitude and with season are likely to be significant, and are presently unknown as well. The solar heating rate will be measured directly in the stratosphere by DISR on the probe, and the aerosol sizes and optical properties will be measured by DISR solar aureole and spectral flux measurements and by the PIRLS nephelometer. Temperature profiles and aerosol properties will be mapped from the orbiter by CIRS, CSS, and C-VIMS.

The haze particles, together with a possible methane condensation cloud in the troposphere, are also effective at limiting the penetration of sunlight to Titan's surface. Titan's surface temperature is known to be elevated above

its effective temperature; a fact attributed to a small "greenhouse" effect on Titan. Sufficient solar energy must penetrate and be absorbed at the surface to provide this warming in the presence of the opacity of the atmosphere to radiative cooling at thermal wavelengths. The cloud and haze particles must be sufficiently transmitting to permit significant solar heating at the surface, and yet sufficiently opaque at thermal wavelengths to trap enough heat to raise the surface temperature to the observed value. Neither the penetration of sunlight to the surface nor the opacity of the cloud particles at either solar or thermal wavelengths are known at present. The solar heating profile throughout the atmosphere will be measured by the DISR, and the DISR spectral flux data and aerosol measurements will determine the location, thickness, and optical properties of cloud and haze particles. The cloud/haze structure and its optical properties will also be measured in-situ by the PIRLS nephelometer. Direct thermal flux measurements are difficult due to the very low atmospheric temperatures, so the thermal fluxes will have to be calculated from the particle size, and optical properties inferred from measurements at shorter wavelengths by DISR and from other indirect measurements.

3.2.2.5 Surface

The surface of Titan has yet to be probed directly except by microwave radio emission and radar. Prior to Voyager, lack of knowledge of atmospheric composition severely limited modeling of the surface. The Voyager encounters provided some information on atmospheric composition, thermal structure and photolysis rates and products of methane. Models of the surface state must be consistent with this information. The simplest model which achieves such consistency is a liquid hydrocarbon layer, containing dissolved methane and nitrogen: a so-called "ethane-methane" ocean. The properties of such a layer can be summarized as follows:

1. Gaseous methane is in vapor equilibrium with the ocean; for the range of tropospheric methane mole fractions allowed by Voyager data, the ocean contains 15-60% methane;
2. The ocean depth, calculated for the current rate of methane photolysis extrapolated over 4.5 billion years, is roughly one kilometer. Since ethane is the primary product of methane photolysis on Titan, it dominates the ocean composition; and,
3. The solubility of molecular nitrogen, the dominant atmospheric constituent in liquid ethane and methane, implies a mixing ratio in the ocean of at least several percent. The ocean and atmosphere contain comparable amounts of nitrogen. Higher hydrocarbons either dissolve in the ocean or sink to the bottom.

Alternative models in which the surface is covered largely by solid polyacetylenes and other complex hydrocarbons require modification to the photochemical schemes, frequent endo- or exogenic resupply of methane, and/or reinterpretation of the lower atmospheric temperature profiles. A model in which the "bedrock" of Titan, solid ice, is significantly exposed runs into conflict with the inferred rate of methane photolysis.

Few remote-sensing tests of the hydrocarbon ocean hypothesis are available. Ground-based measurements of Titan's microwave emission argue weakly against the ocean hypothesis; polarization measurements are

ambiguous. Recent attempts to measure radar return from Titan have proved unsuccessful in diagnosing the surface physical state. Determination by Cassini of the presence and extent of a hydrocarbon ocean on Titan's surface carries profound implications for the long-term evolution of this body, as well as for the physical and chemical cycles which determine its present state.

The MSAR will probe emission and polarization from the surface of Titan, using dual-polarized 2-cm receivers, to determine the physical state of the material present. The polarization is a strong function of the surface dielectric constant, and the measurement should yield maps of regions covered by liquids (ethane, etc.) and regions covered by rough ice. Ice will exhibit dielectric constants of about 3, while that for liquid ethane is 1.8. With accurate knowledge of the dielectric properties of candidate Titan surface materials (which requires a suite of laboratory experiments prior to the mission), the presence and global extent of a hydrocarbon ocean will be determined. It may also be possible, depending upon the depth and purity of such an ocean, to detect emission from the base of the ocean. If the surface is largely solid, the experiment will map the real extent of polymeric hydrocarbons/nitriles and exposed water-ice or rock.

The DISR will provide images of the surface of Titan, providing direct information on the presence or absence of an ocean at a single location on the body. Reflection spectra of the surface, obtained before and possibly after impact, will provide compositional information on the solid or liquid material at the landing site. Information on the morphology of the clouds and thermal structure obtained by the experiment will permit more detailed modeling of the physical and chemical interactions between a surface ocean layer and atmosphere.

The theoretical basis for and implications of various Titan surface models is developed in Lunine, J.I., S.K. Atreya and J.B. Pollack, *Present State and Chemical Evolution of the Atmospheres of Titan, Triton and Pluto*, in Origin and Evolution of Planetary and Satellite Atmospheres (eds. Atreya, Pollack and Matthews), Univ. of Arizona Press, Tucson, 1988, in press.

3.2.2.6 Science Summary of Individual Instruments

MSAR

o Thermal structure and dynamics

- Retrieval of tropospheric and stratospheric temperatures from 400 km down to the surface from CO and HCN line shape measurements

o Composition and chemistry

- Vertical distributions of CO, HCN, and HC₃N and their variations over the globe
- Isotopic ratios for H, C, O, and N

o Surface

- Map of the surface emissivity from brightness temperature measurements in the centrimetric range

- Map of the surface emissivity from polarization measurements- Measure surface roughness and search for liquids on Titan

CIRS

o Thermal structure and dynamics

- Retrieval of tropospheric temperatures between 20 and 750 mb from nadir measurements in the $N_2+CH_4+H_2$ pressure-induced absorption range
- Retrieval of stratospheric temperature between 0.01 to 10 mbar from limb measurement in CH_4

o Composition and chemistry

- Major constituents: CH_4 relative humidity, H_2 abundance, presence of Ar and N_2-H_2 dimers
- Study of the CH_4+N_2 photochemical products: vertical distribution of hydrocarbons and nitriles- Study of oxygenated compounds: CO, CO_2 , H_2O , etc. ?
- Isotopic ratios: $^{12}C/^{13}C$, D/H
- Search for condensed material: water ice, hydrocarbons, nitriles, polymers
- Prebiotic chemistry: search for complex nitriles
- Compositional variations: polar enhancements, dayside vs. nightside compositions

o Photochemical haze and condensation clouds

- Global mapping of tropospheric clouds/haze
- Global mapping of stratospheric haze

CSS

o Thermal structure and dynamics

- Global mapping of stratospheric temperature profiles between the 0.01 and 10-mbar levels on Titan with high vertical resolution, using limb measurements in CH_4

o Composition and chemistry

- Global mapping of vertical distribution, spatial variation and temporal variation of CH_4 and selected key chemical species in the stratosphere of Titan (candidates CH_4 , C_2H_2 , C_2H_6 , and HCN)

o Condensation clouds and haze

- Global mapping of vertical profiles of aerosol coefficients in the stratosphere of Titan at several wavelengths from 7-14 μm .

C-VIMS

o Composition and chemistry

- Global mapping of CH_4 variability

o Condensation clouds and haze

- Global mapping of vertical structure of clouds using phase angle coverage. Particle sizes, mass loading for clouds.

DISR

o Photochemical haze and condensation clouds

- Spectral characteristics between 0.4 and 2 μm and/or vertical profile below 160 km for the extinction optical depth, the single scattering albedo and phase function, the mean particle size, number density and refractive index
- Morphology

o Thermal balance

- Solar heating rate at altitudes below 160 km from measurements between 0.4 and 2 μm

o Surface

- Morphology
- Spectral reflectivity from 0.4 to 2 μm

o Gaseous composition

- Vertical profile of mixing ratio of methane from 160 km to surface

PIRLS

o Composition and chemistry

- Gaseous composition down to 10^{-9} volume mixing ratios from stratosphere to surface
- Vertical profile of CH_4 mixing ratio from 160 km to surface
- Vertical profiles of hydrocarbons and nitriles such as HCN , C_2H_2 , C_2N_2 , C_3H_4 , C_3H_8 , HC_3N , C_4H_2 and isotopic ratios for C and H
- Vertical profiles of oxygen compounds CO and CO_2 (and H_2O)
- Search for H_2O and NH_3
- Vertical profile of particle size distributions from entry with 100-m resolution
- Particle sizes from 0.2 to 50 microns in diameter
- Refractive index computed from independent forward and back scatter measurements.

APPENDIX A MSAR BACKGROUND INFORMATION AND FIGURES

PRECEDING PAGE BLANK NOT FILMED

SATURN ATMOSPHERE BRIGHTNESS TEMPERATURE

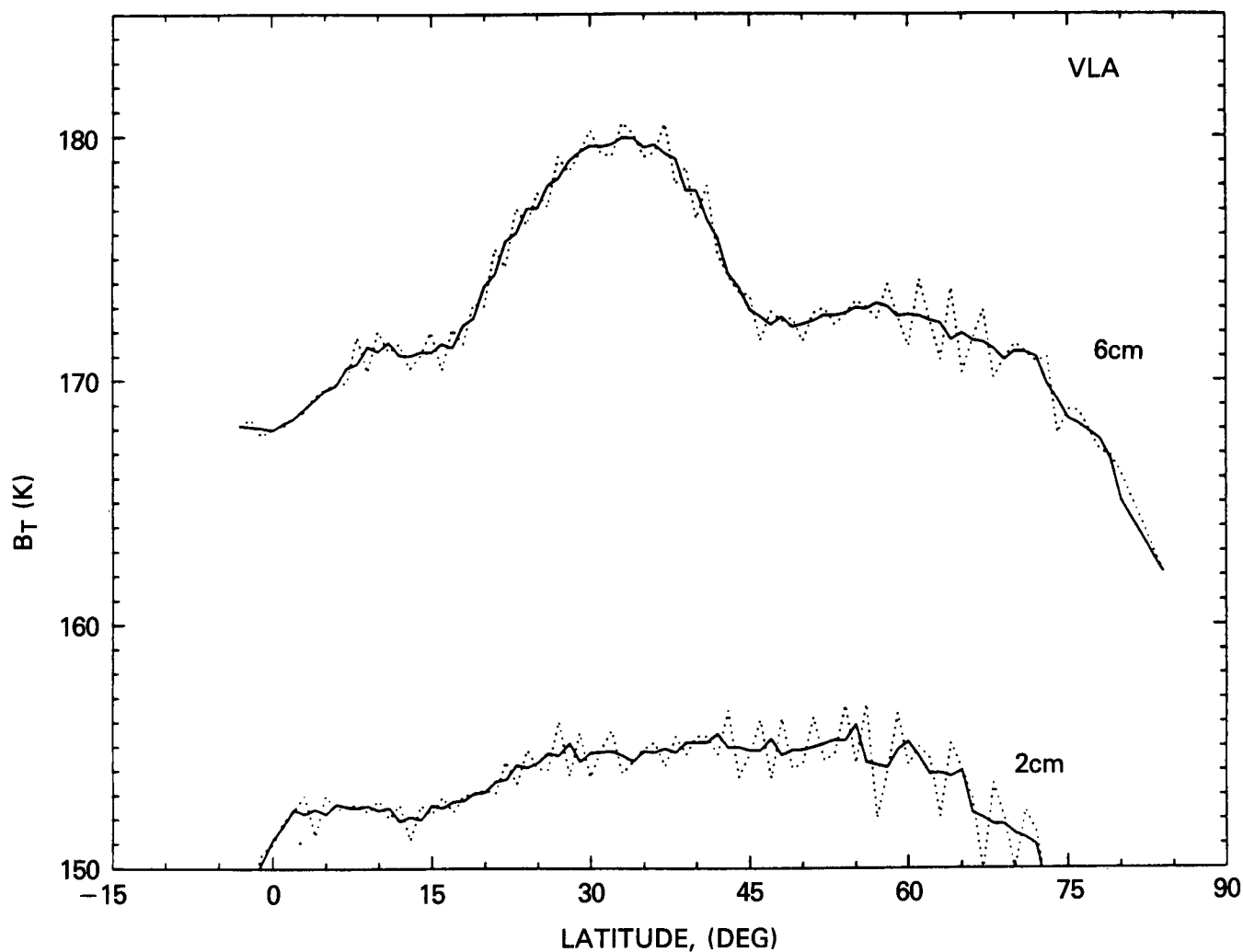


Figure A1 Equator to North pole scans on VLA maps of Saturn made at wavelengths of 2 and 6 cm, B_T is the brightness temperatures in Kelvin.

PRECEDING PAGE BLANK NOT FILMED

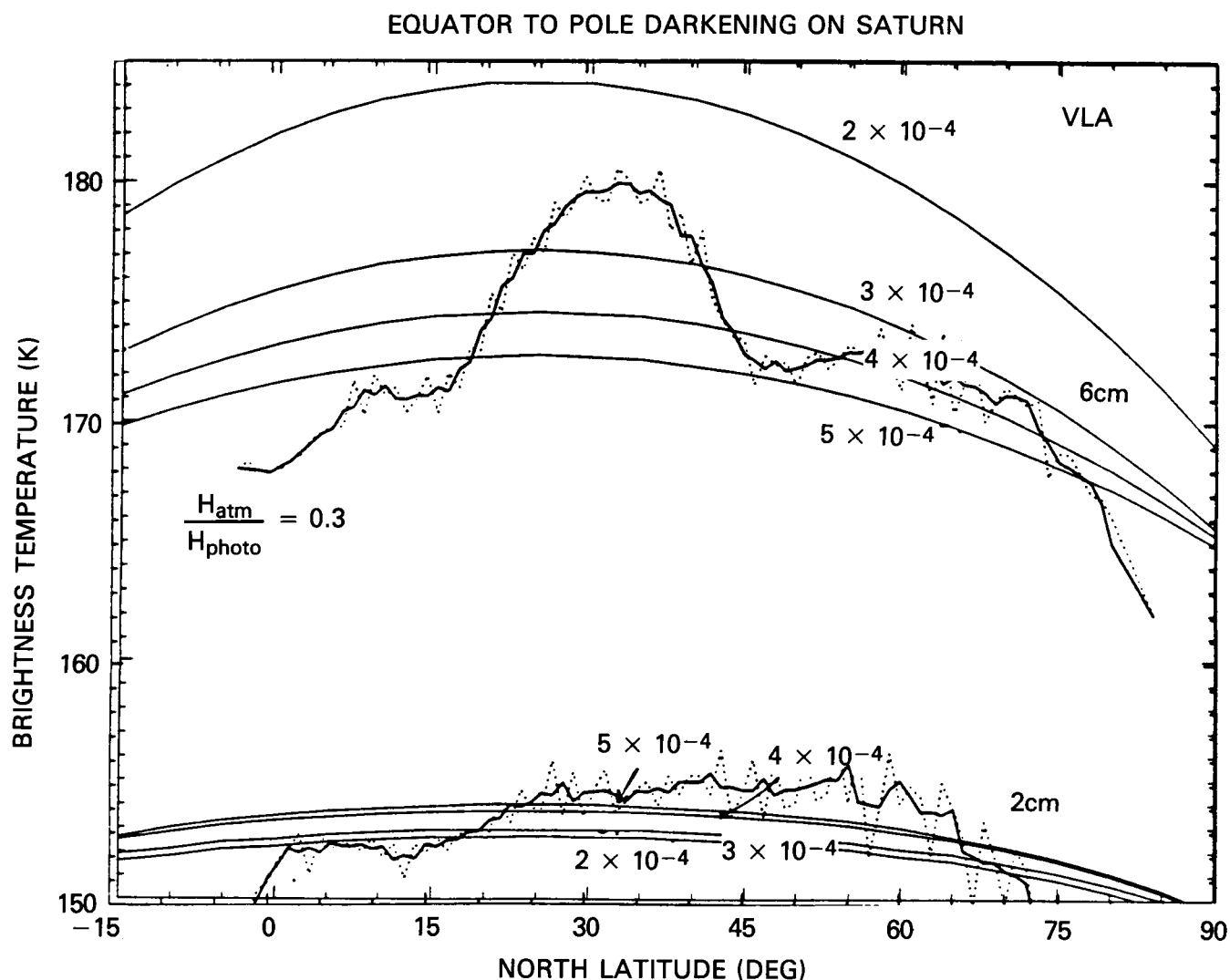


Figure A2 Same as fig. A1 with model predictions as a function of the NH_3 mixing ratio (assumed to be uniform with depth below the NH_3 saturation level). To simultaneously fit the data at 2 wavelengths it was necessary to assume that NH_3 is subsaturated above the clouds, i.e., the NH_3 relative humidity falls exponentially with scale height 113 km above the clouds.

S/X LIMB DARKENING ON SATURN: NH₃ MIXING RATIOS = 2X10⁻⁴ AND 4X10⁻⁴

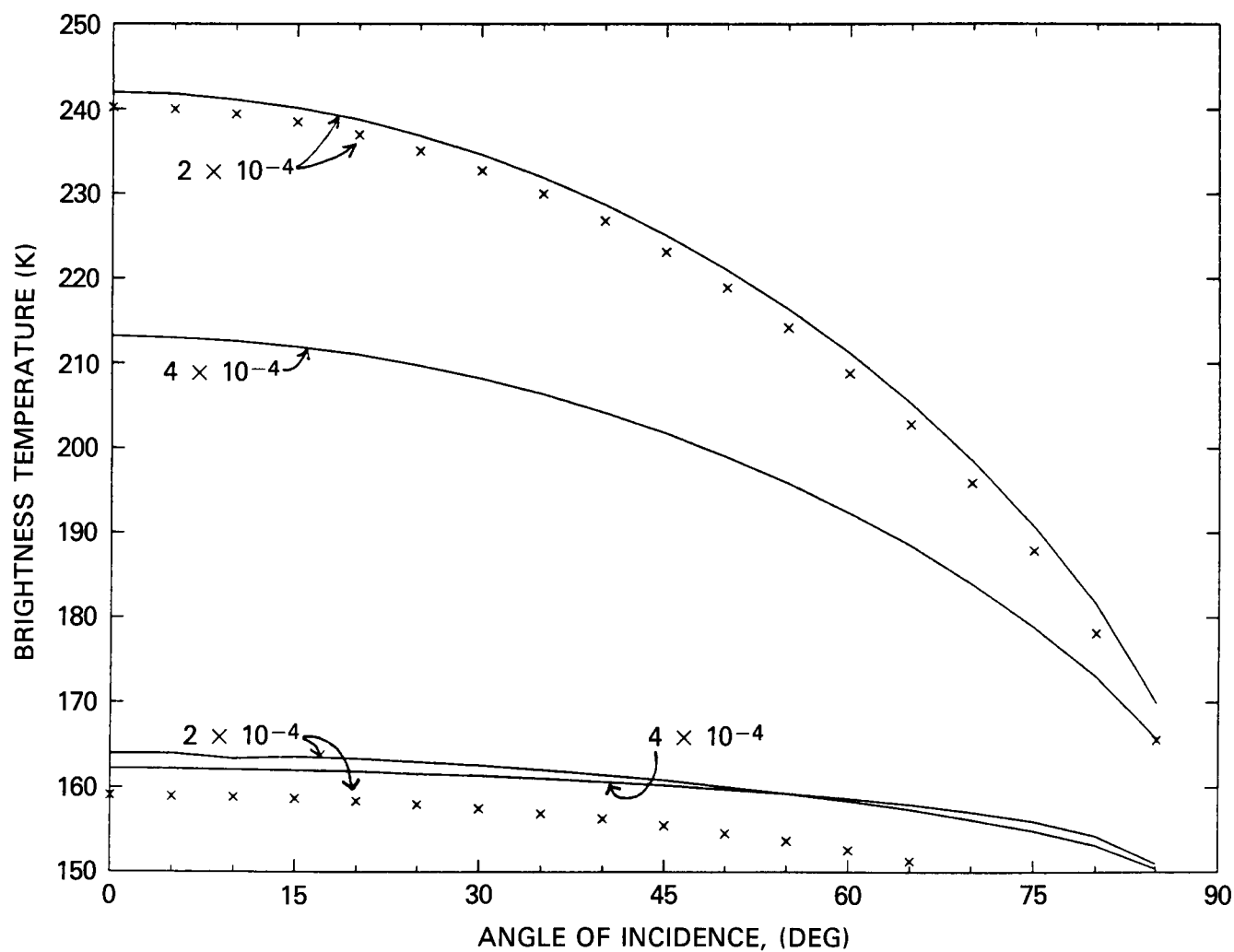


Figure A3 Similar models for wavelengths proposed for the Cassini Ammonia Sounder: 3.5 and 13 cm.

$$\frac{[\text{CO}]}{[\text{N}_2]} = 6 \times 10^{-6}$$

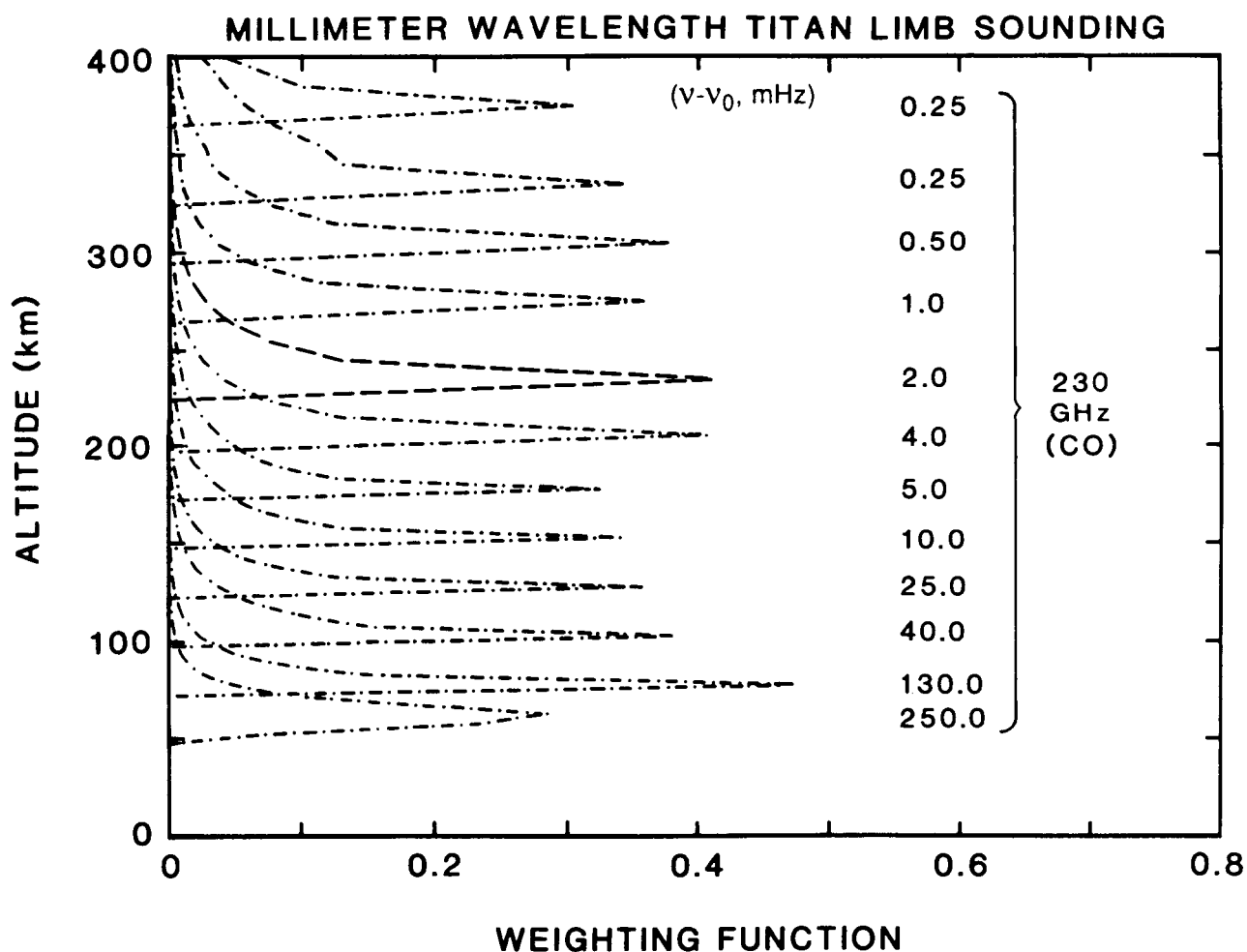


Figure A4 Limb sounding weighting functions for CO(2-1) line at 230 GHz with minimum CO mixing ratio of 6×10^{-6} . Functions are labeled by the frequencies from the line center in MHz. Curves show that CO can be used as a sounding gas to altitudes of 400 km on Titan.

$$\frac{[\text{CO}]}{[\text{N}_2]} = 6 \times 10^{-6}$$

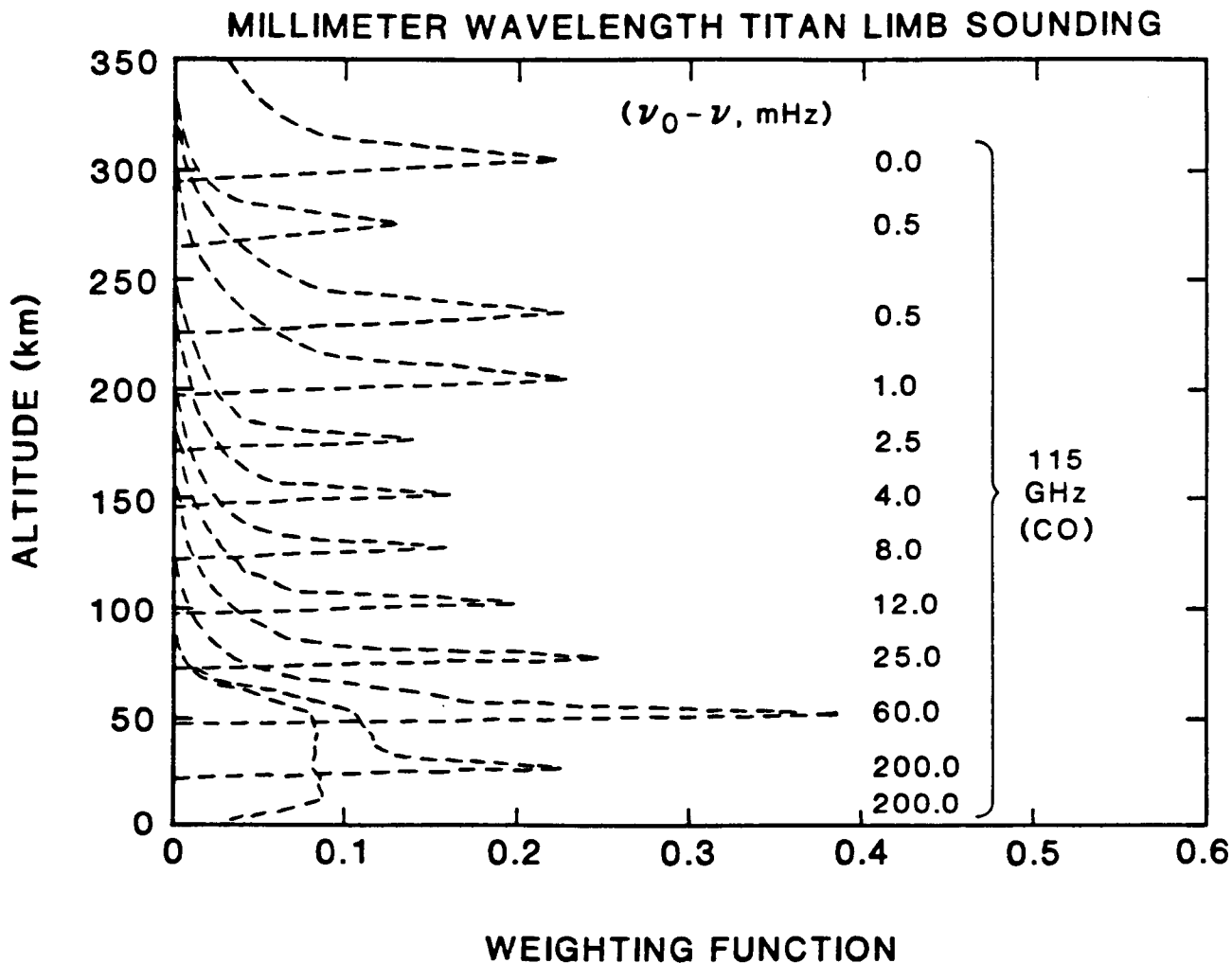


Figure A5 Limb viewing weighting functions on Titan. Mixing ratio is significantly smaller than expected on Titan. Crudely, weighting functions for the 230-GHz line would be about 8 times stronger.

$$\frac{[\text{CO}]}{[\text{N}_2]} = 6 \times 10^{-5}$$

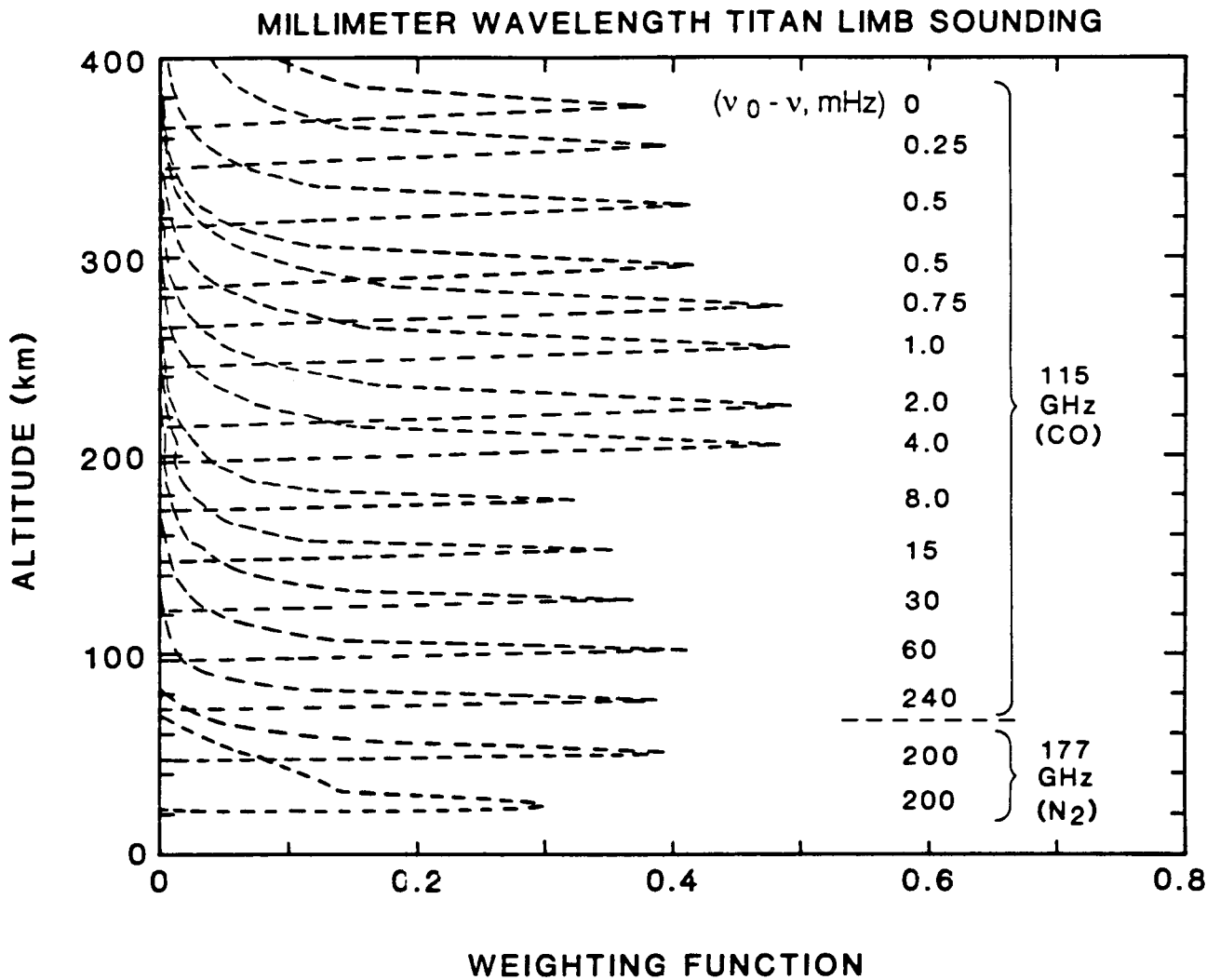


Figure A6 Limb viewing weighting functions on Titan. The functions are labeled with the frequency from line center in MHz. Mixing ratio is near the mean value expected for Titan.

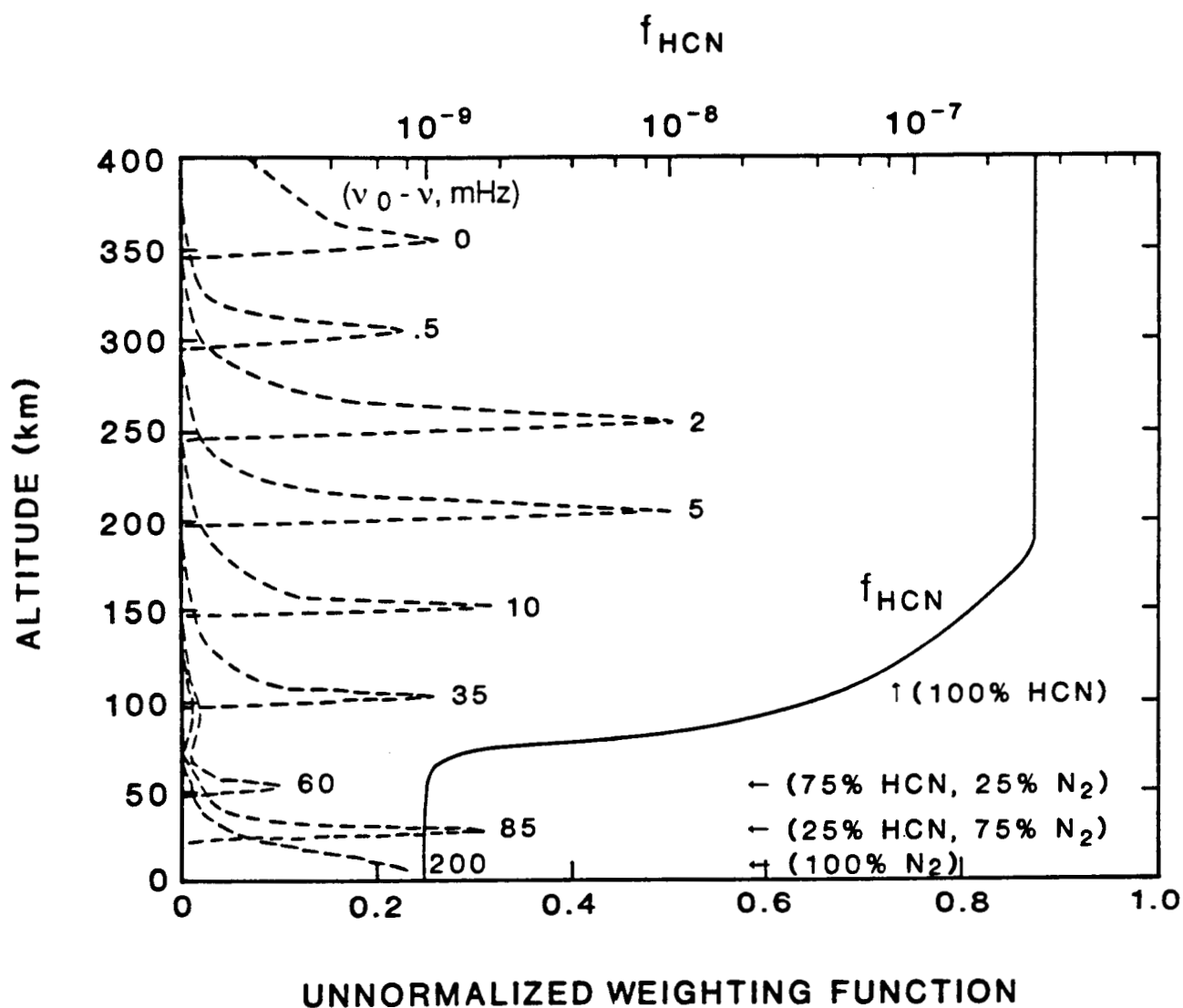
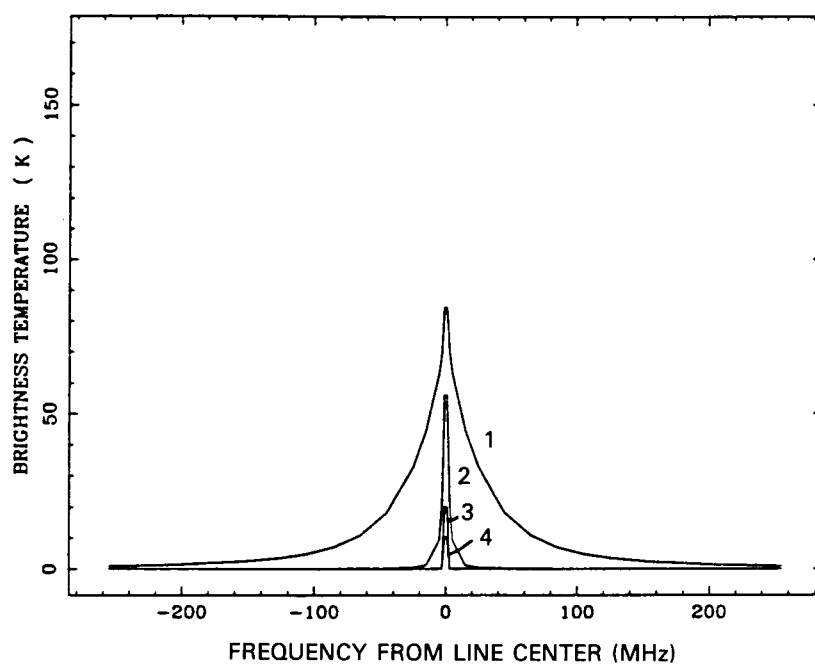


Figure A7 HCN weighting functions on the Titan limb, f is the HCN mixing ratio profile. For 177 GHz.

CO (1-0) TITAN LIMB SPECTRA WITH ALTITUDE MIX = 3×10^{-6}



CO (2-1) TITAN SPECTRA WITH ALTITUDE MIX = 3×10^{-6}

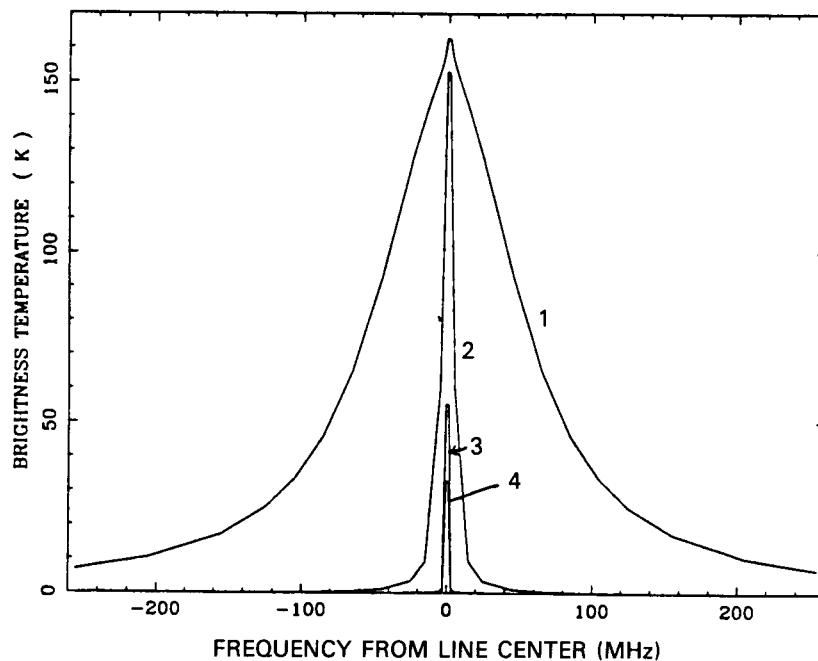


Figure A8 CO (1-0) 115 GHz and (2-1) 230 GHz for an extremely low value of the stratospheric CO mixing ratio (3×10^{-6}). Limb scans at tangent heights (1) 100 km, (2) 200 km, (3) 300 km and (4) 350 km.

SCHEMATIC SPECTRA IN 1.3 MM RECEIVER

230 GHz CO(2-1) RECEIVER

1st. LO 22520 GHz
2nd. LO 5.19 MHz
Not to scale

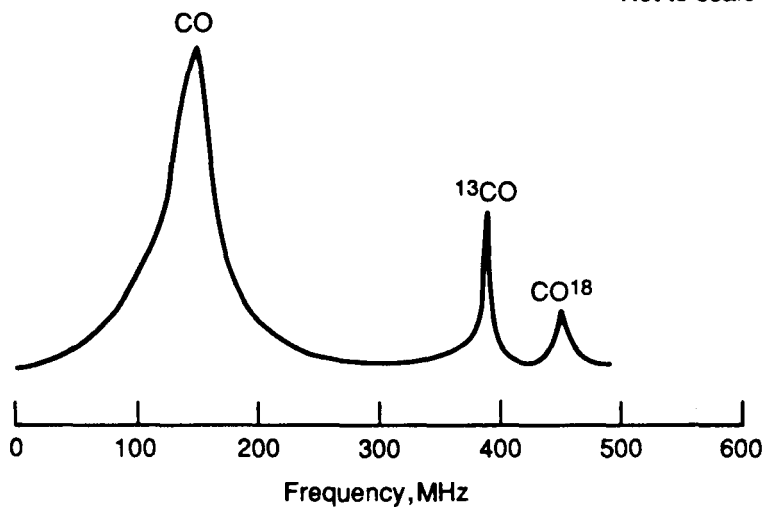


Figure A9 Spectra in a single bandpass for the 230 GHz mixer.

SCHEMATIC SPECTRA IN 1.7 MM RECEIVER

177 HCN RECEIVER

1st. LO 174.80000 GHz
2nd. LO 2.3000 GHz
Not to scale

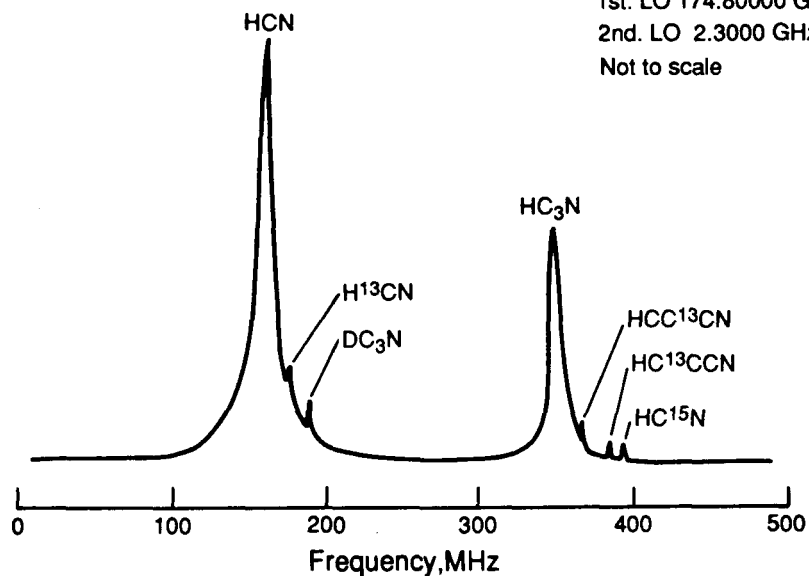
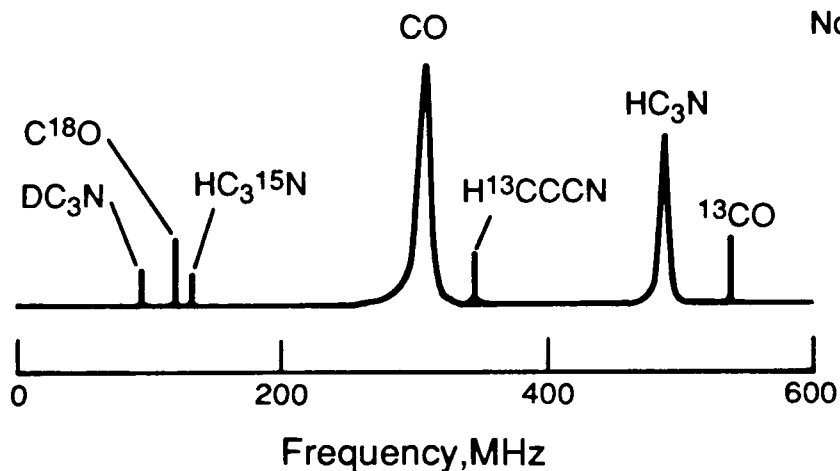


Figure A10 Spectra in a single bandpass for the 177 GHz mixer.

SCHEMATIC SPECTRA IN 3 MM RECEIVERS

115 GHz CO RECEIVER

1st. LO 112312 MHz
2nd. LO 2605 MHz
Not to scale



88 GHz HCN RECEIVER

1st. LO 87415 MHz
2nd. LO 875 Mhz

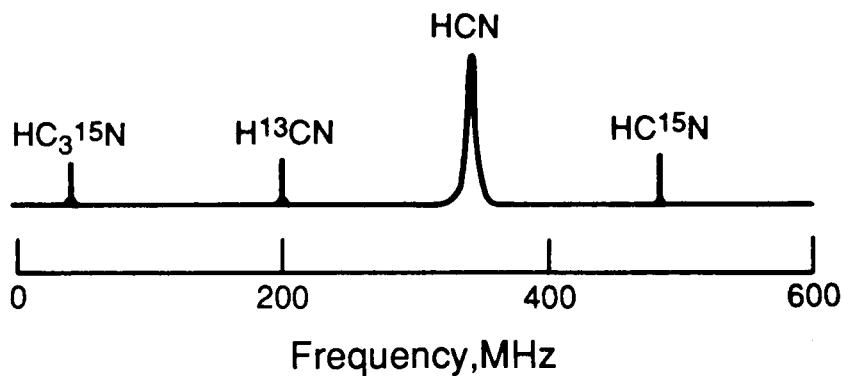
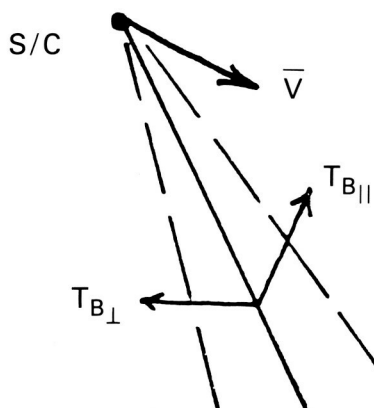


Figure A11 Spectra in a single bandpass for the 115-GHz mixer.



ORIGINAL PAGE IS
OF POOR QUALITY

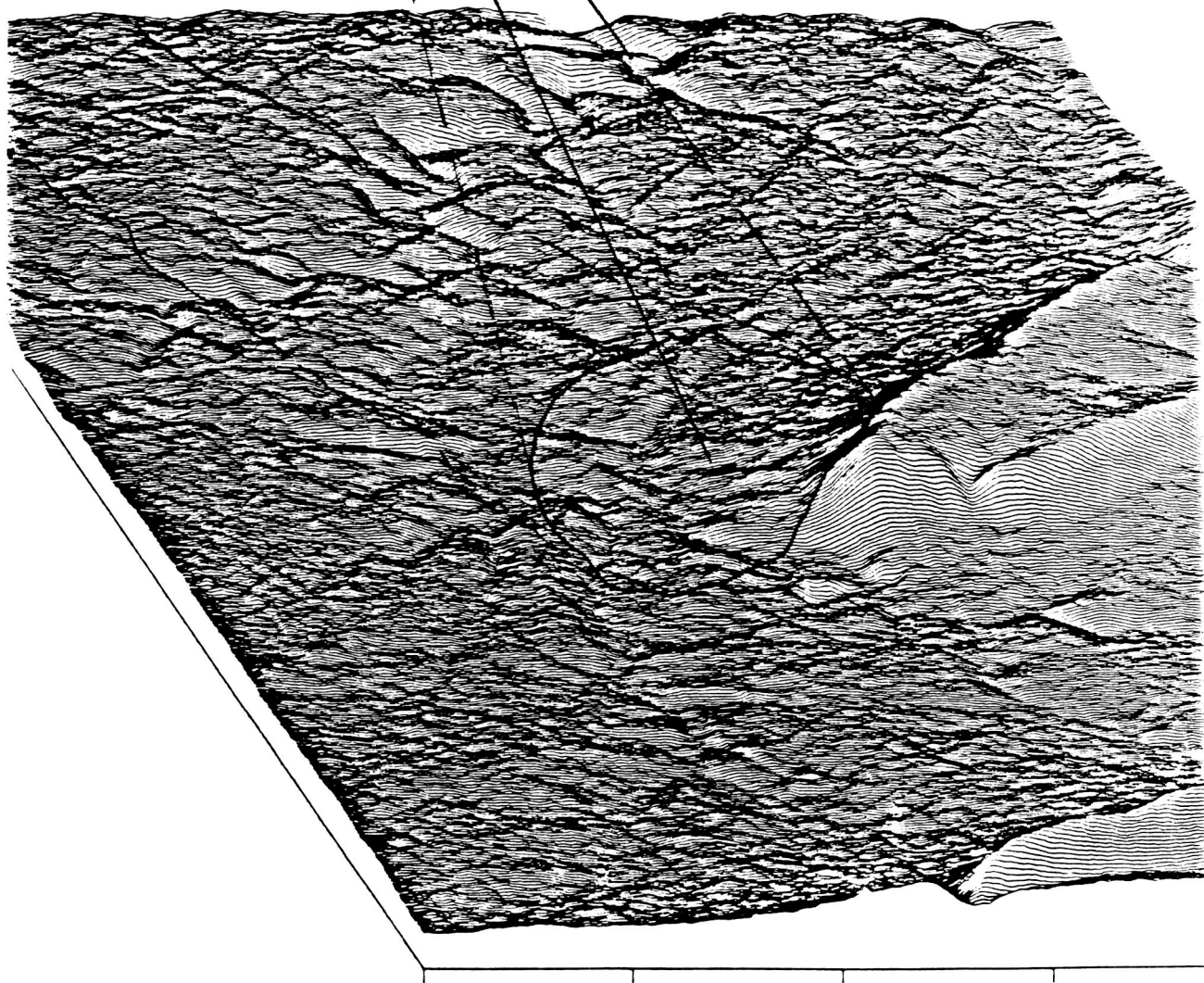


Figure A12 Illustration of 2 cm polarimetry for the Titan surface.

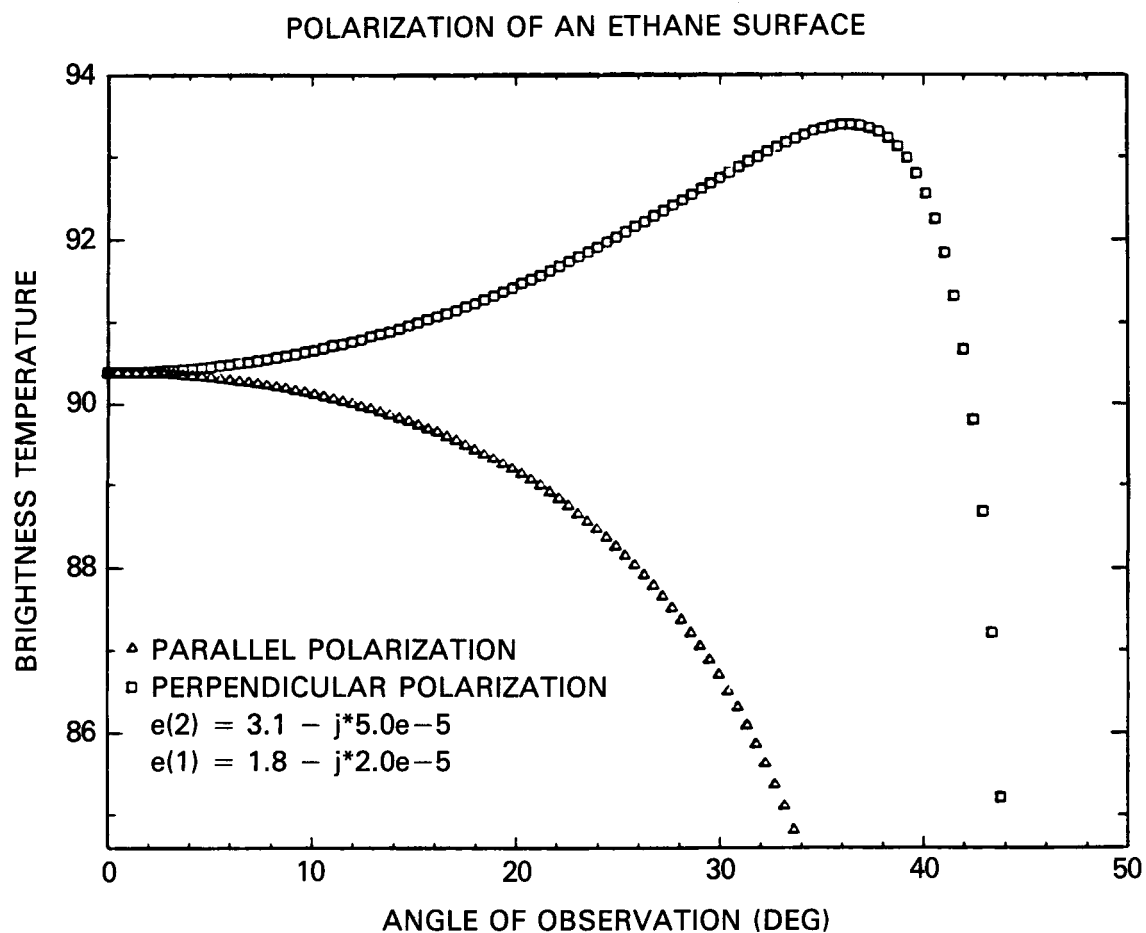


Figure A13 Expected brightness temperature response of the Titan surface vs. elevation angle for a smooth ethane ocean. The 2 cm polarimeter will measure these temperatures to an accuracy of about 2 K, their ratios far better.

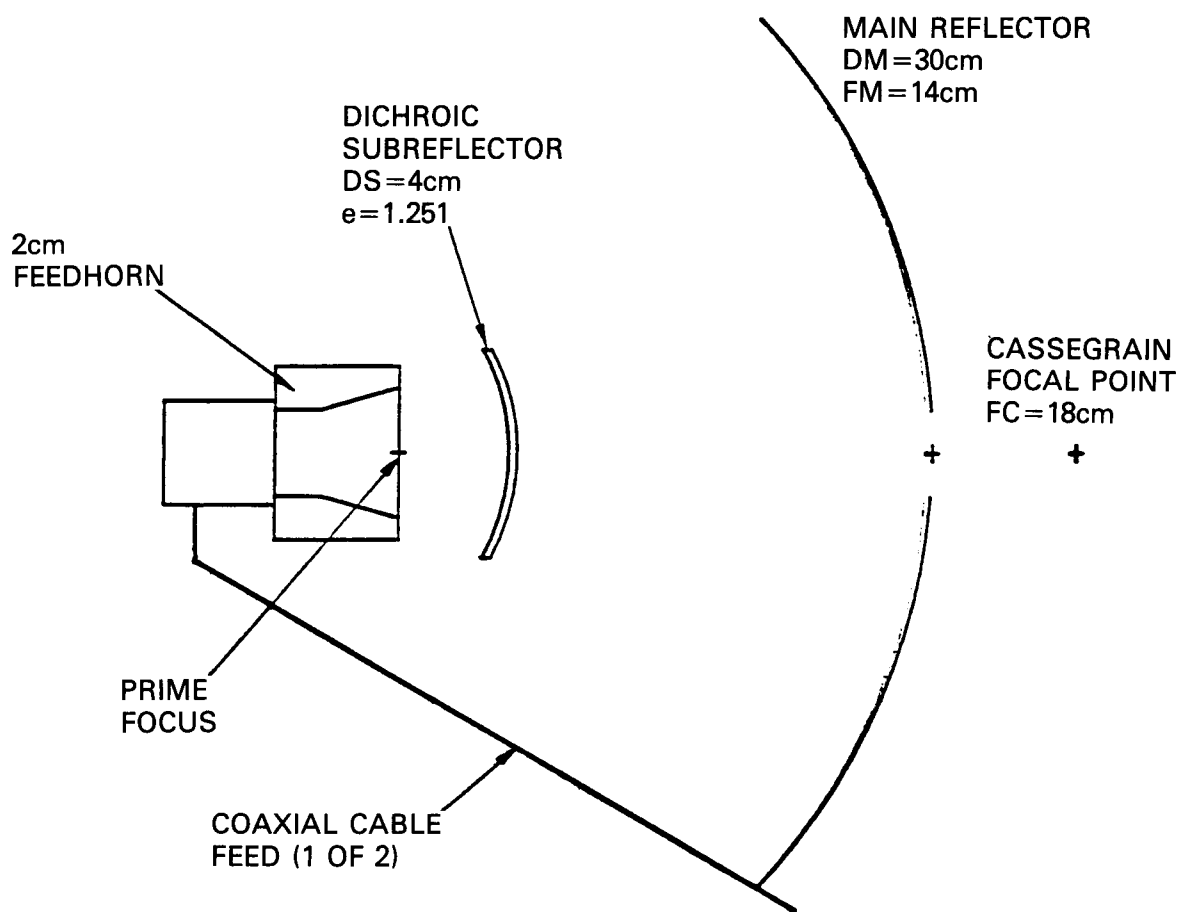


Figure A14 Optics of the Millimeter Spectrometer and Radiometer.

CASSINI MICROWAVE INSTRUMENT ANTENNA BEAMWIDTHS¹

Wavelength(cm)	FWHM Beamwidth ¹	Full Width to -10 dB Beamwidth ¹	Titan Resol.	
			<u>Nadir</u>	<u>Limb</u>
2.00	0.0760 (4.35°)	0.130 (7.46°)	76 km	188 km
0.28	0.0106 (0.61°)	0.018 (1.05°)	11 km	26 km
0.17	0.0065 (0.37°)	0.011 (0.64°)	7 km	16 km

Notes

(1) The first values given in each column are in radians, and those in parentheses are in degrees.

Figure A15 MSAR spatial resolution on Titan.

OVERALL CASSINI MICROWAVE INSTRUMENT WEIGHT CALCULATION

Mechanical Components	299.4 oz.	8.5 Kg.
2cm Radiometer	58.7	1.7 Kg.
3mm Radiometer	65.9	1.9 Kg.
2mm Radiometer	67.6	1.9 Kg.
Common Millimeter Electronics	37.0	1.05 Kg.
<hr/>		
Total	528.6 oz.	15.0 Kg.
	= 33.0 lbs.	
	= 15.0 Kgm.	

Weight of the AOS spectrometer: 1 to 2 Kgm.

Current plan is for the Radio Astromomy Group at Meudon, France to provide the flight AOS.

Figure A16 Weight estimated for MSAR.

SUMMARY OF POWER REQUIREMENTS FOR CASSINI MICROWAVE INSTRUMENT

Power Consumption for 2cm Radiometer with Calibration System	7.76 W
---	--------

Power Consumption for 3mm Radiometer with Phaselock and Calibration Systems	18.55 W
--	---------

Power Consumption for 2mm Radiometer with Phaselock and Calibration Systems	17.55 W
--	---------

Power Consumption for 2mm and 3mm Radiometers with Phaselock and Calibration Systems	31.55 W
---	---------

Estimated power for the French AOS	5 W
------------------------------------	-----

Total Power Consumption for 2cm, 3mm, and 2mm Radiometers with Phaselock and Calibration Systems	39.31 W
---	---------

Current plan is to operate the instrument with only a single system "on" at a time.
Last listed mode on for ground testing.

Figure A17 Power estimates for MSAR.

APPENDIX B CIRS BACKGROUND INFORMATION AND FIGURES

PRECEDING PAGE BLANK NOT FILMED

CIRS INSTRUMENT PARAMETERS

TELESCOPE DIAMETER (CM): 50

INTERFEROMETERS:

	<u>FAR-IR</u>	<u>MD-IR</u>
TYPE:	polarizing	michelson
SPECTRAL RANGE (cm^{-1}):	10-700	700-1400
SPECTRAL RESOL (cm^{-1}):	.50	.50
INTEG TIME (sec):	25	25

FOCAL PLANES:

	<u>#1</u>	<u>#2</u>	<u>#3</u>
SPECTRAL RANGE (cm^{-1})	10-700	700-1200	1200-1400
DETECTORS:	Thermopile (1×5)	HgCdTe (1×43)	HgCdTe (1×43)
PIXEL F-O-V (mrad):	4.3×12.9	.1×.3	.1×.3
PIXEL AΩ (cm^2sr):	1.1×10 ⁻¹	6.1×10 ⁻⁵	6.1×10 ⁻⁵
NEP ($\text{W Hz}^{-1/2}$):	2×10 ⁻¹¹	8×10 ⁻¹⁴	2×10 ⁻¹⁴
NESR ($\text{W cm}^{-2} \text{sr}^{-1}/\text{cm}^{-1}$):	7×10 ⁻¹⁰	5×10 ⁻⁹	1×10 ⁻⁹
DATA BAND (Hz):	.8-56	56-96	96-106
TEMPERATURE (K):	170	90	90

INSTRUMENT TEMPERATURE (K): ~ 170

Figure B1 CIRS Instrument Parameters.

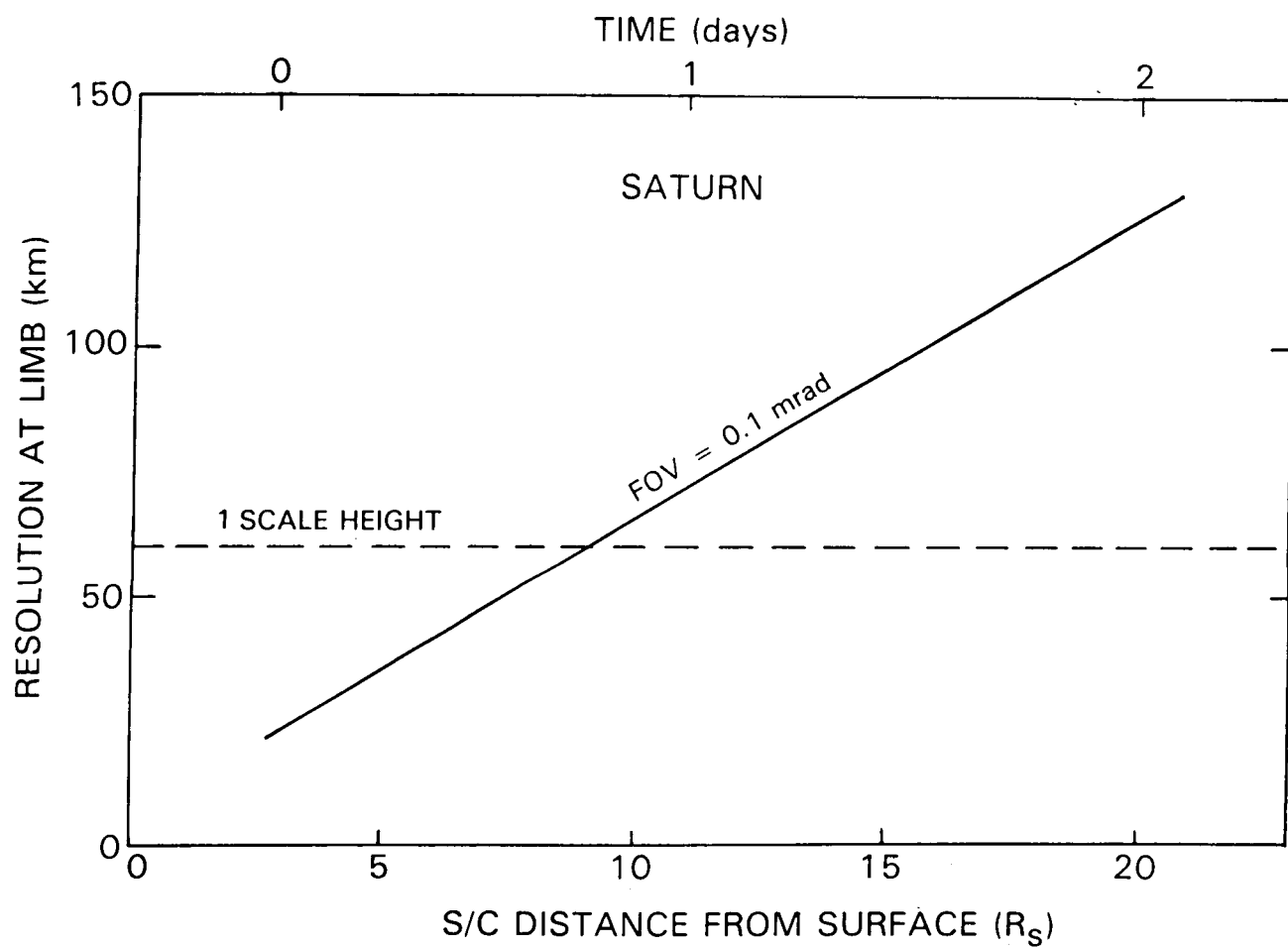


Figure B2 Saturn limb geometry.

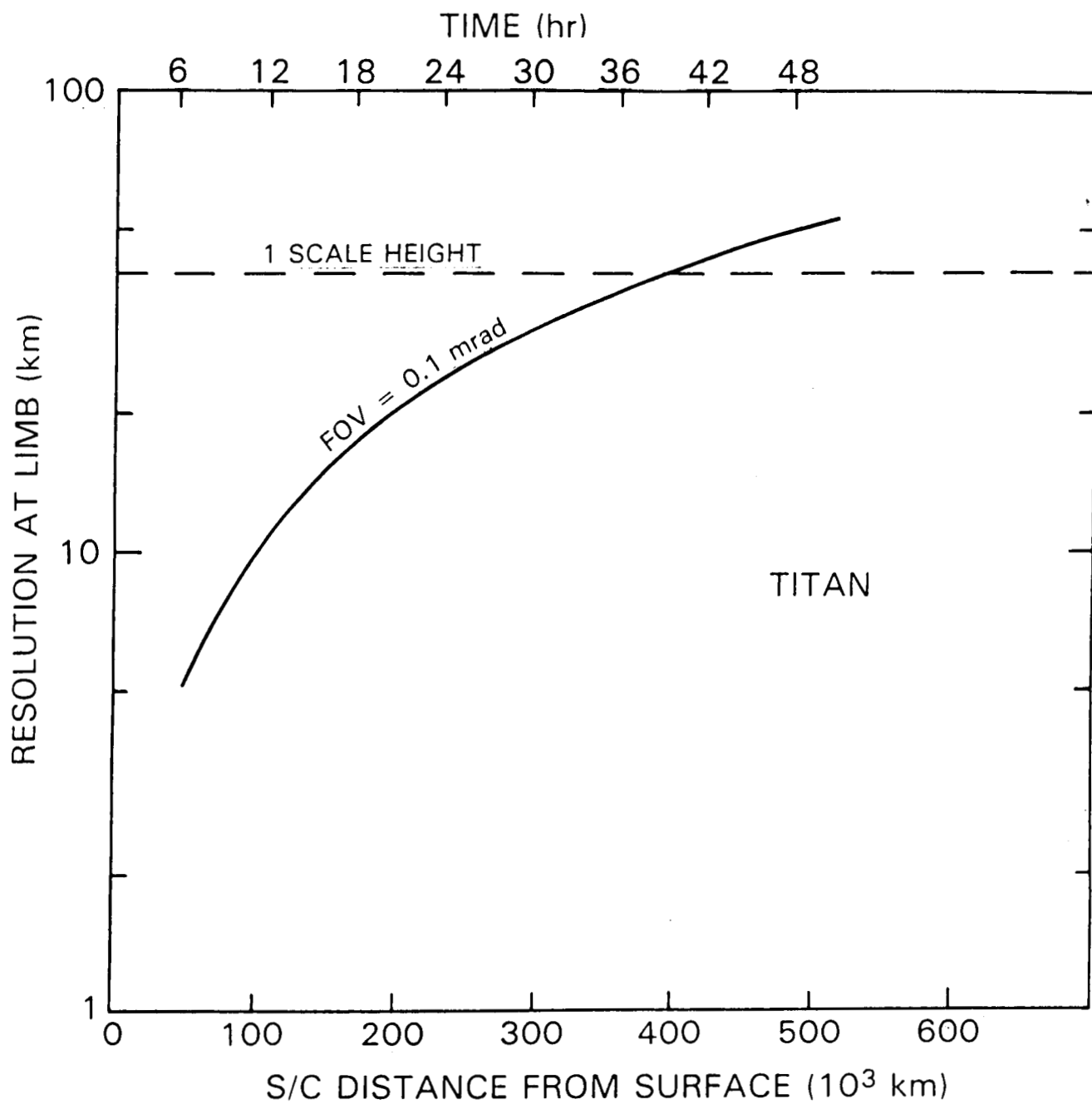


Figure B3 Titan limb geometry.

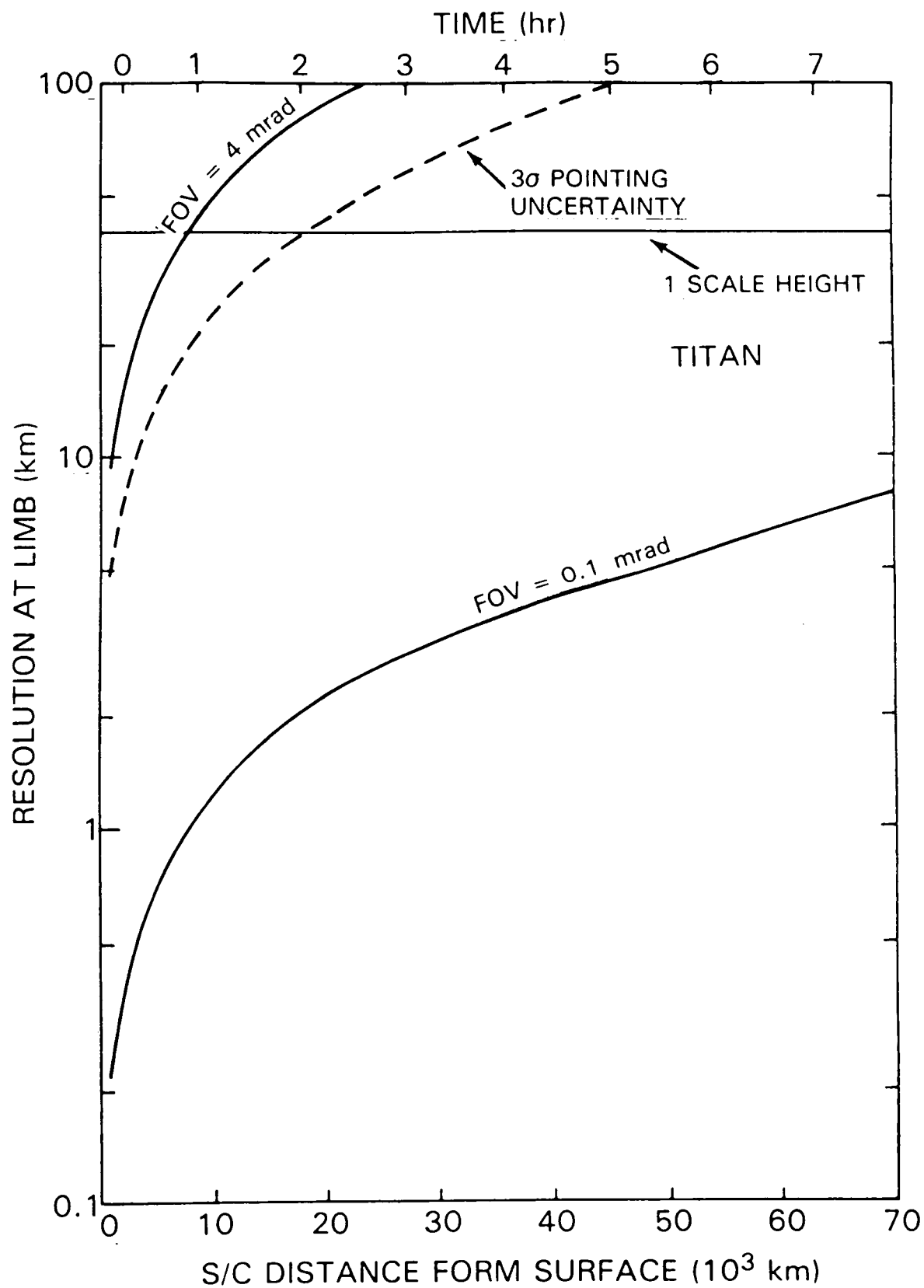
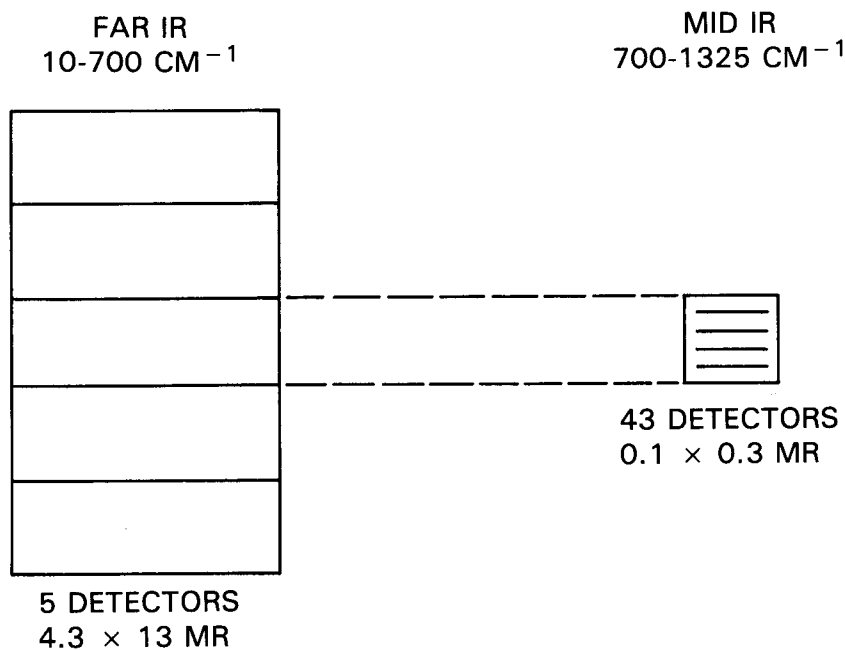


Figure B4 Titan limb geometry and scan platform pointing uncertainty.

CIRS FIELDS OF VIEW



CIRS OBSERVATIONAL MODES

	<u>LIMB 1</u>	<u>LIMB 2</u>	<u>NADIR</u>
VERTICAL RES.	≤ 1 H	≤ 1 H	0.5 to 2.5 H
TIME:			
TITAN	±0 to 0.5 hr	±10 to 20 hr	±0.5 to 10 hr
SATURN	NA	±0 to 20 hr	1 to 60 days
SPECTRAL RES.	0.5 cm ⁻¹	20 cm ⁻¹	0.5 cm ⁻¹
FAR IR	5 DETS.	0 DETS	1 OF 5 DETS.
MID IR	AVG.	20 OF 43	AVG.
BIT RATE	3.02 KBIT/S	0.50 KBIT/S	1.01 KBIT/S

Figure B5 CIRS observational modes.

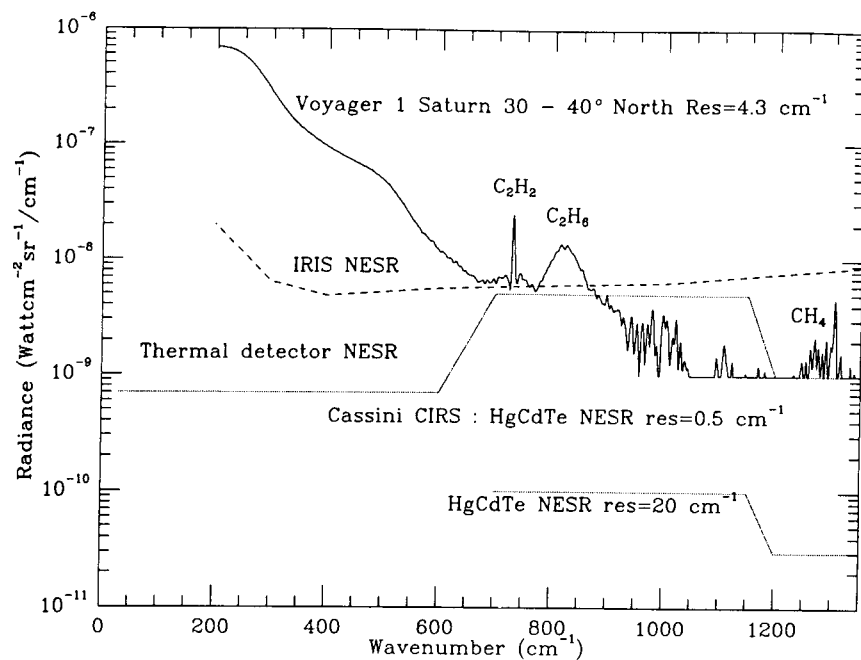


Figure B6 CIRS sensitivity for Saturn.

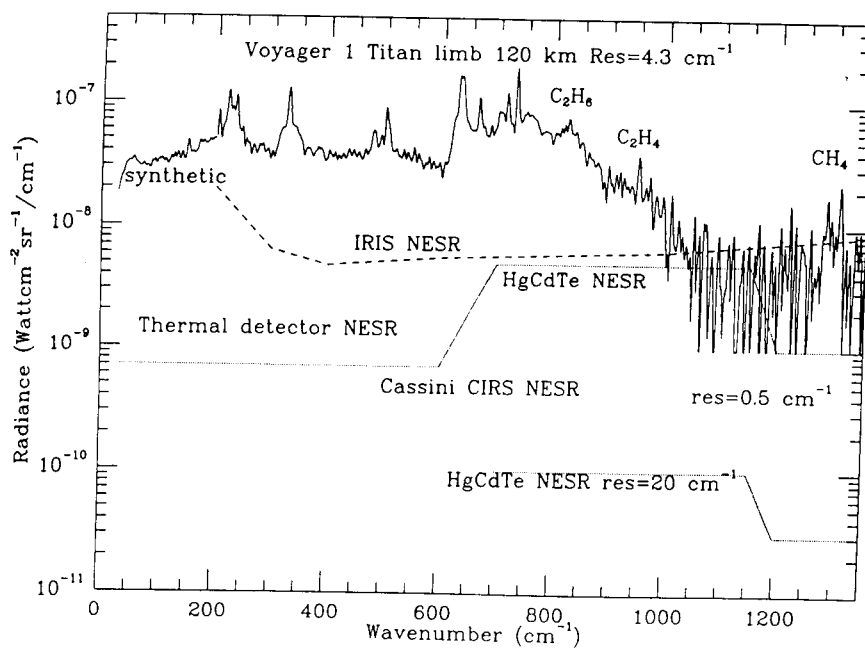


Figure B7 CIRS sensitivity for Titan.

POLARIZING FTS (CIRS)

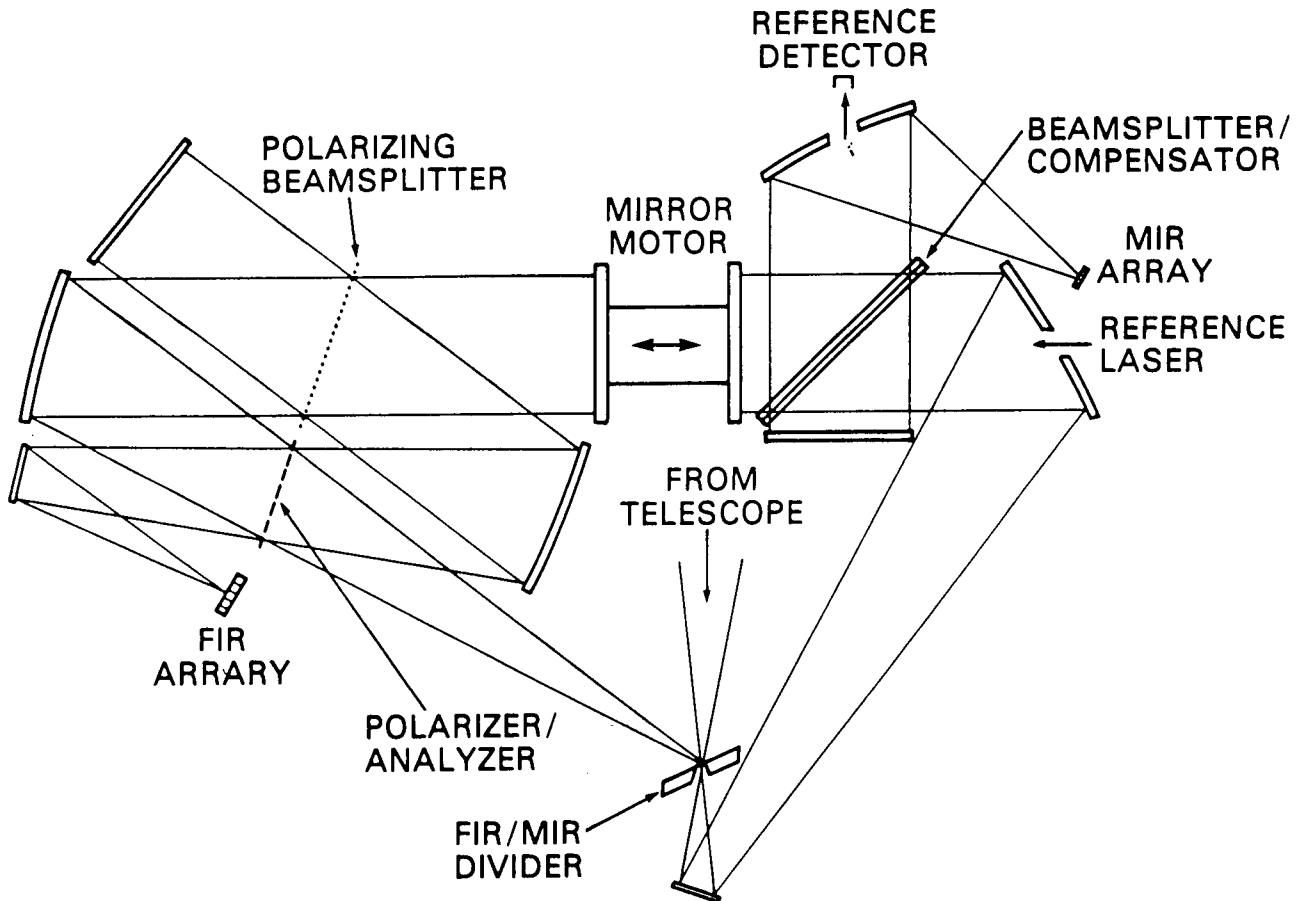


Figure B8 Optical schematic for CIRS.

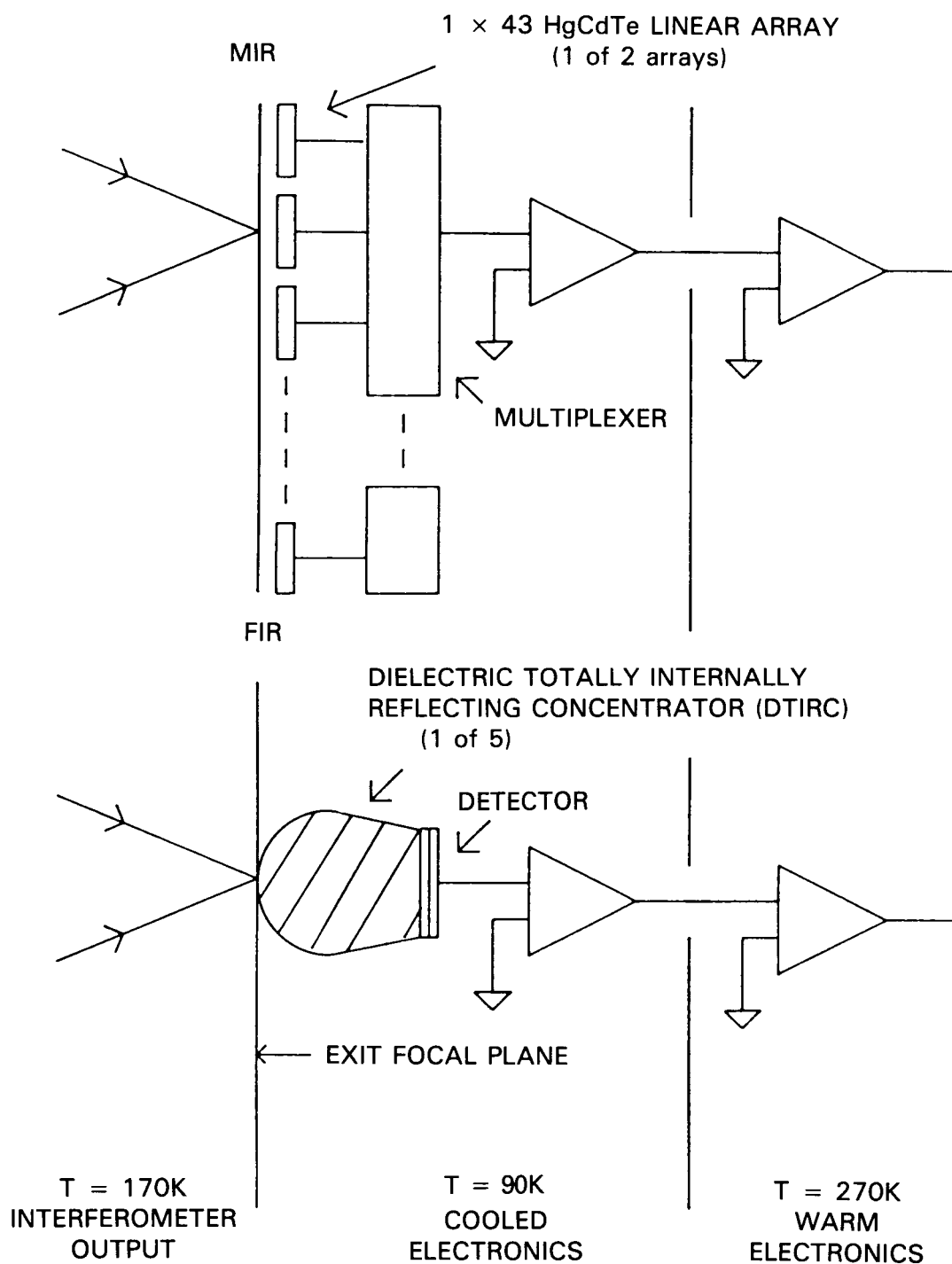
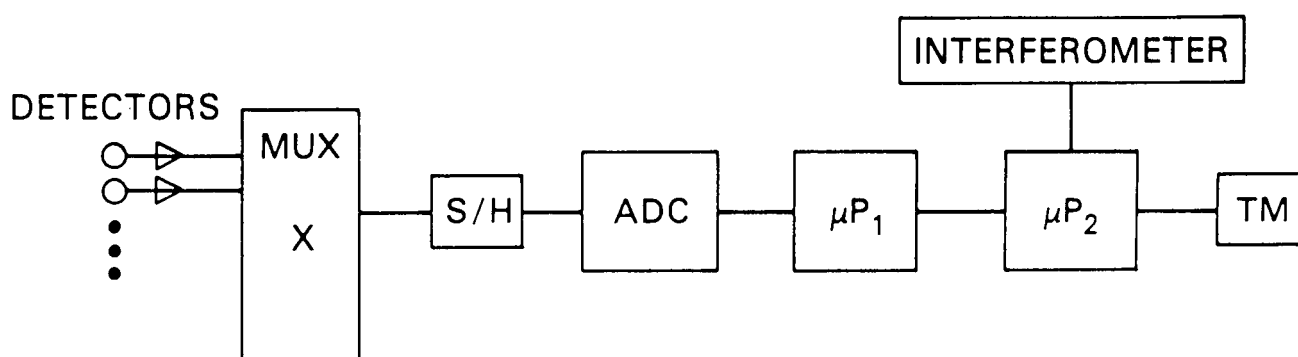


Figure B9 Focal plane layout for CIRS.



μP_1 — DATA AQUISITION, CO-ADD, FILTER, COMBINE

μP_2 — DATA COMPRESSION FOR TM, INTERFEROMETER
CONTROL AND MONITOR

Figure B10 Signal processing schematic for CIRS.

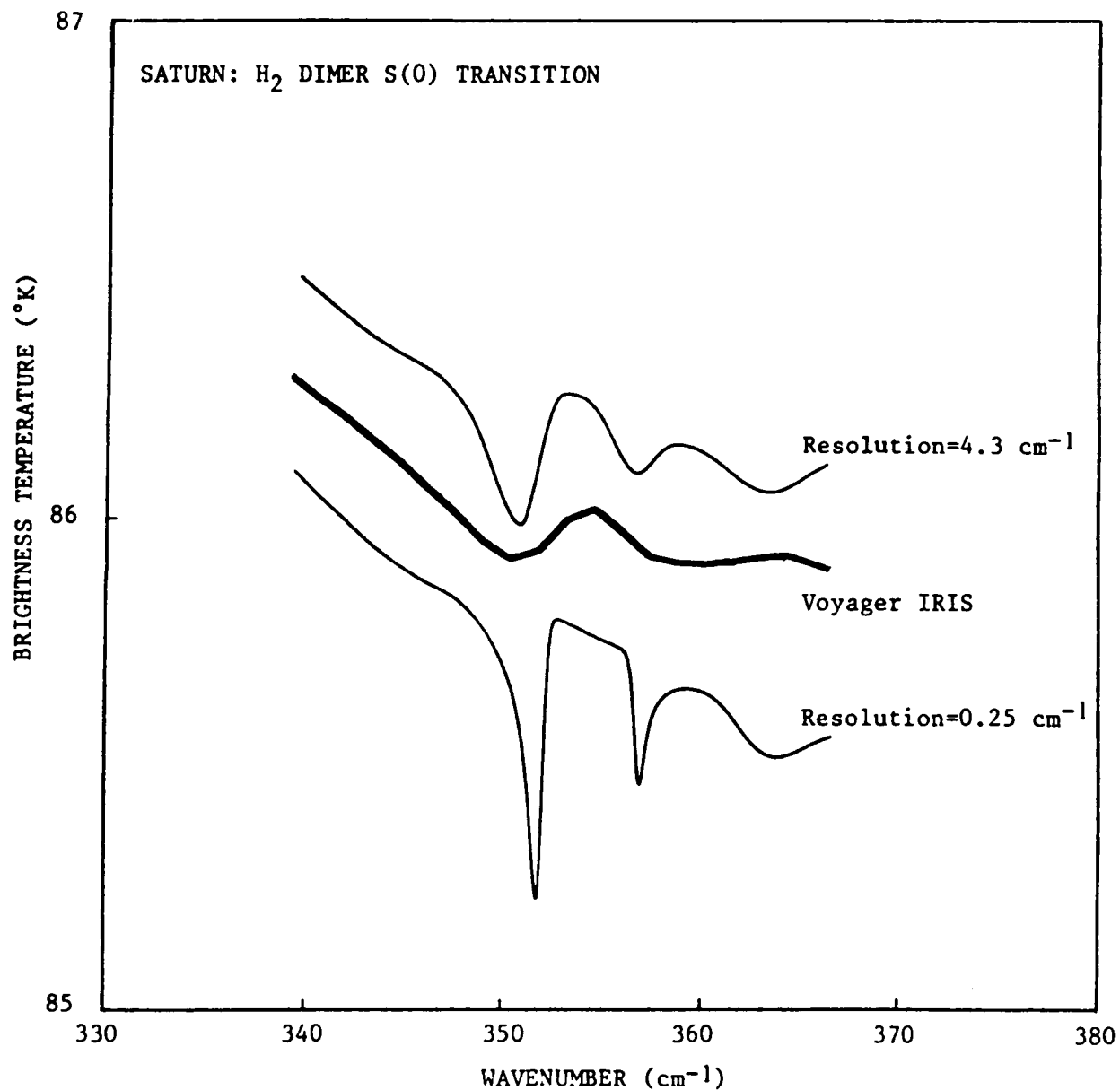


Figure B11 Brightness temperature spectrum in the S(O) rotation line of H₂ showing the fine structure due to the H₂ dimer transitions, at resolutions of 4.3 cm⁻¹ (Voyager IRIS) and 0.25 cm⁻¹ (synthetic spectra have been offset arbitrarily with respect to the observed one).

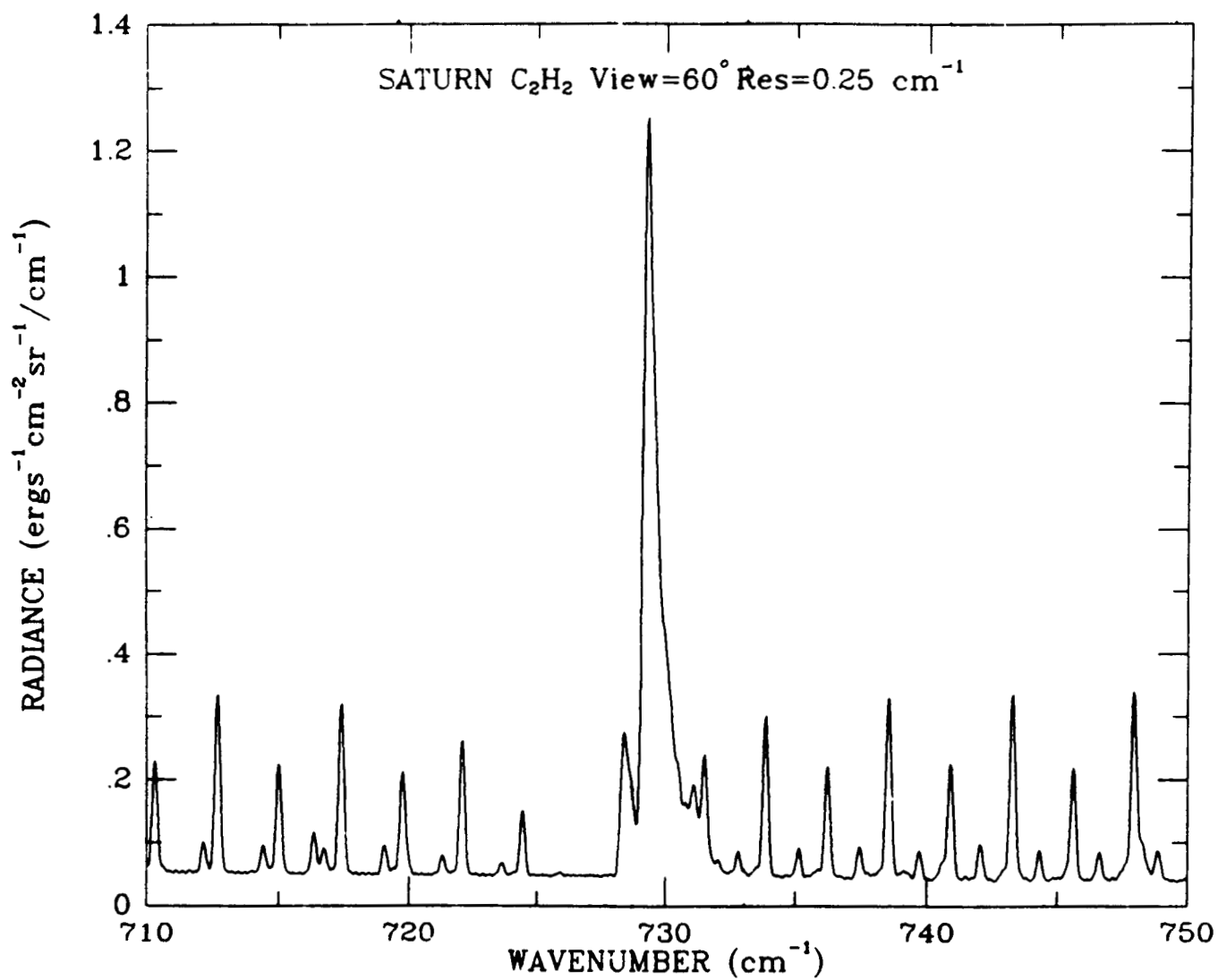


Figure B12 Nadir radiance spectrum for ν_5 band of C₂H₂.

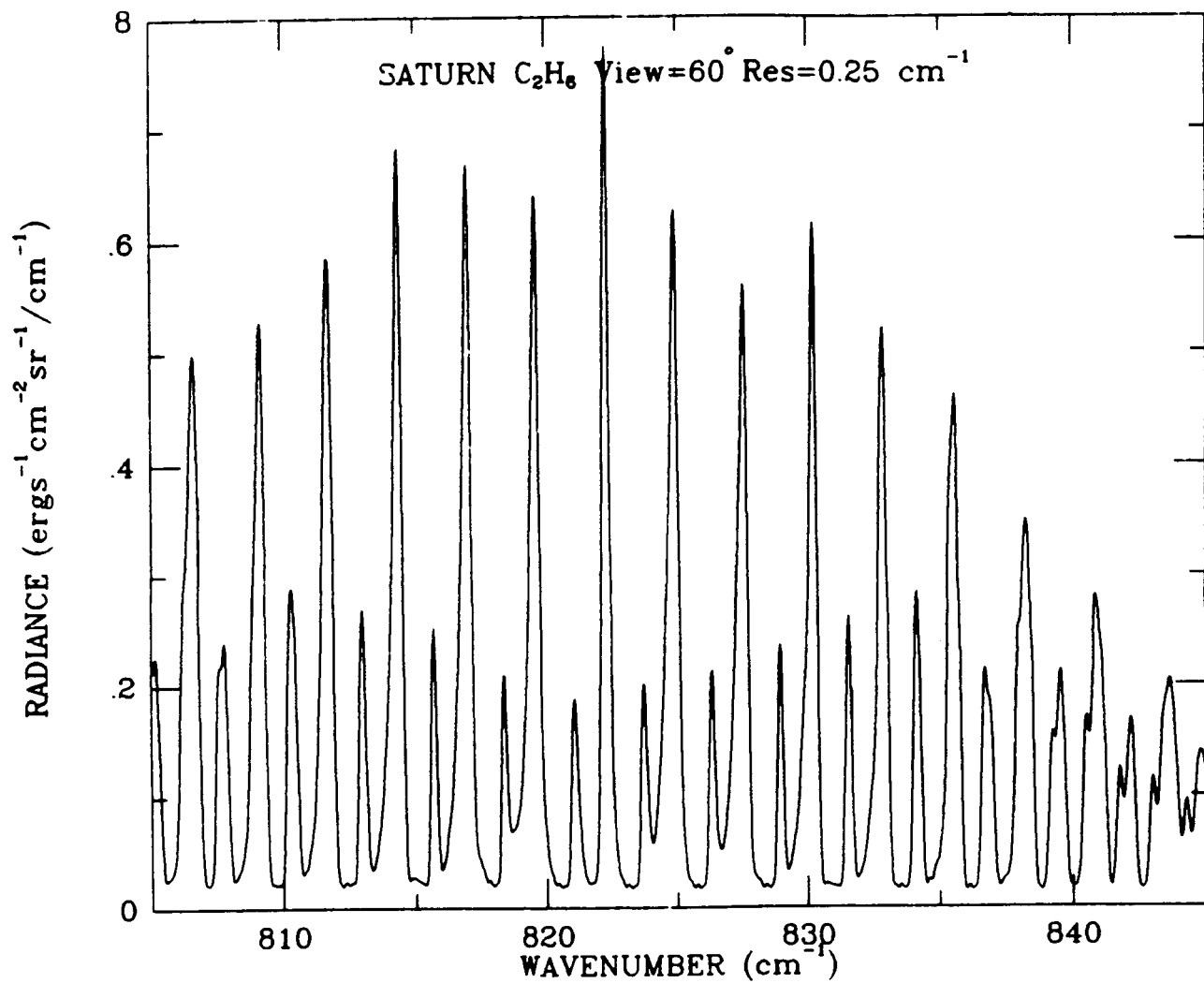


Figure B13 Nadir spectrum for ν_9 band of C₂H₆.

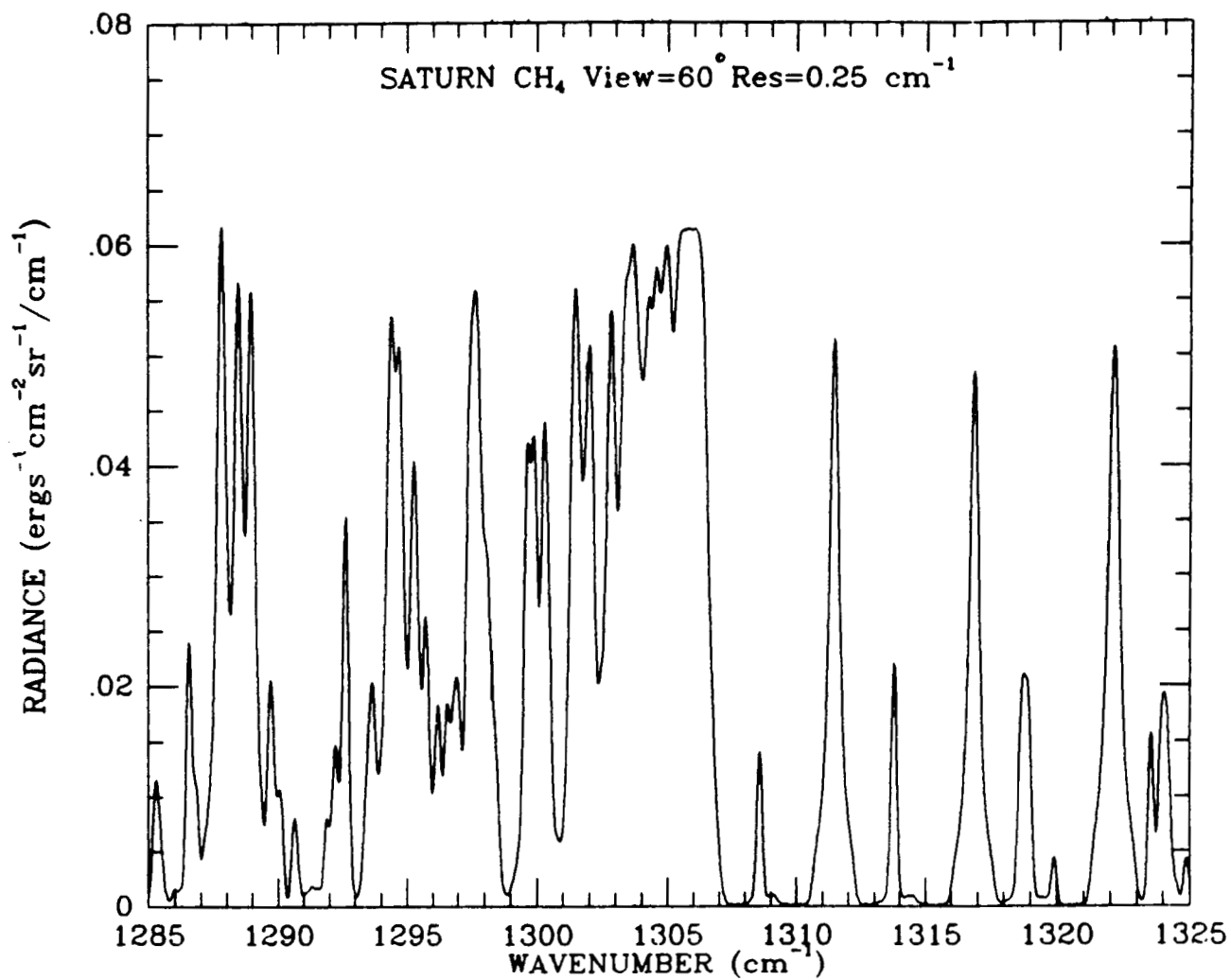


Figure B14 Nadir radiance spectrum for ν_4 band of CH₄.

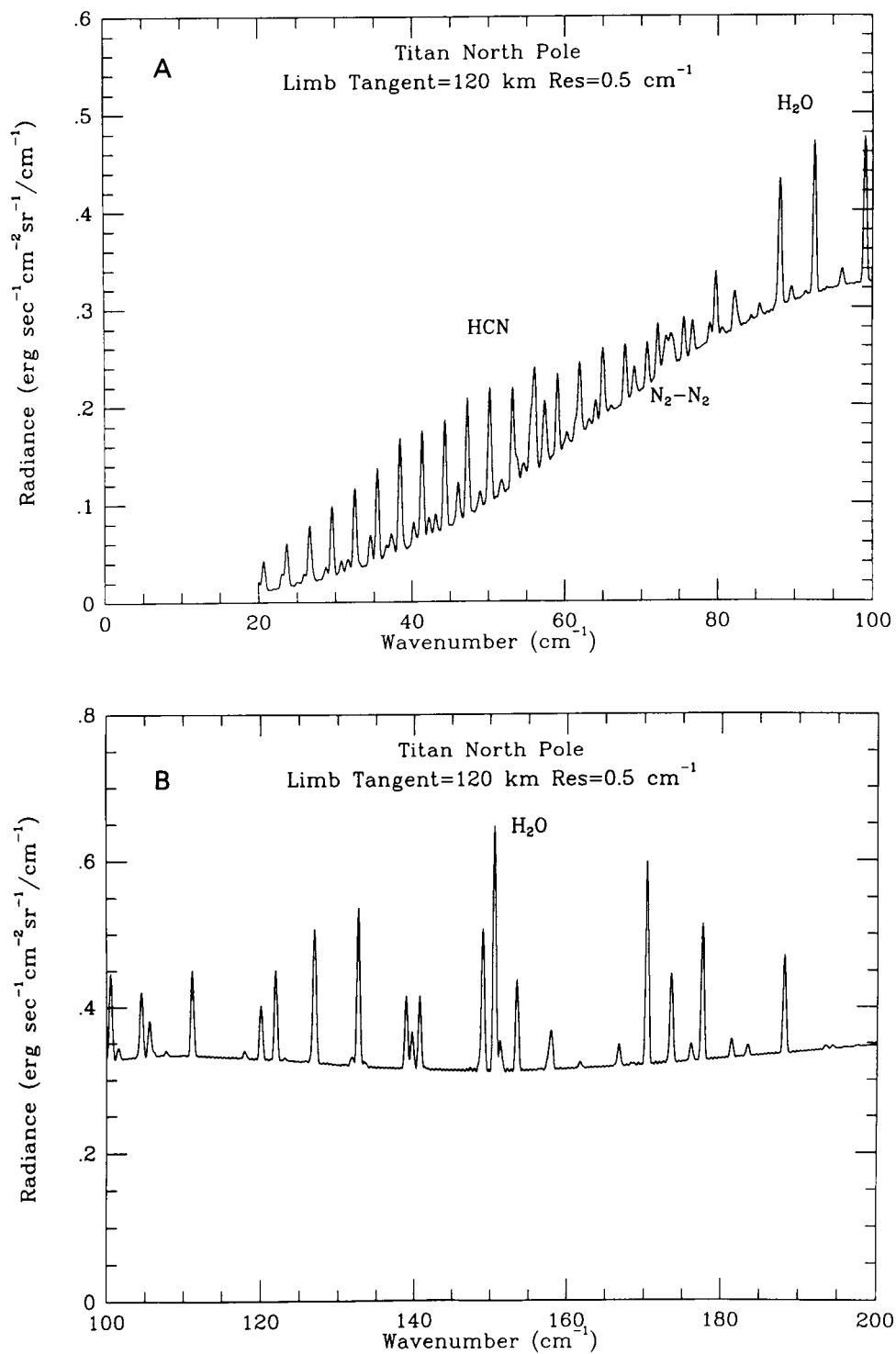


Figure B15 Titan limb spectrum for tangent height of 120 km.

ORIGINAL PAGE IS
OF POOR QUALITY

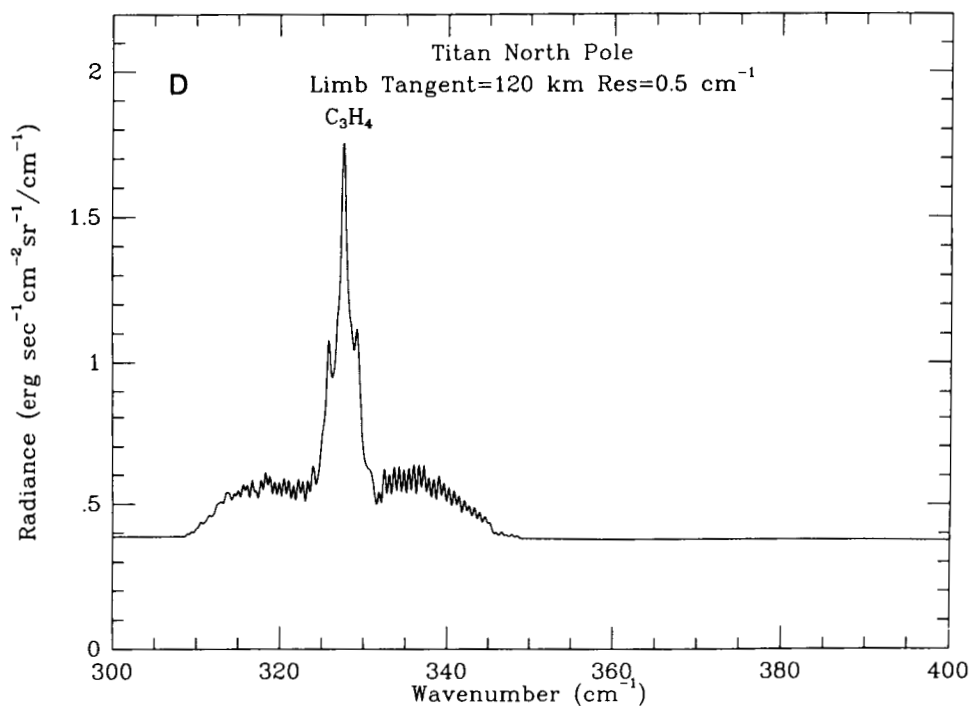
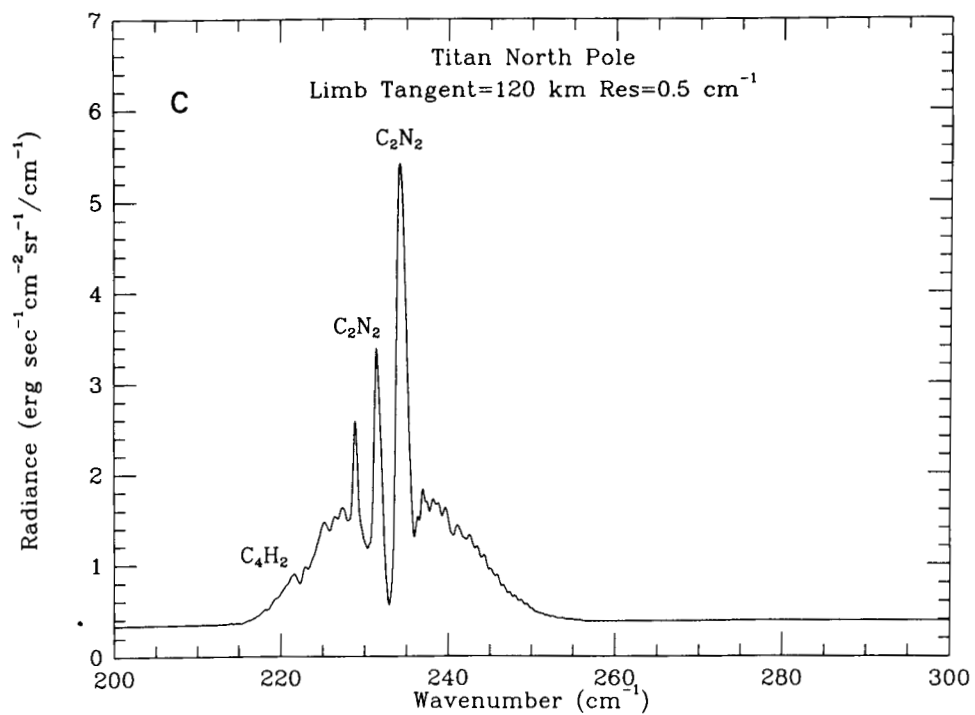


Figure B15 (Continued).

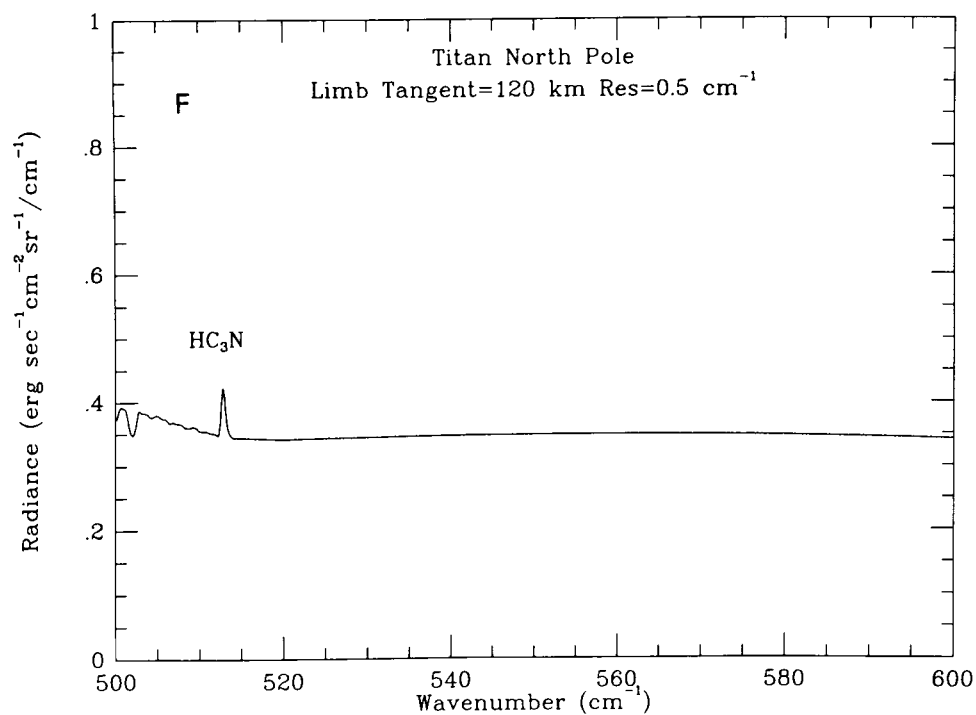
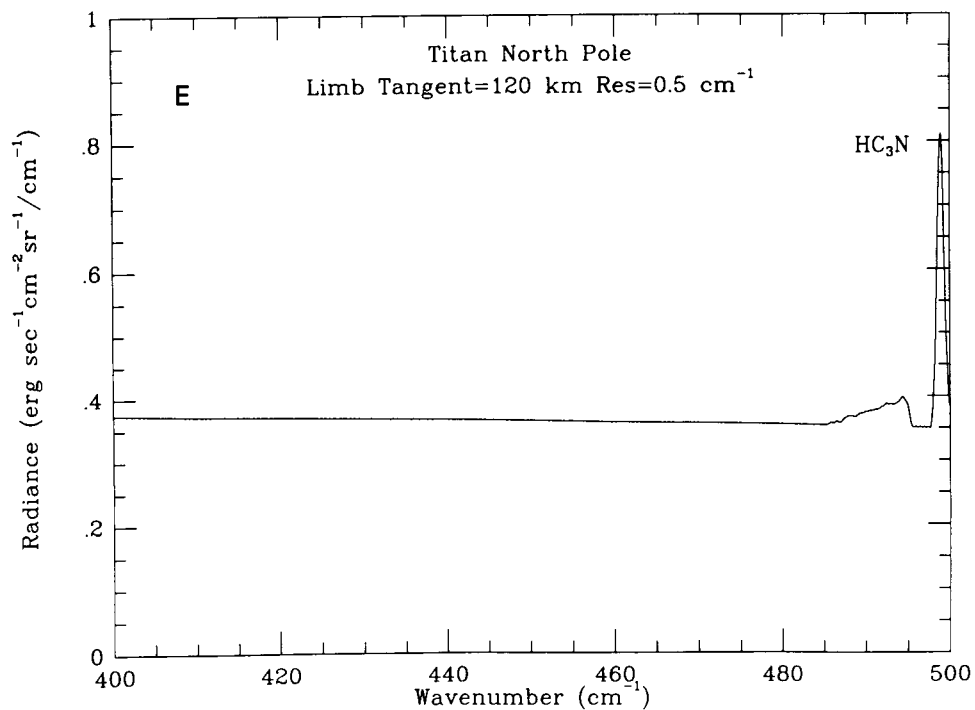


Figure B15 (Continued).

ORIGINAL PAGE IS
OF POOR QUALITY

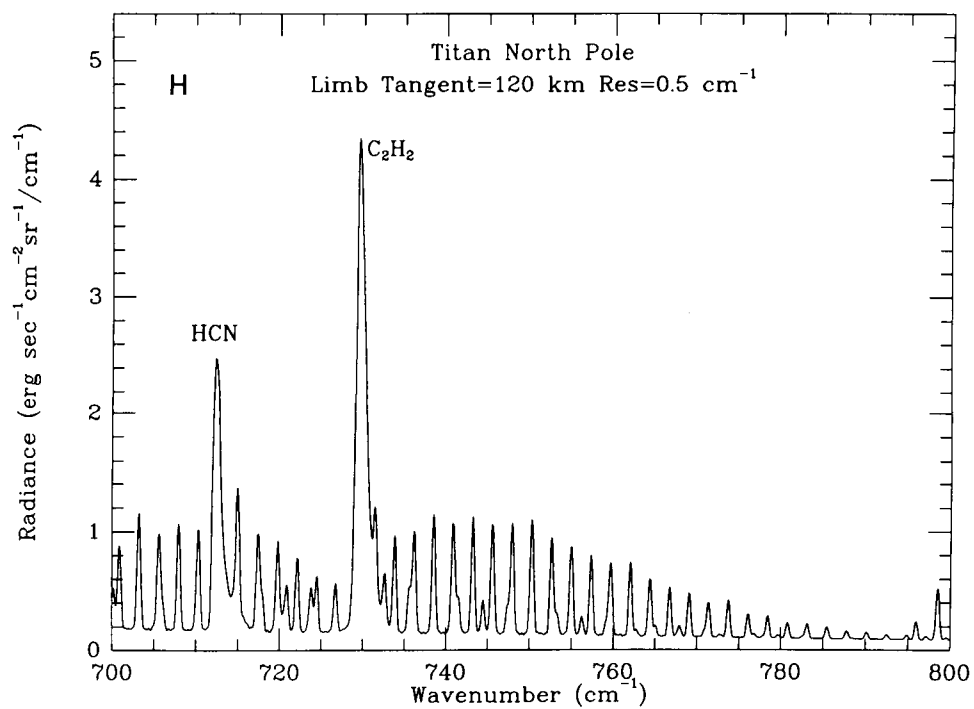
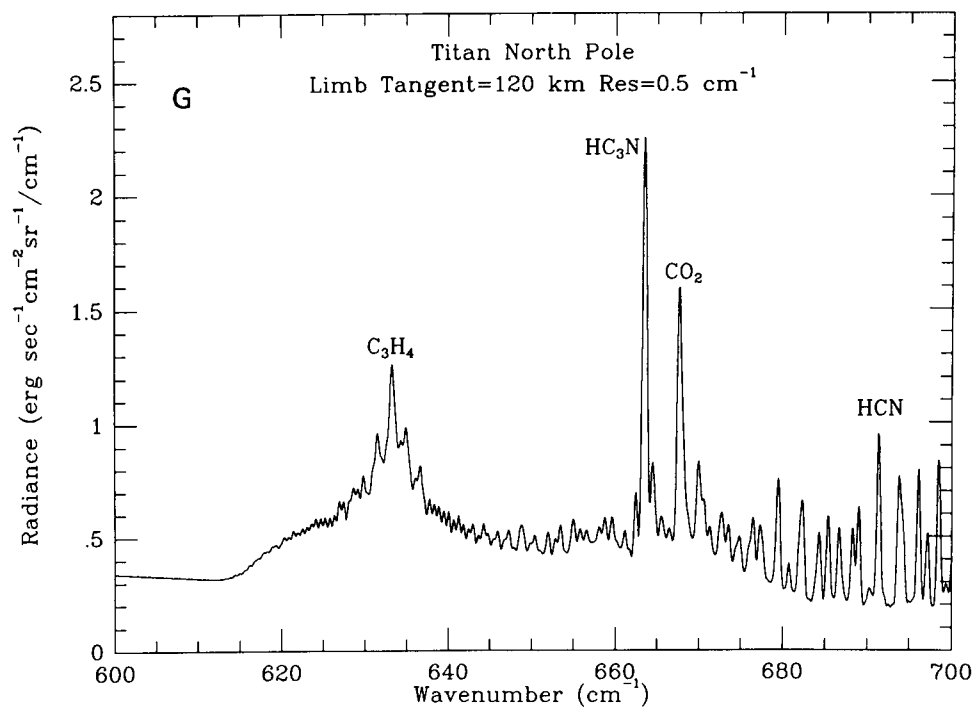


Figure B15 (Continued).

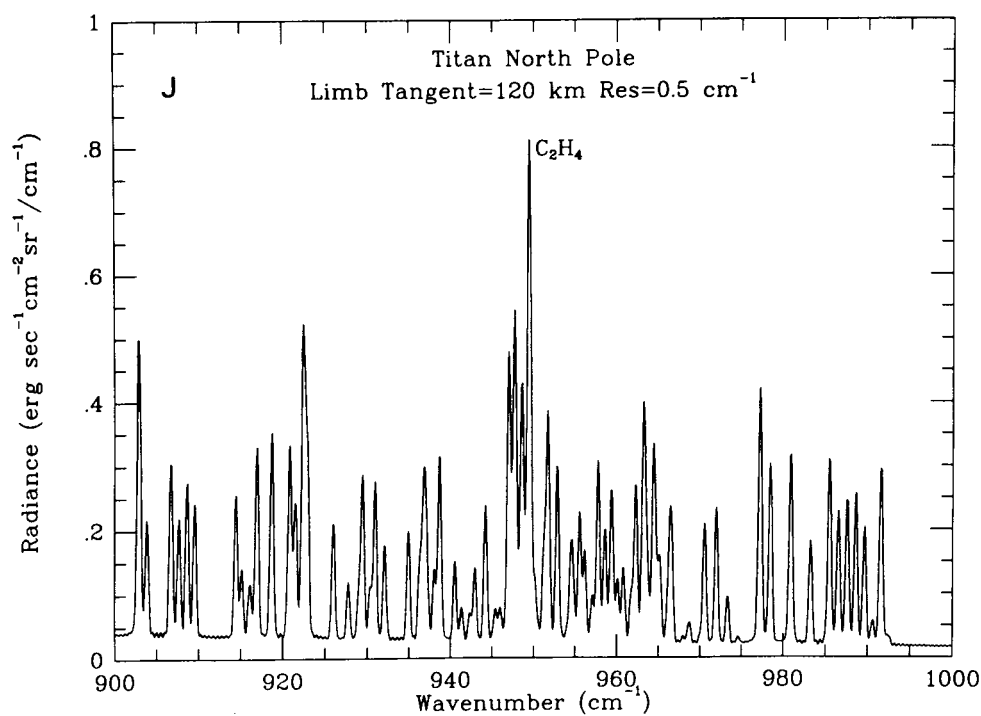
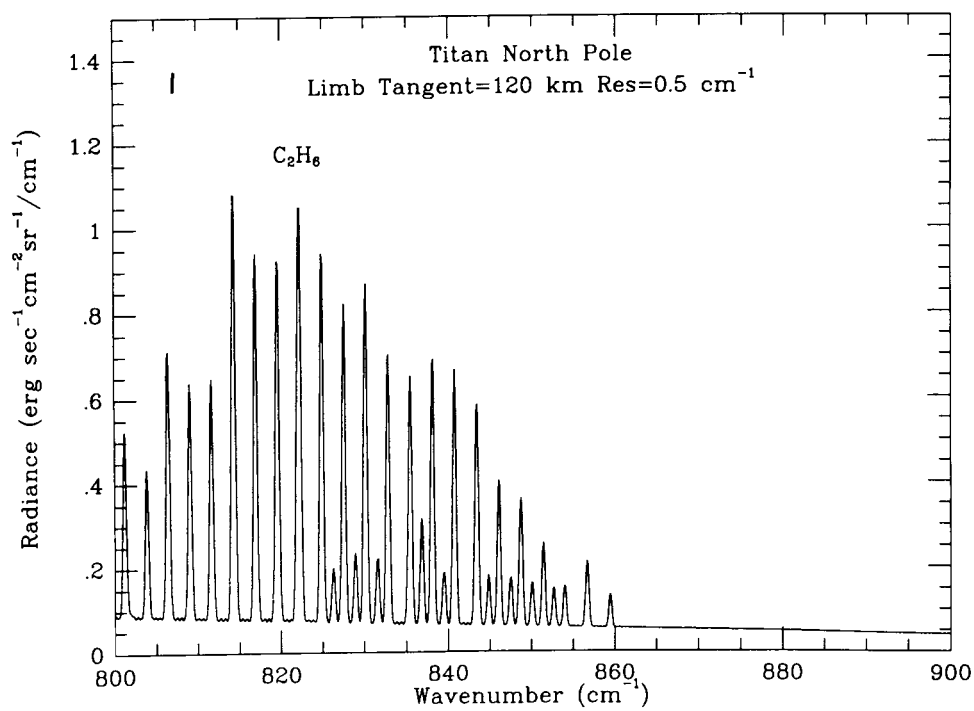


Figure B15 (Continued).

ORIGINAL PAGE IS
OF POOR QUALITY

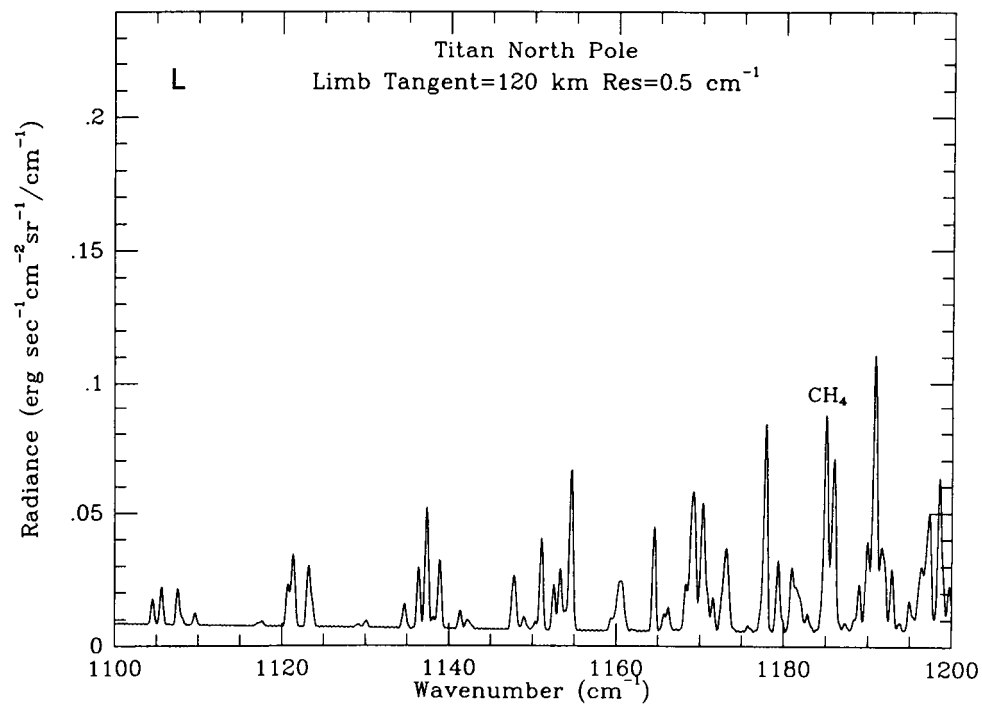
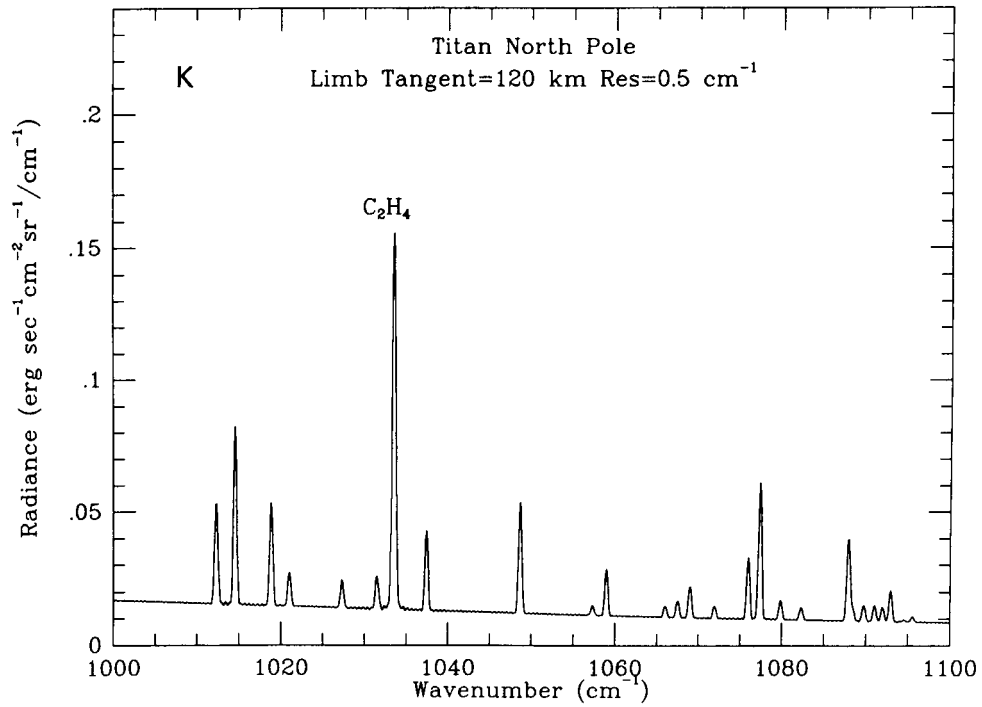


Figure B15 (Continued).

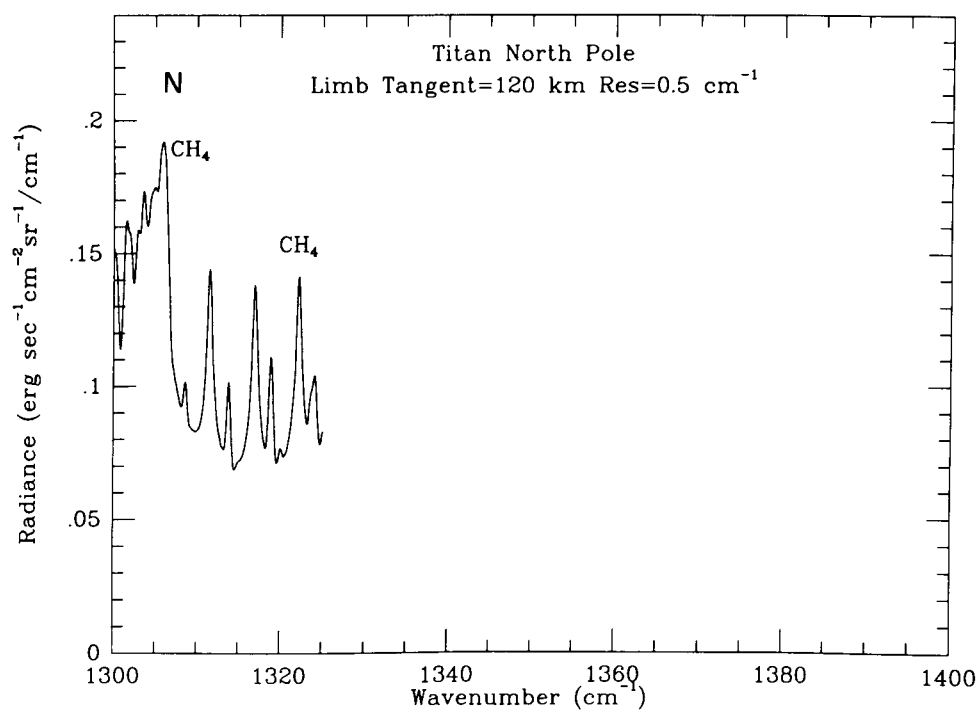
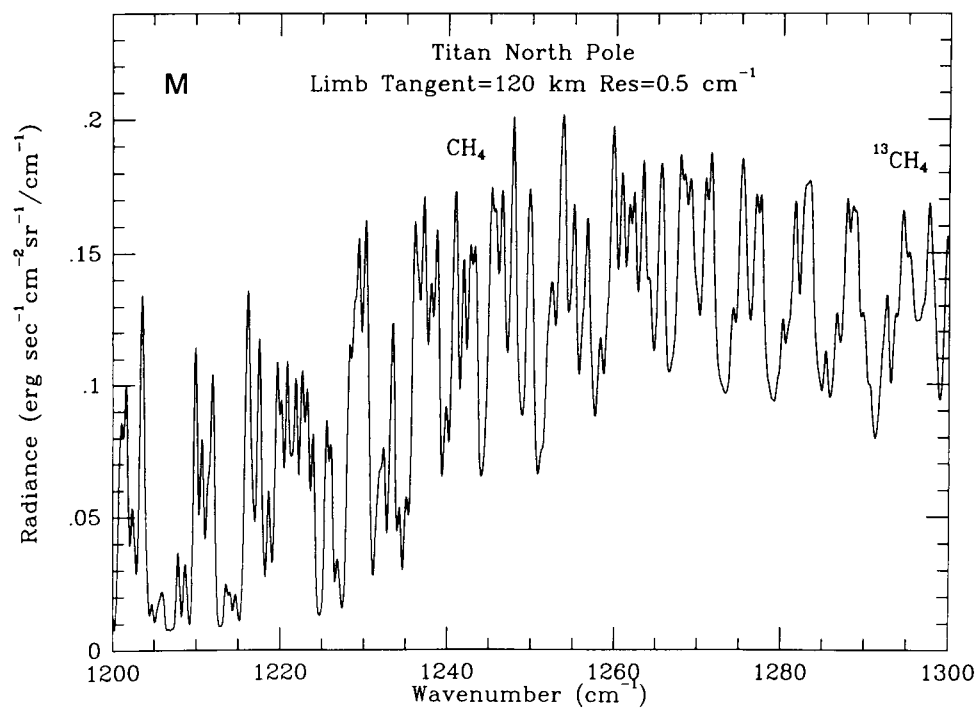


Figure B15 (Continued).

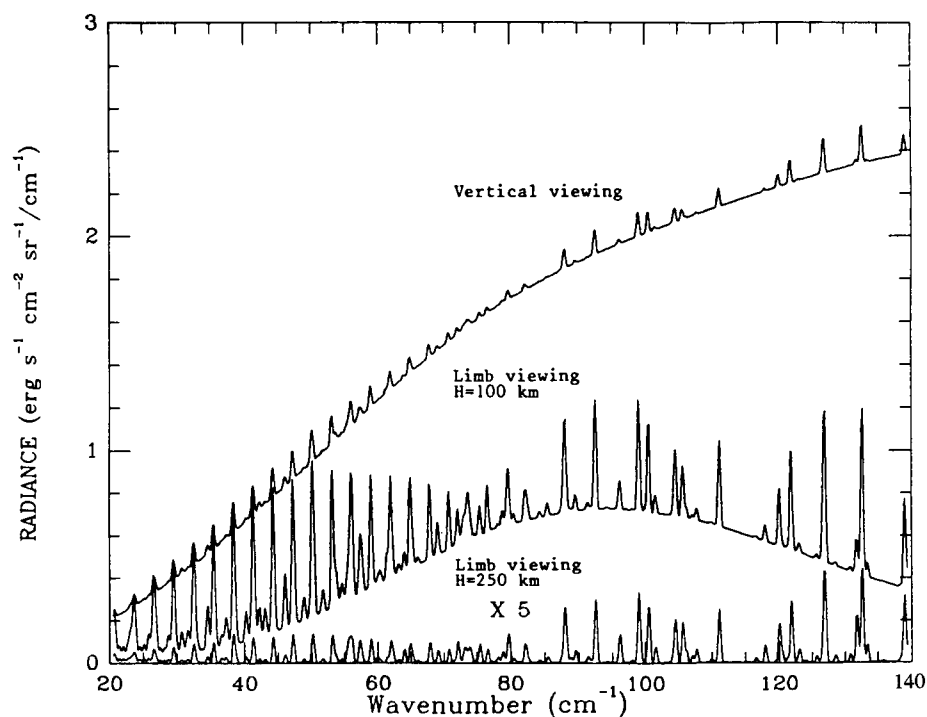


Figure B16. Titan radiance spectra showing emission lines due to HCN and CO, and their isotopes.

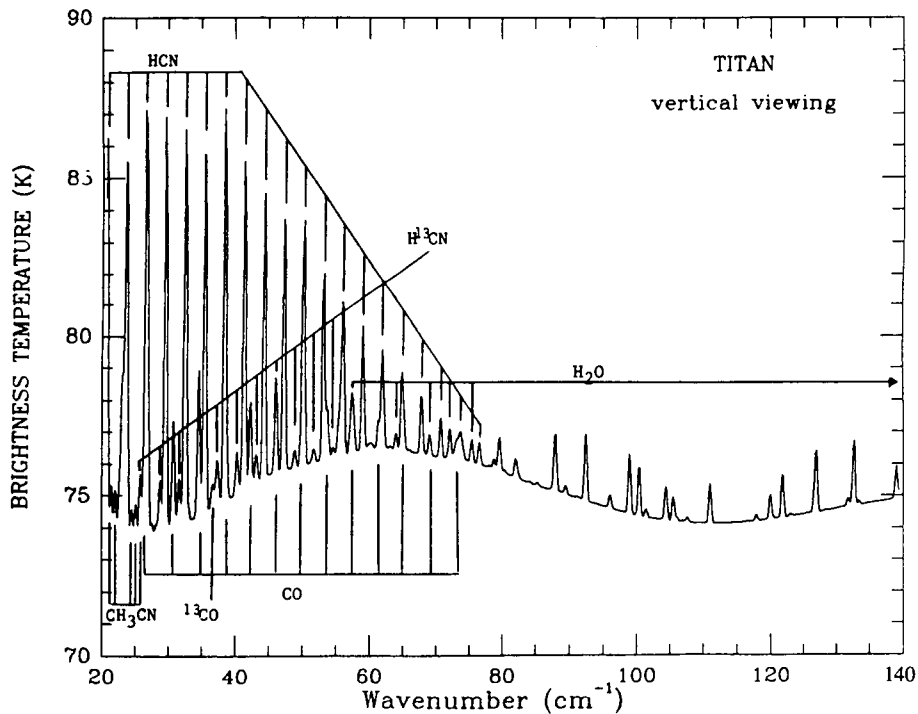


Figure B17 Titan nadir radiance spectrum.

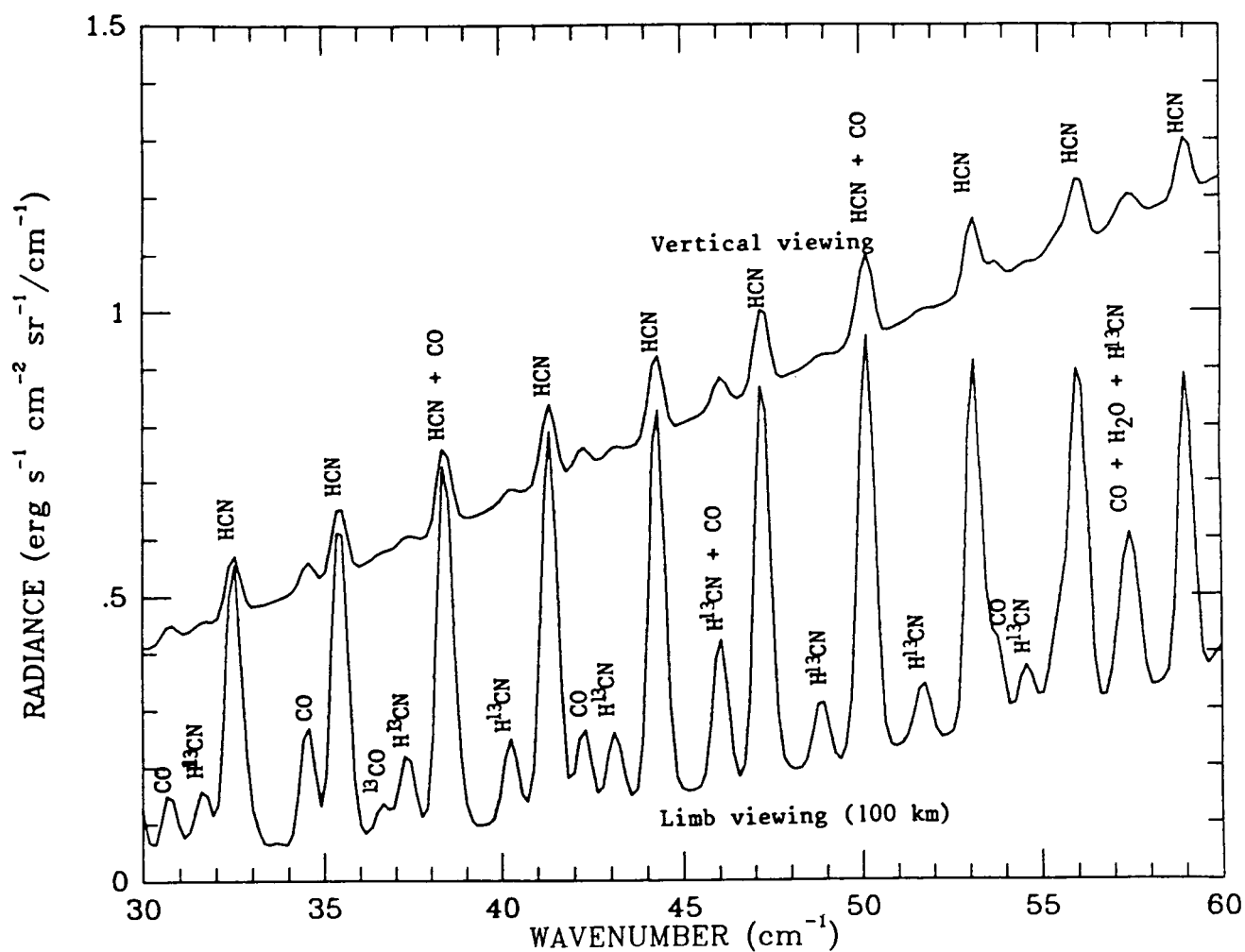


Figure B18 Titan HCN and CO emission lines.

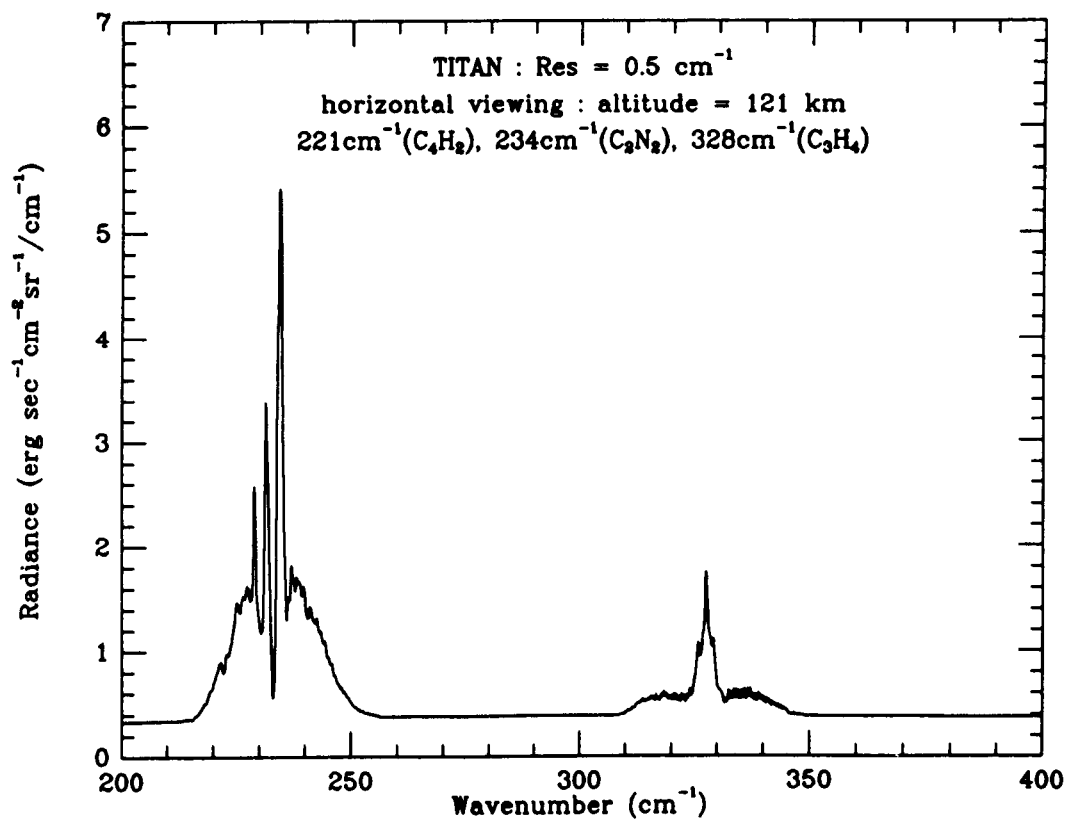
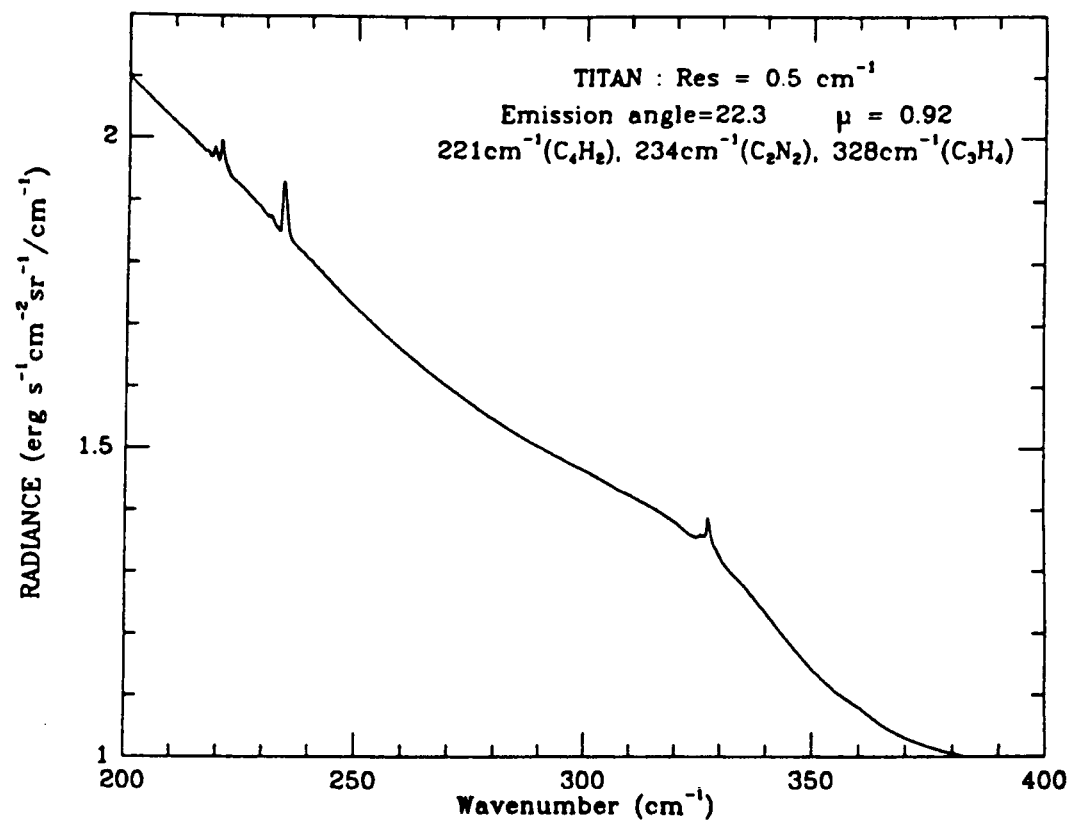


Figure B19 Titan radiance spectra.

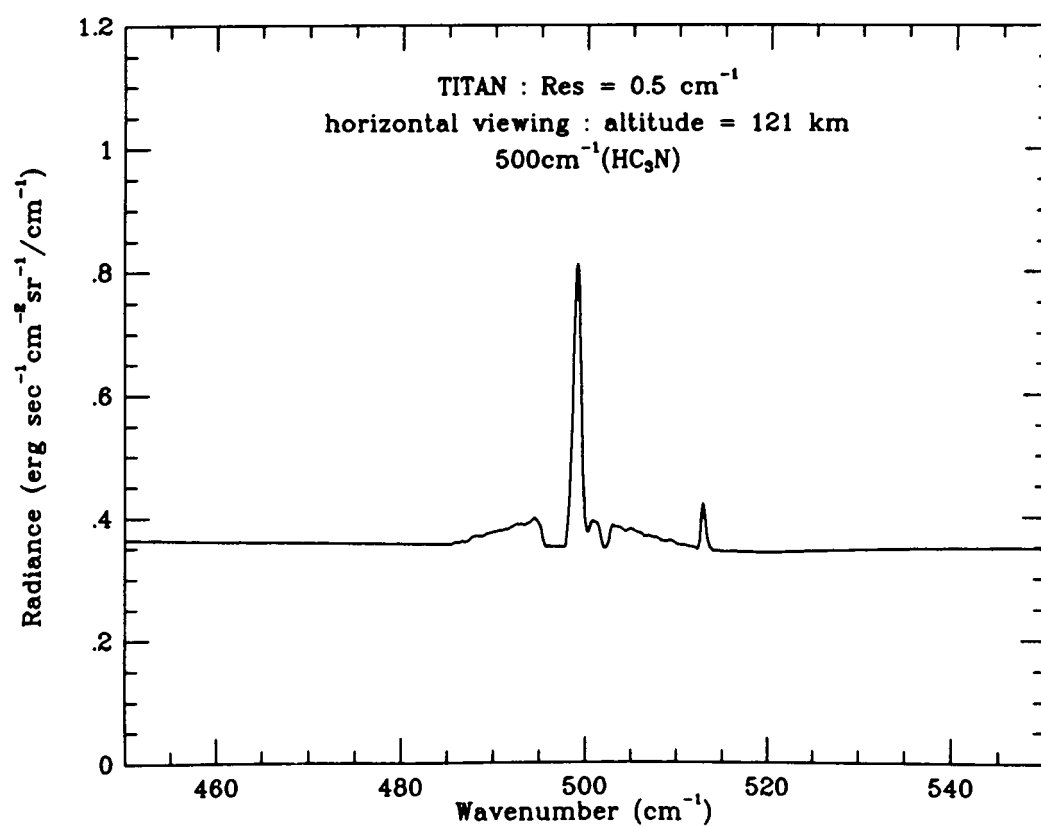
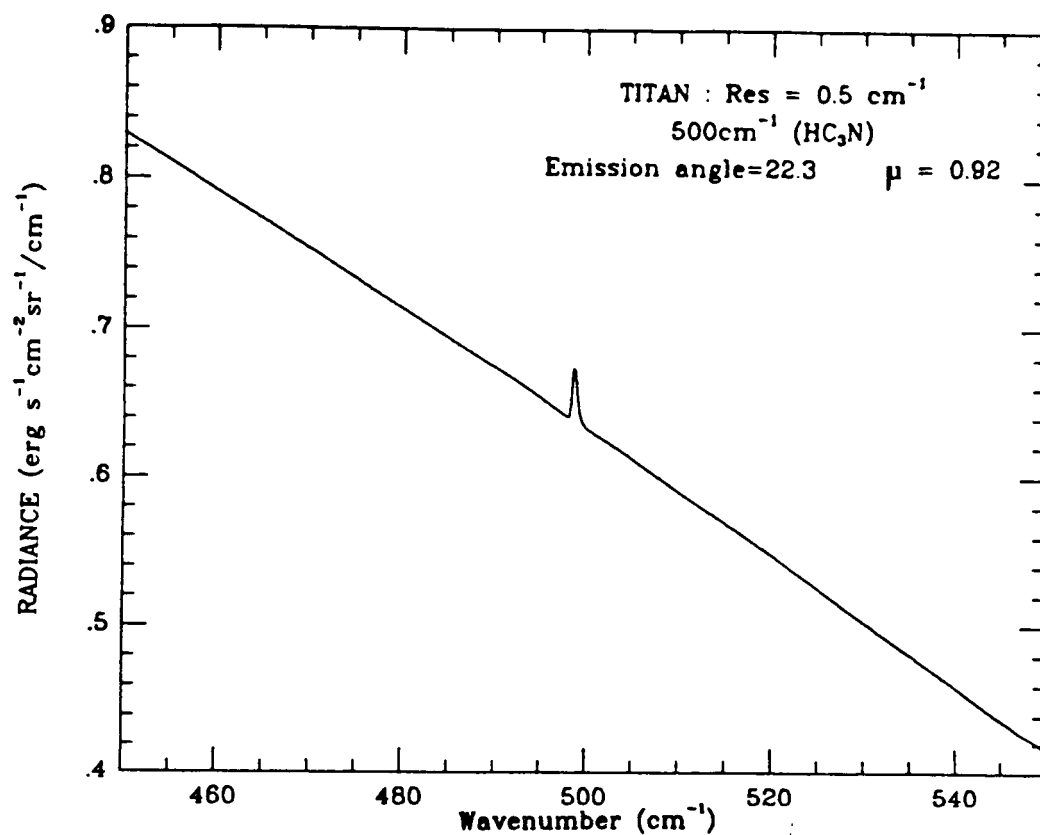


Figure B20 Titan radiance spectra.

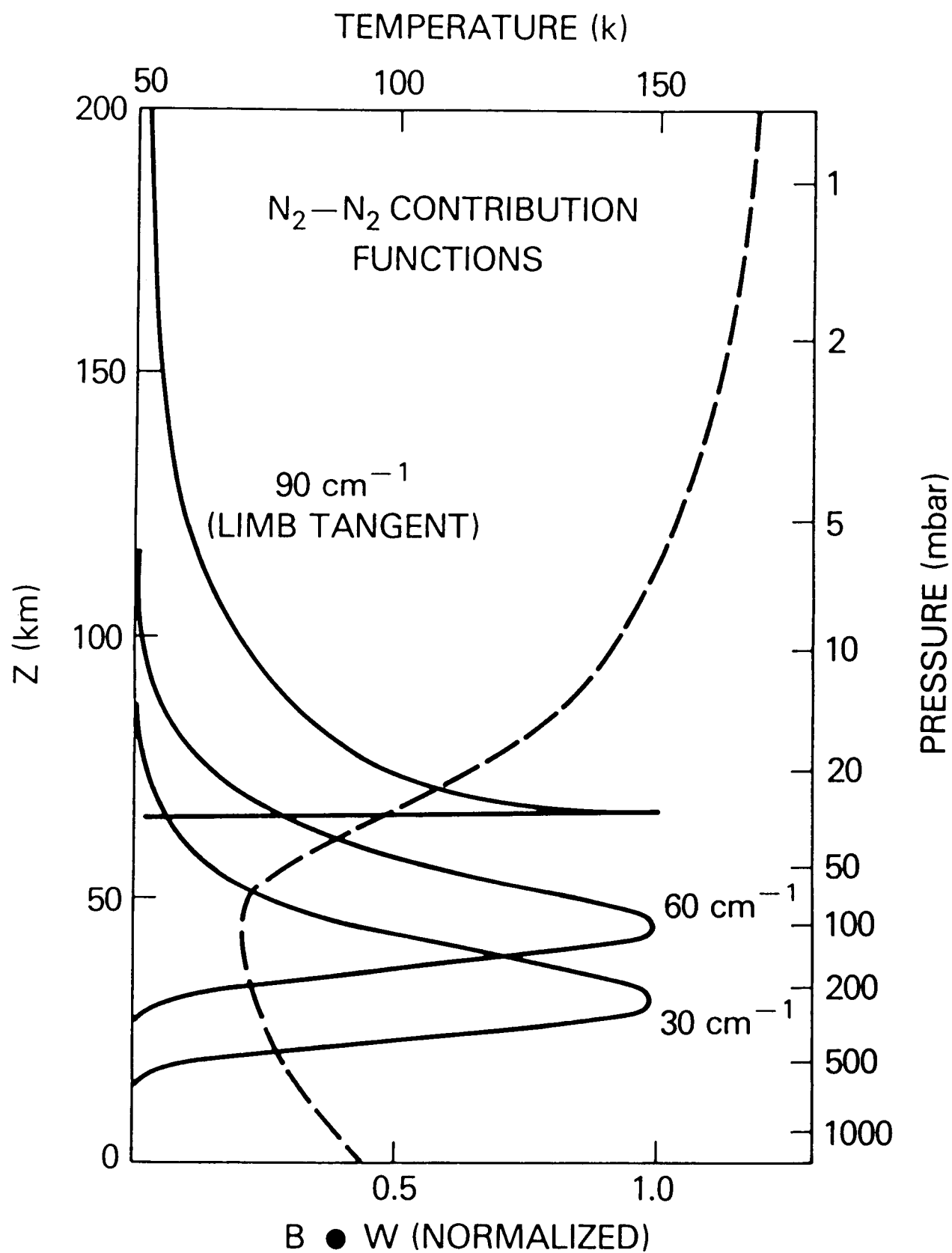


Figure B21 Titan N_2-N_2 contribution functions.

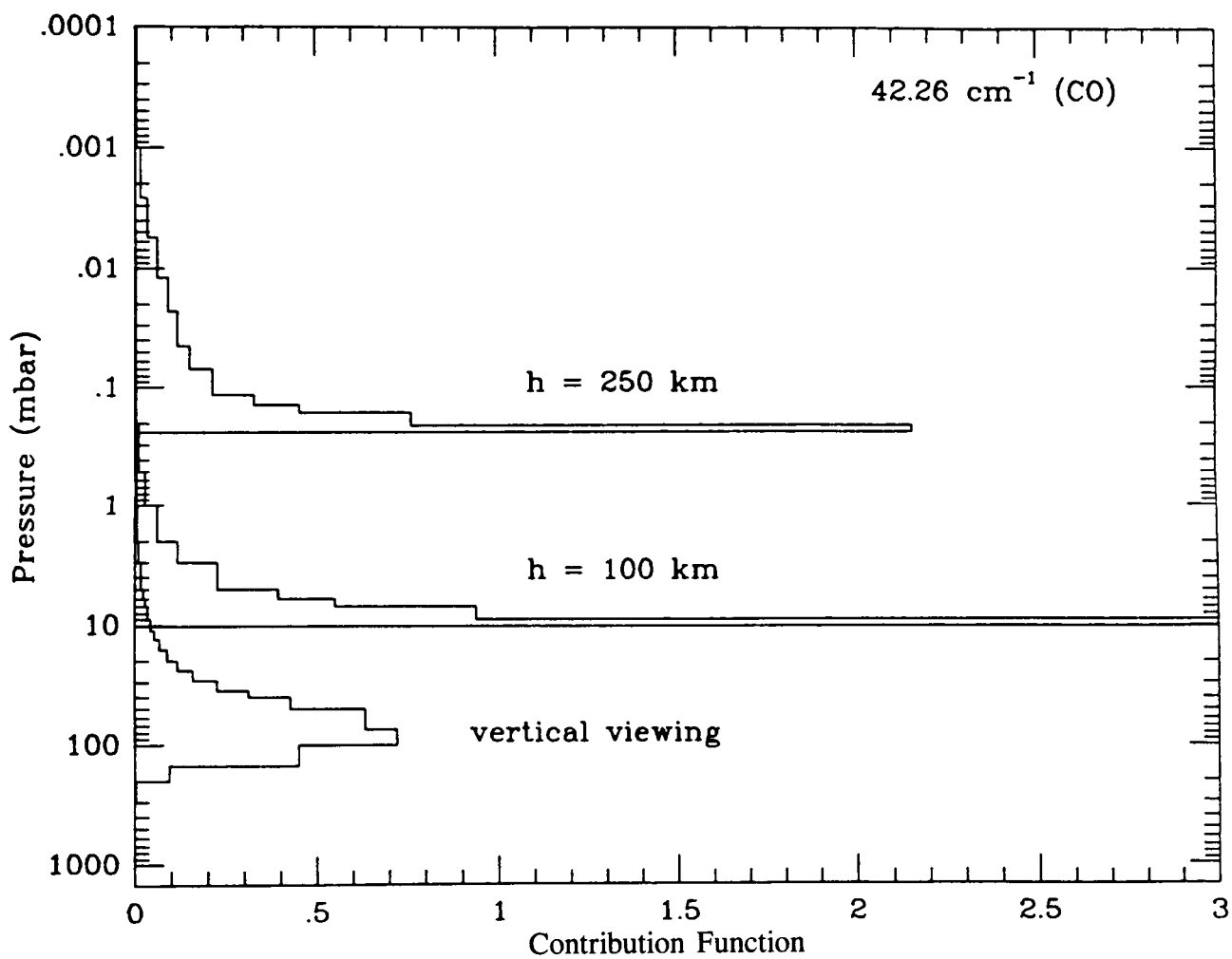


Figure B22 Titan CO contribution function.

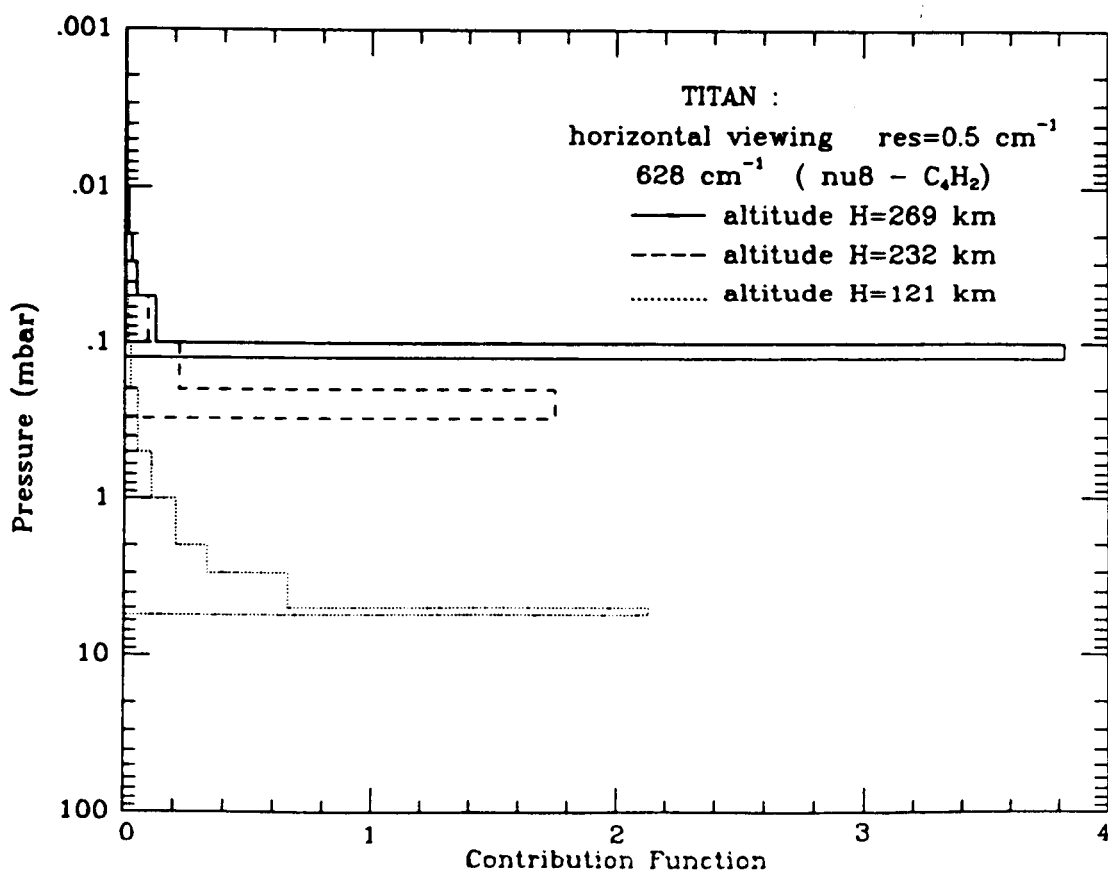
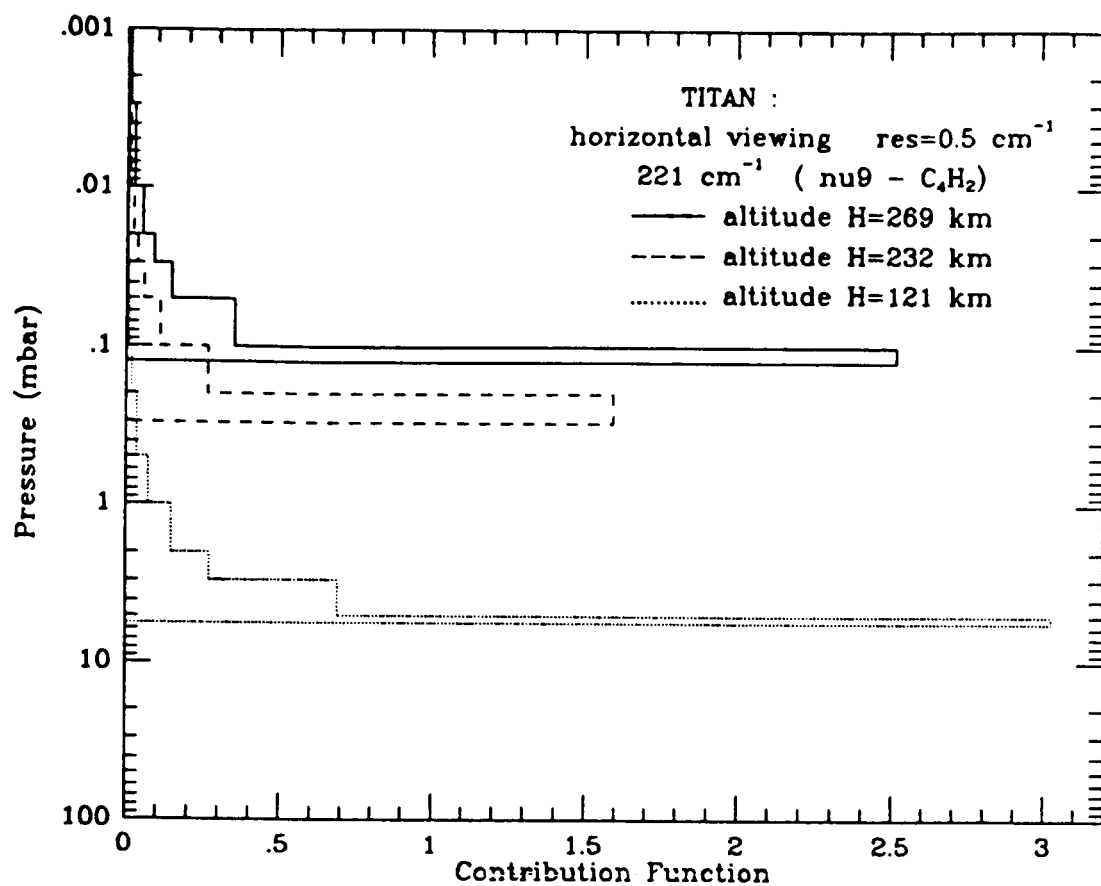


Figure B23 Titan C₄H₂ contribution functions.

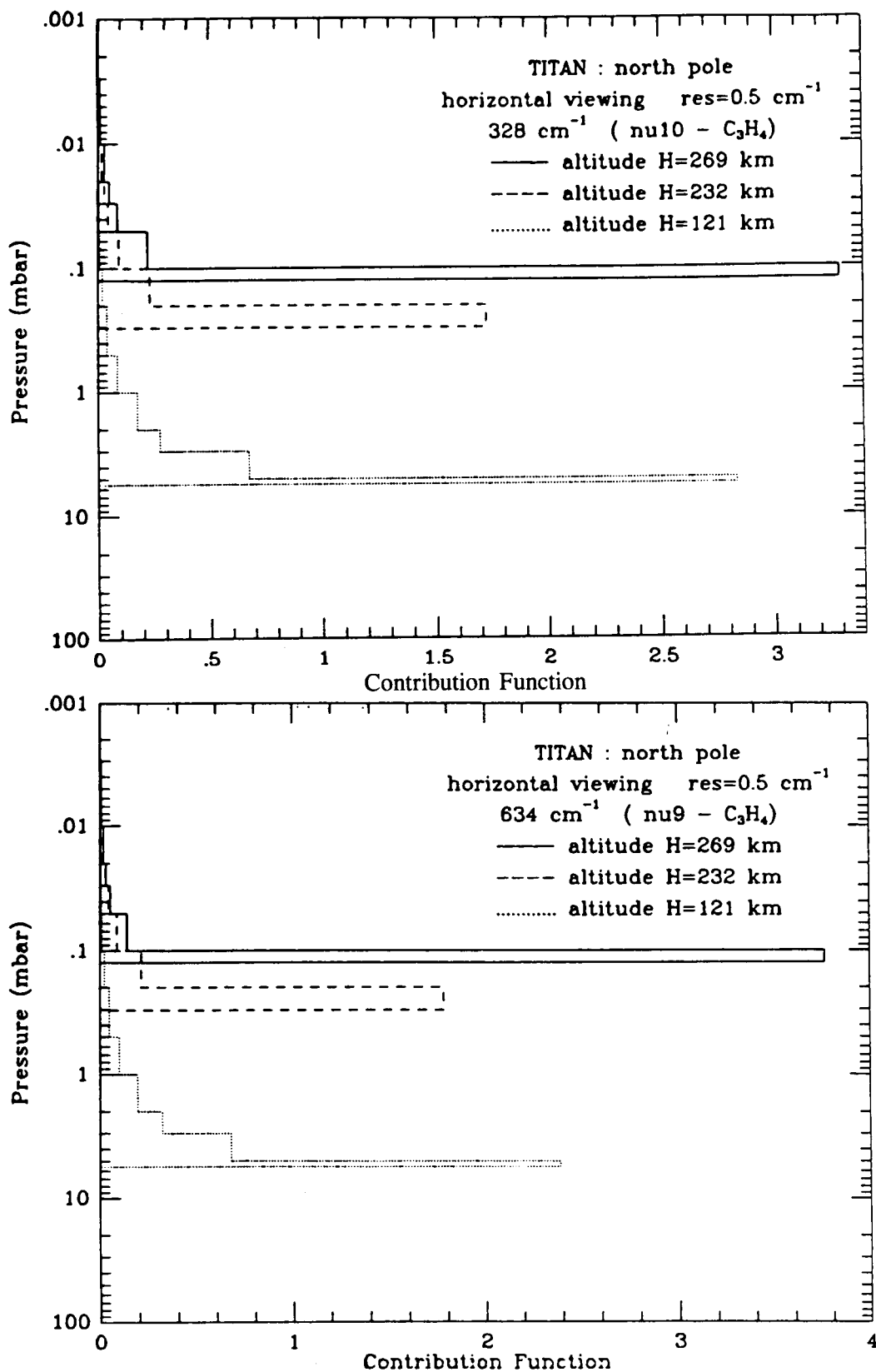


Figure B24 Titan C₃H₄ contribution functions.

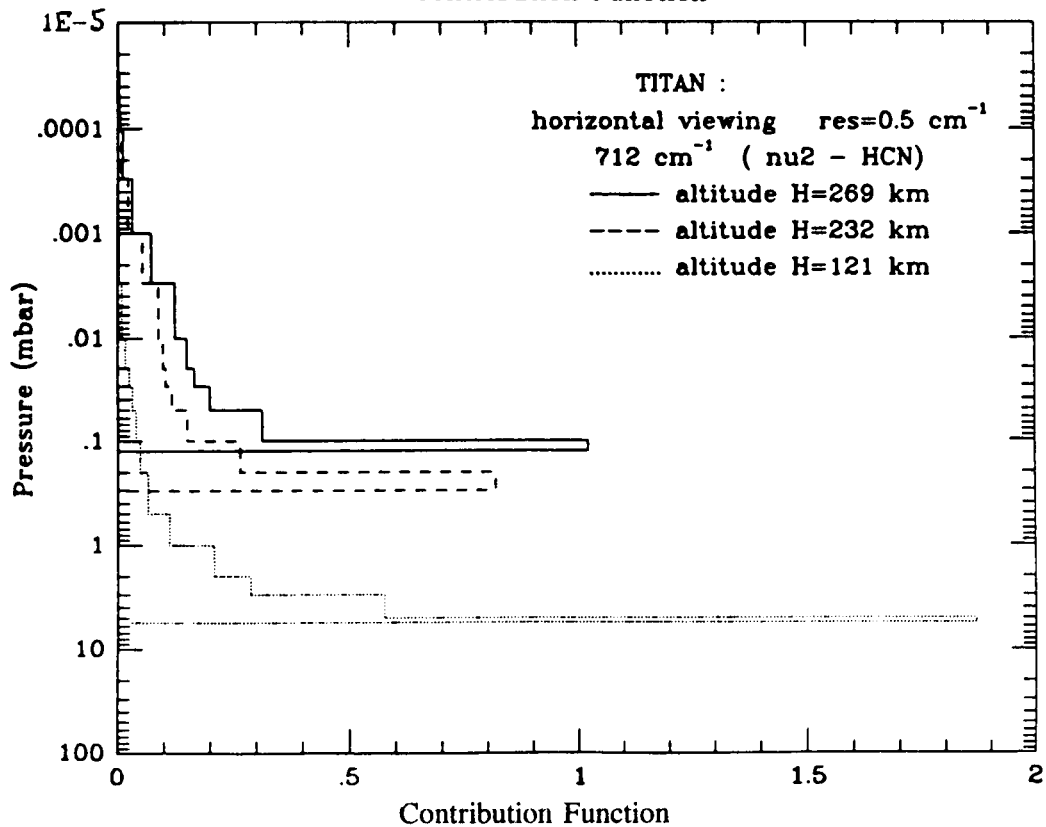
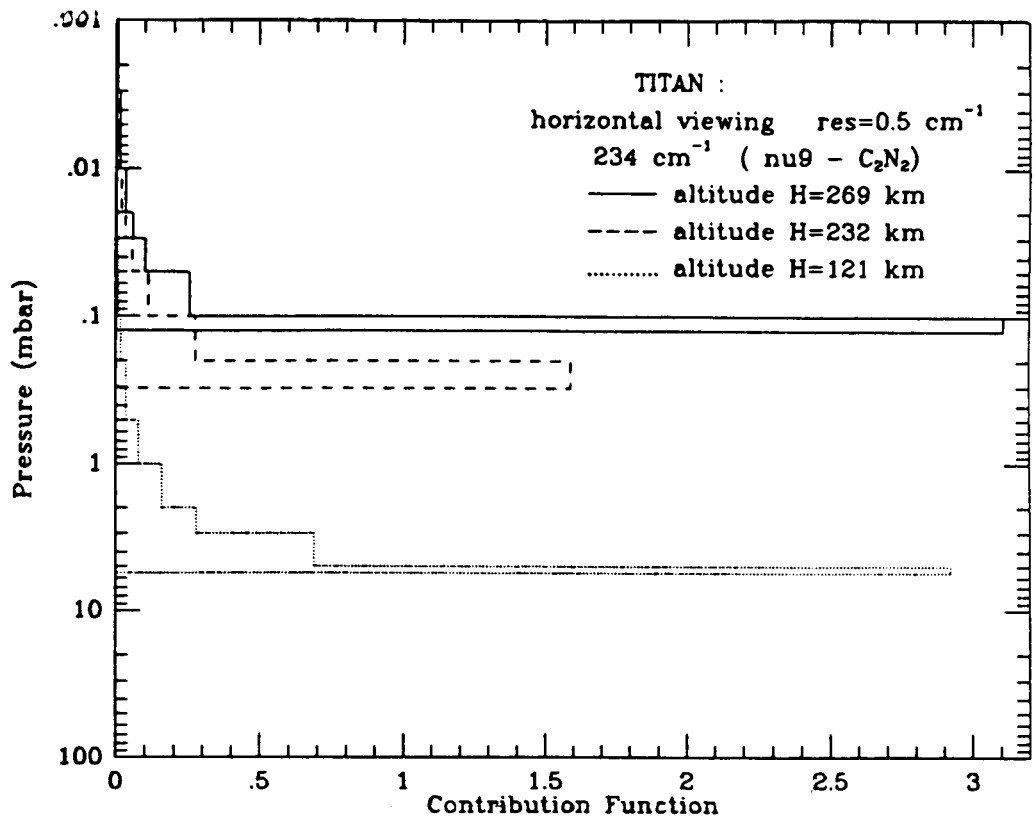


Figure B25 Titan C₂N₂ and HCN contribution functions.

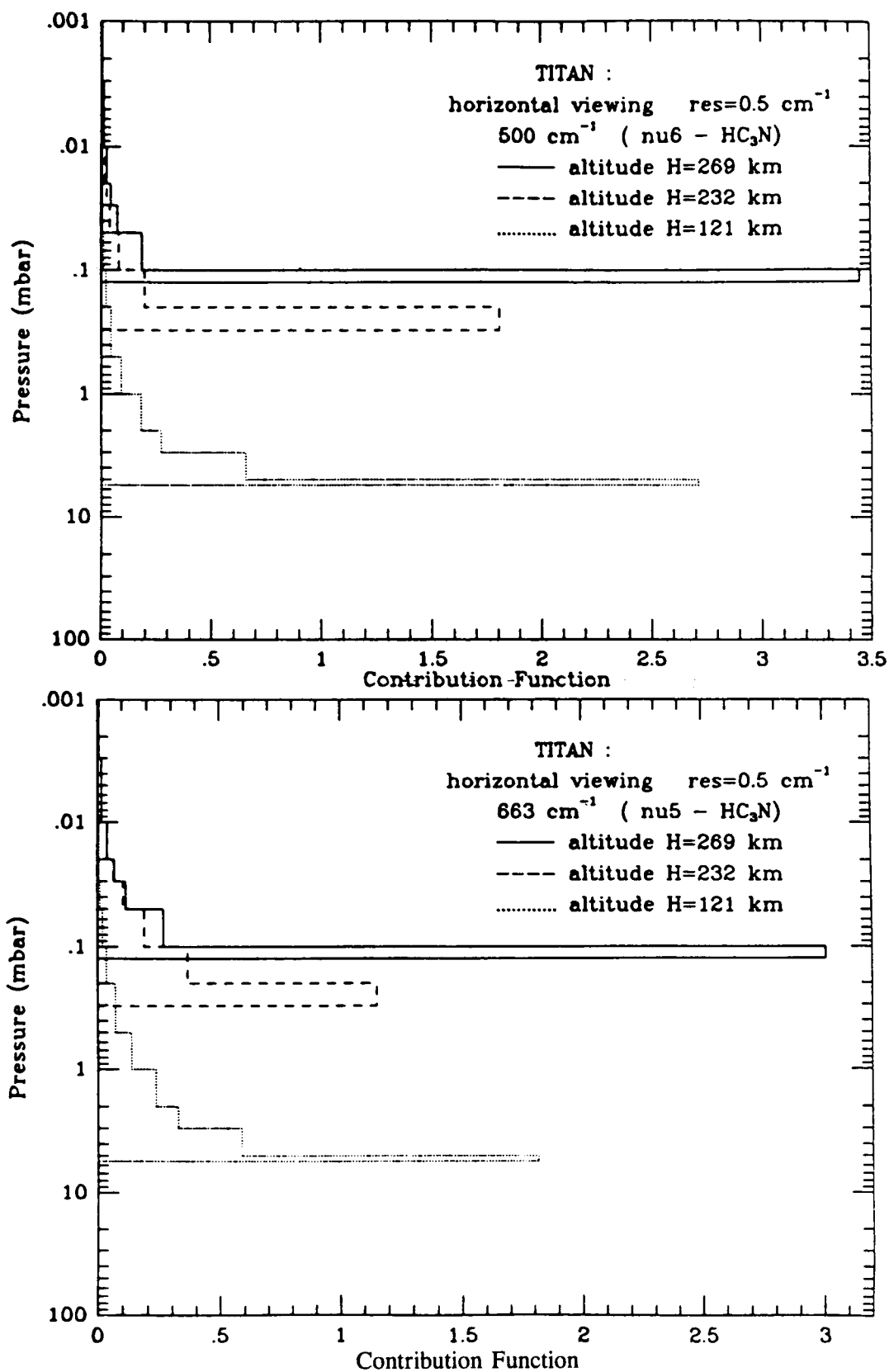


Figure B26 Titan HC_3N contribution functions.

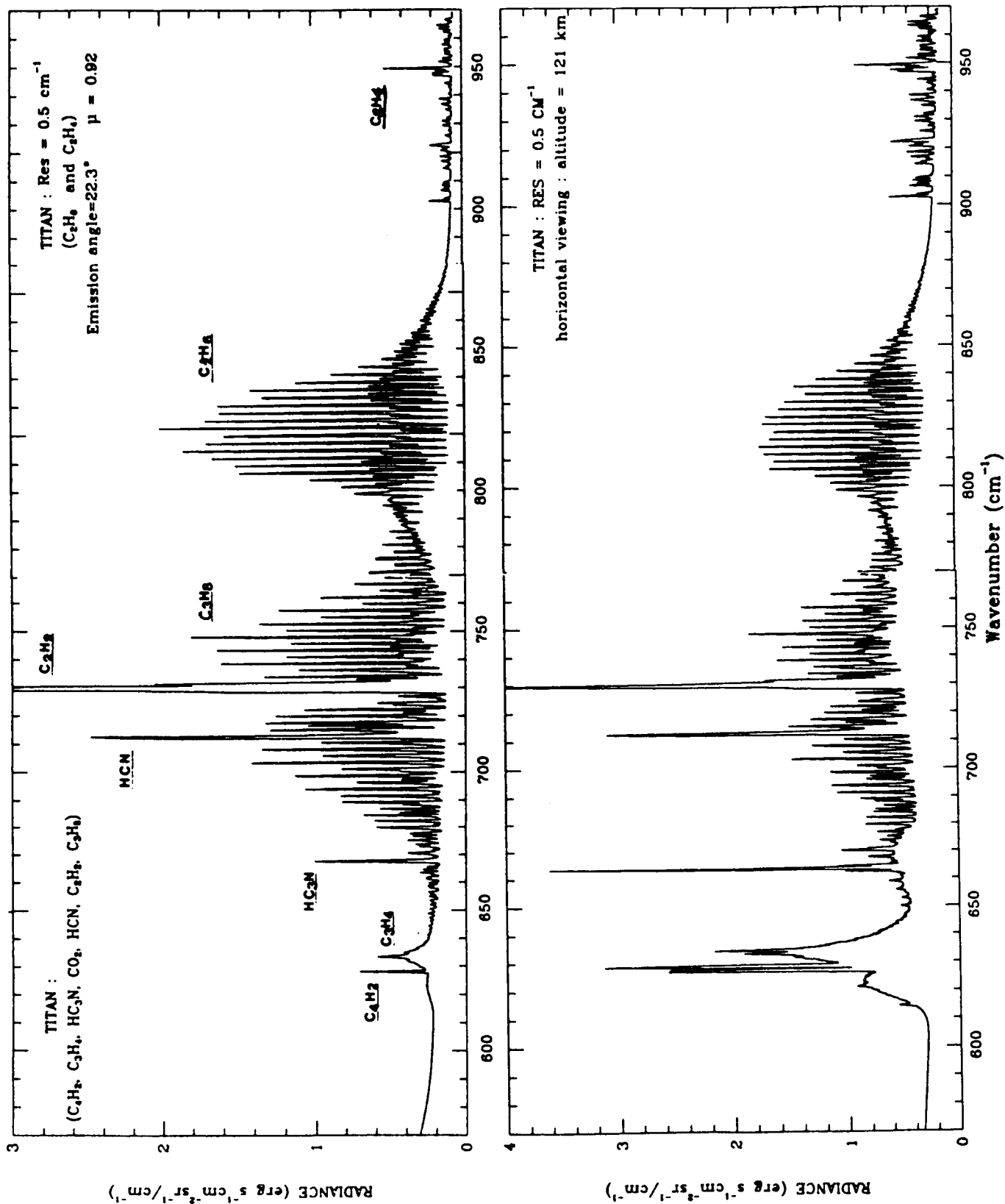


Figure B27 Titan radiance spectra.

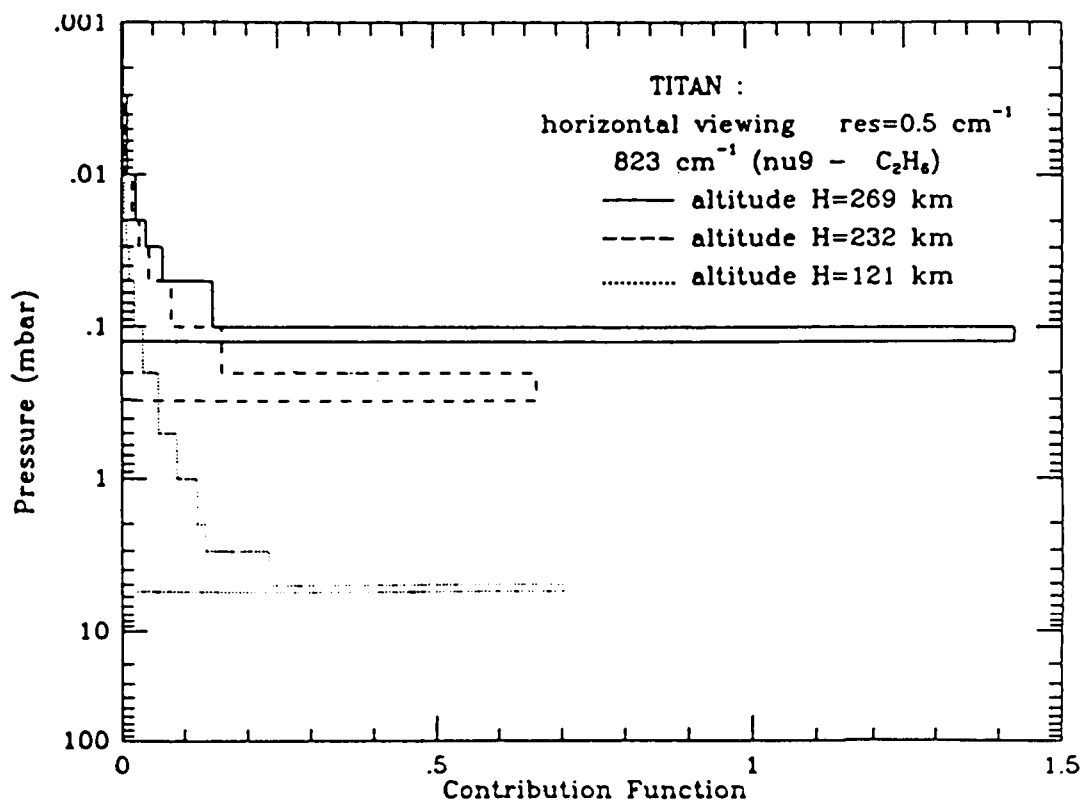
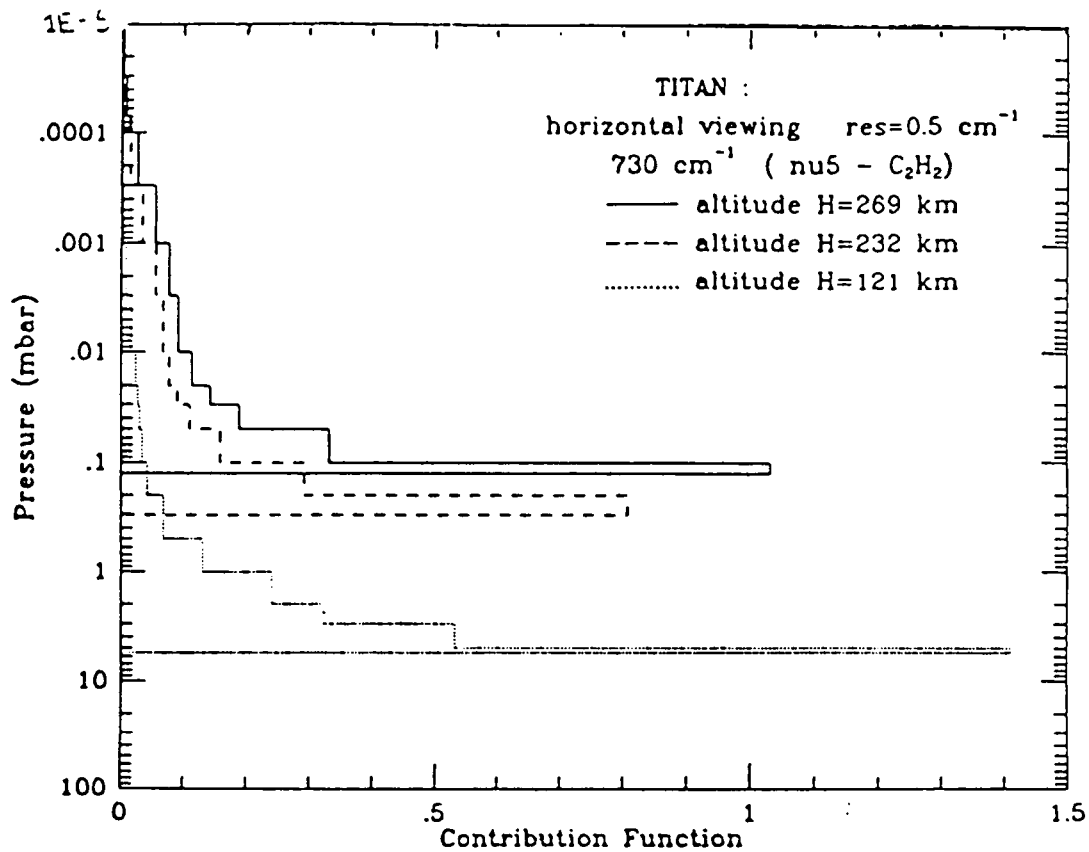


Figure B28 Titan contribution functions.

ORIGINAL PAGE IS
OF POOR QUALITY

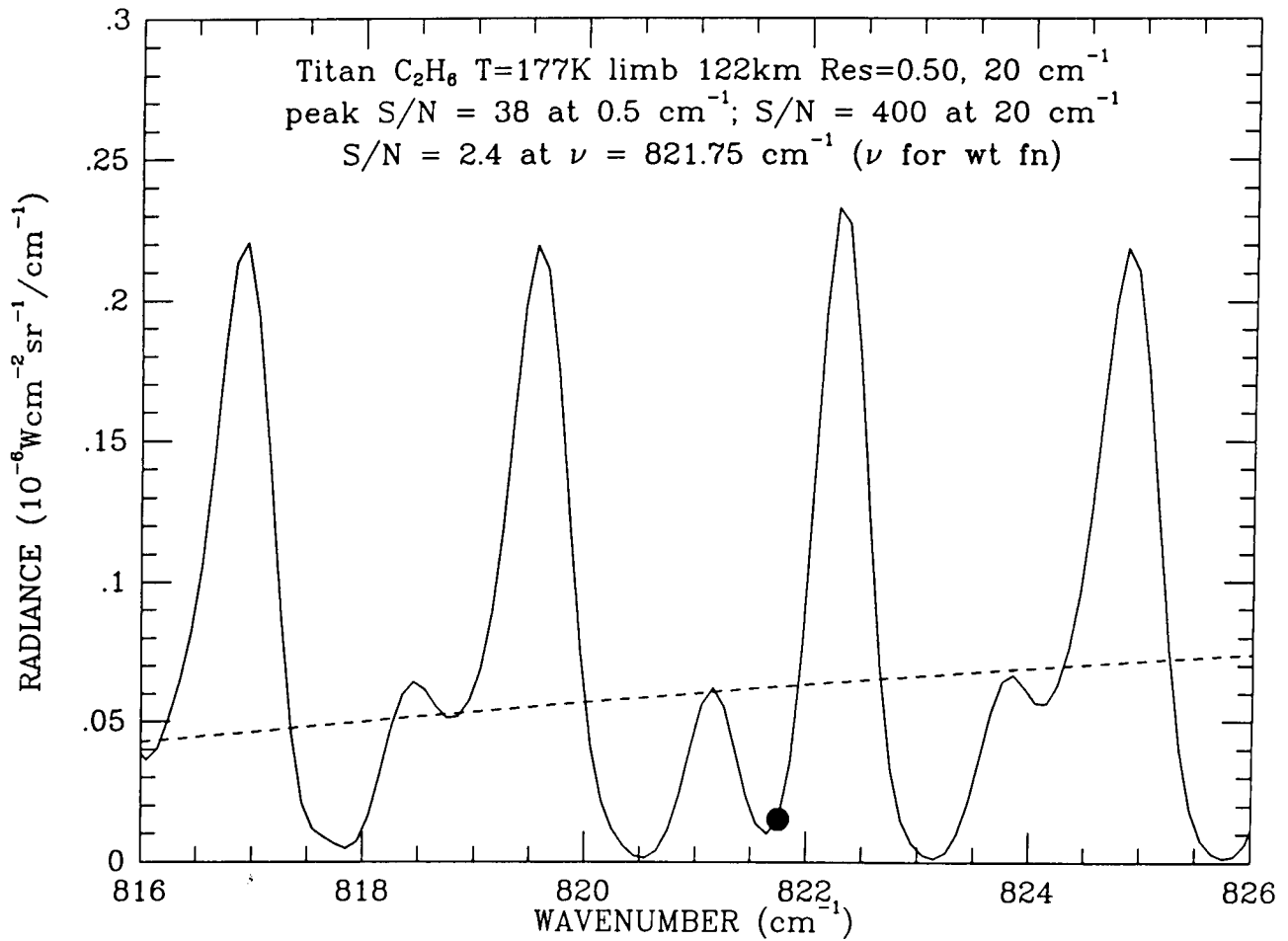


Figure B29 Titan C_2H_6 spectrum.

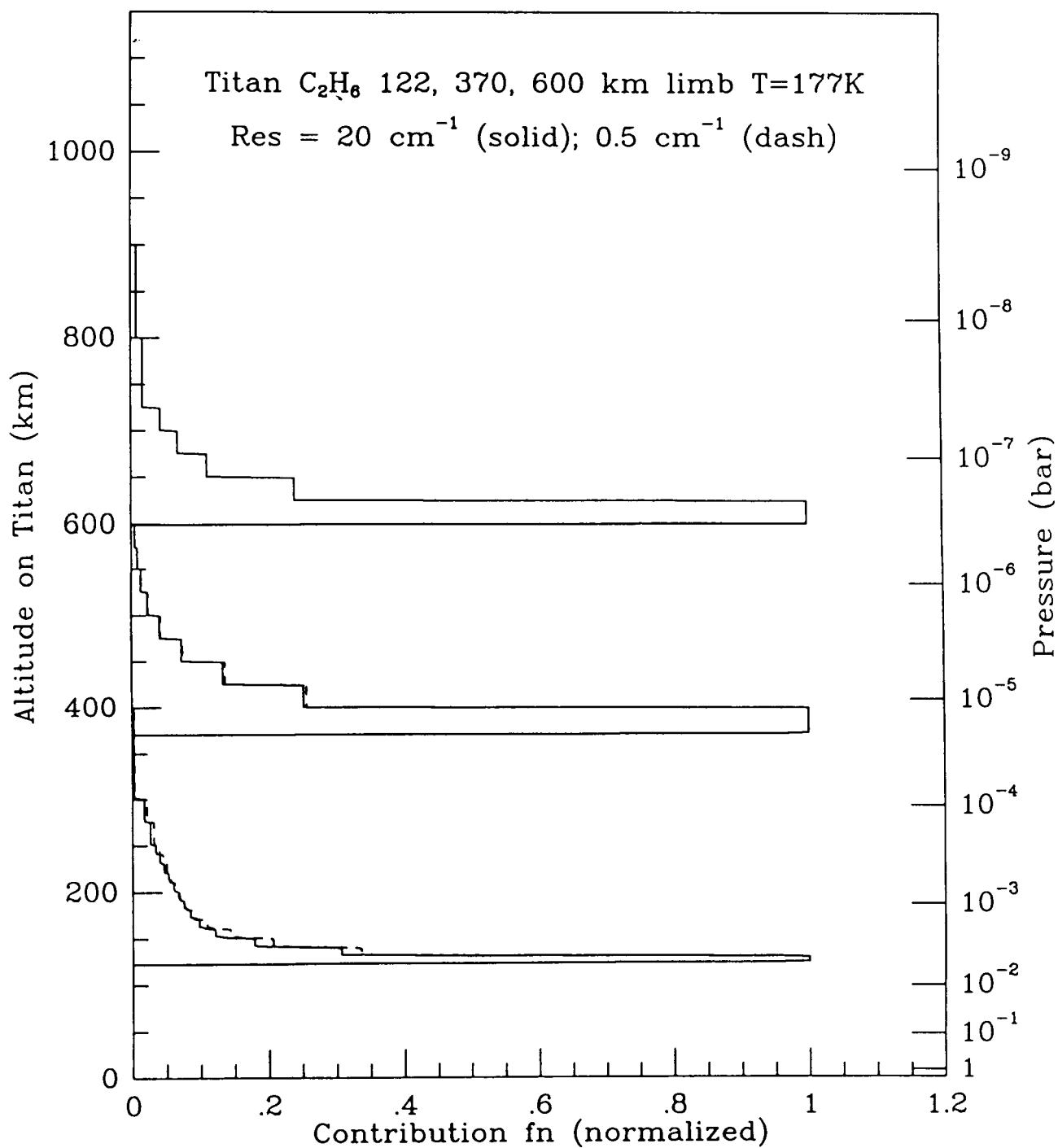


Figure B30 Titan C_2H_6 contribution function.

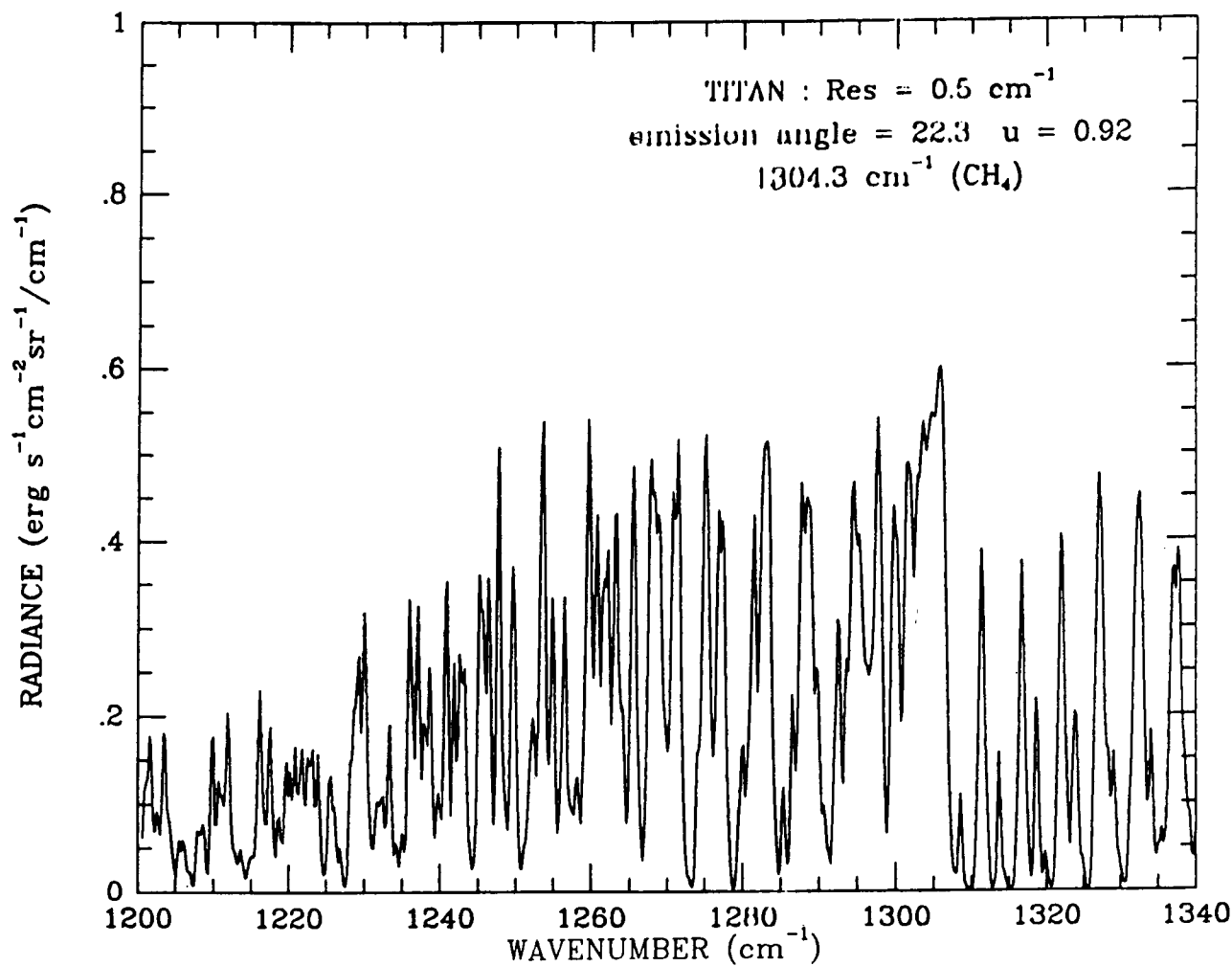


Figure B31 Titan radiance spectrum.

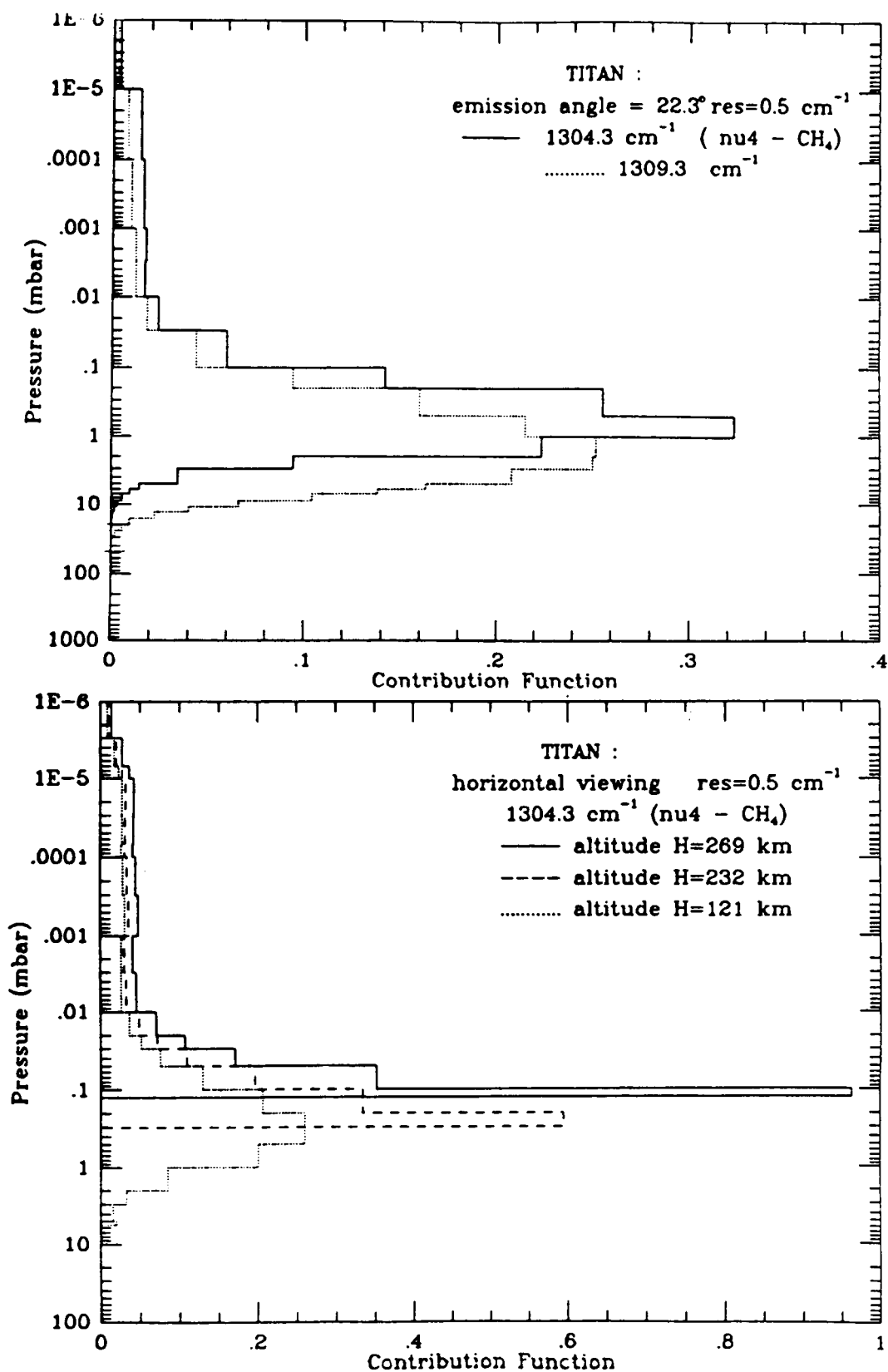


Figure B32 Titan CH_4 contribution function.

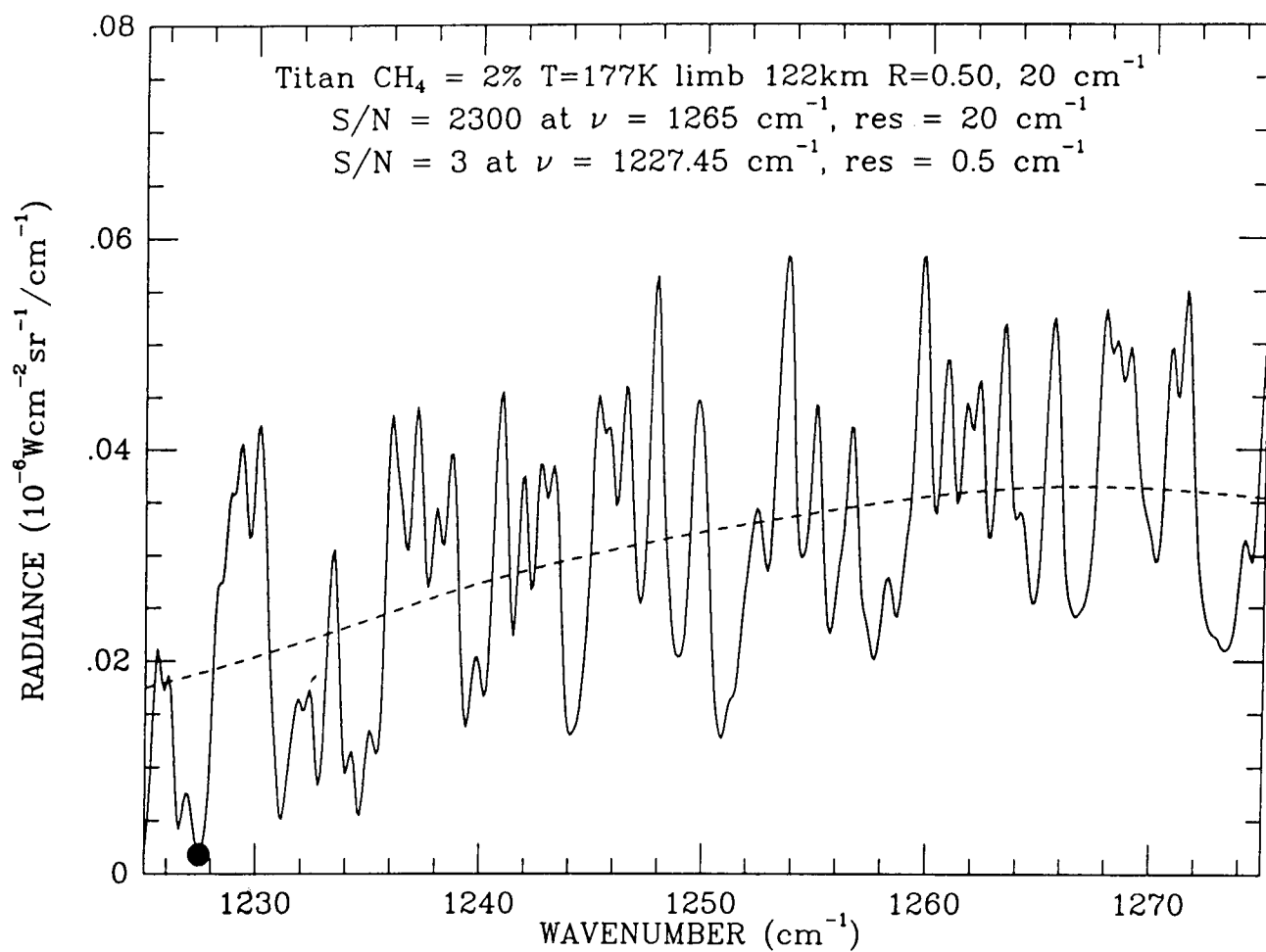


Figure B33 Titan CH₄ radiance spectra.

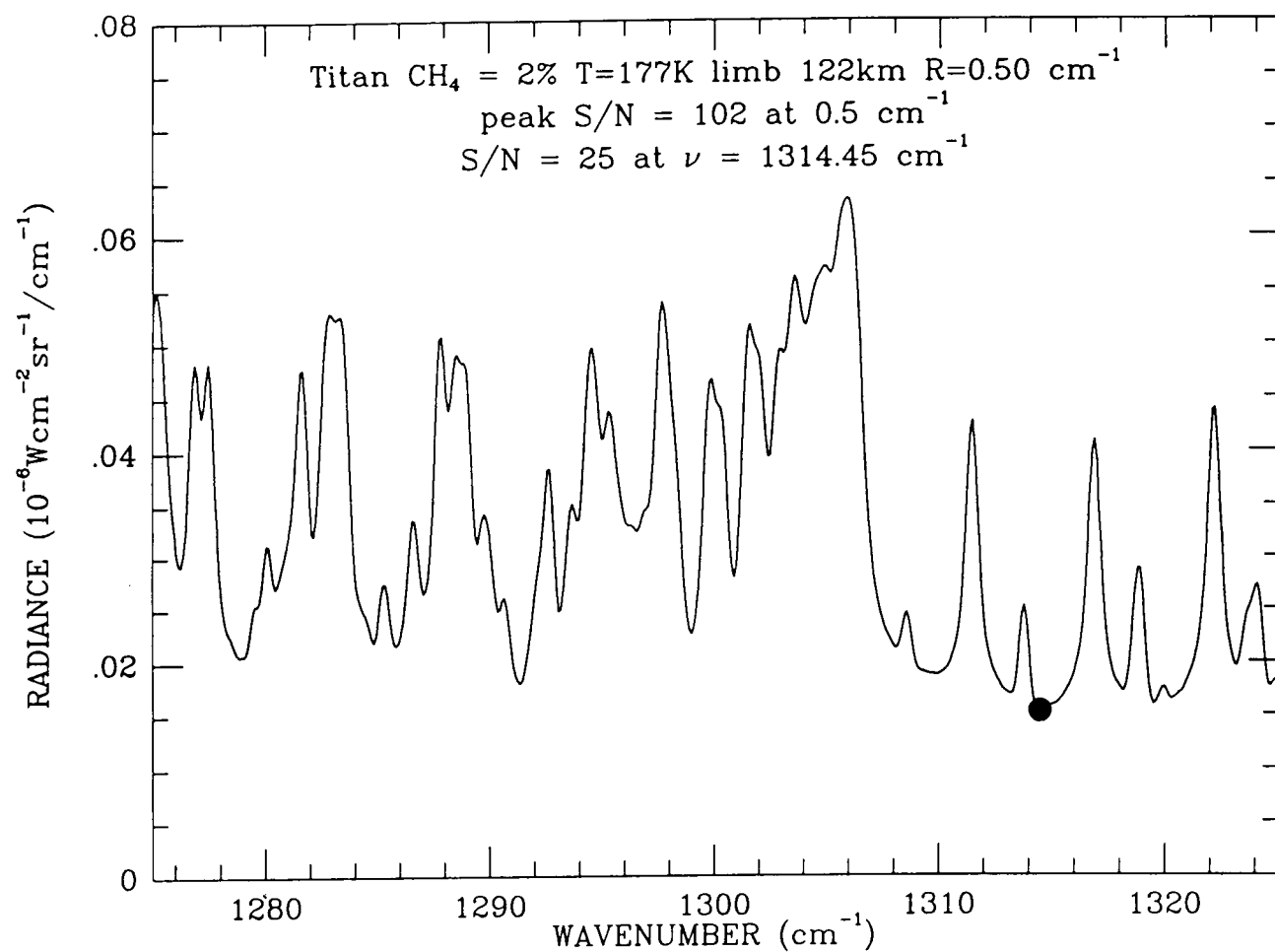


Figure B34 Titan CH₄ radiance spectra.

ORIGINAL PAGE IS
OF POOR QUALITY

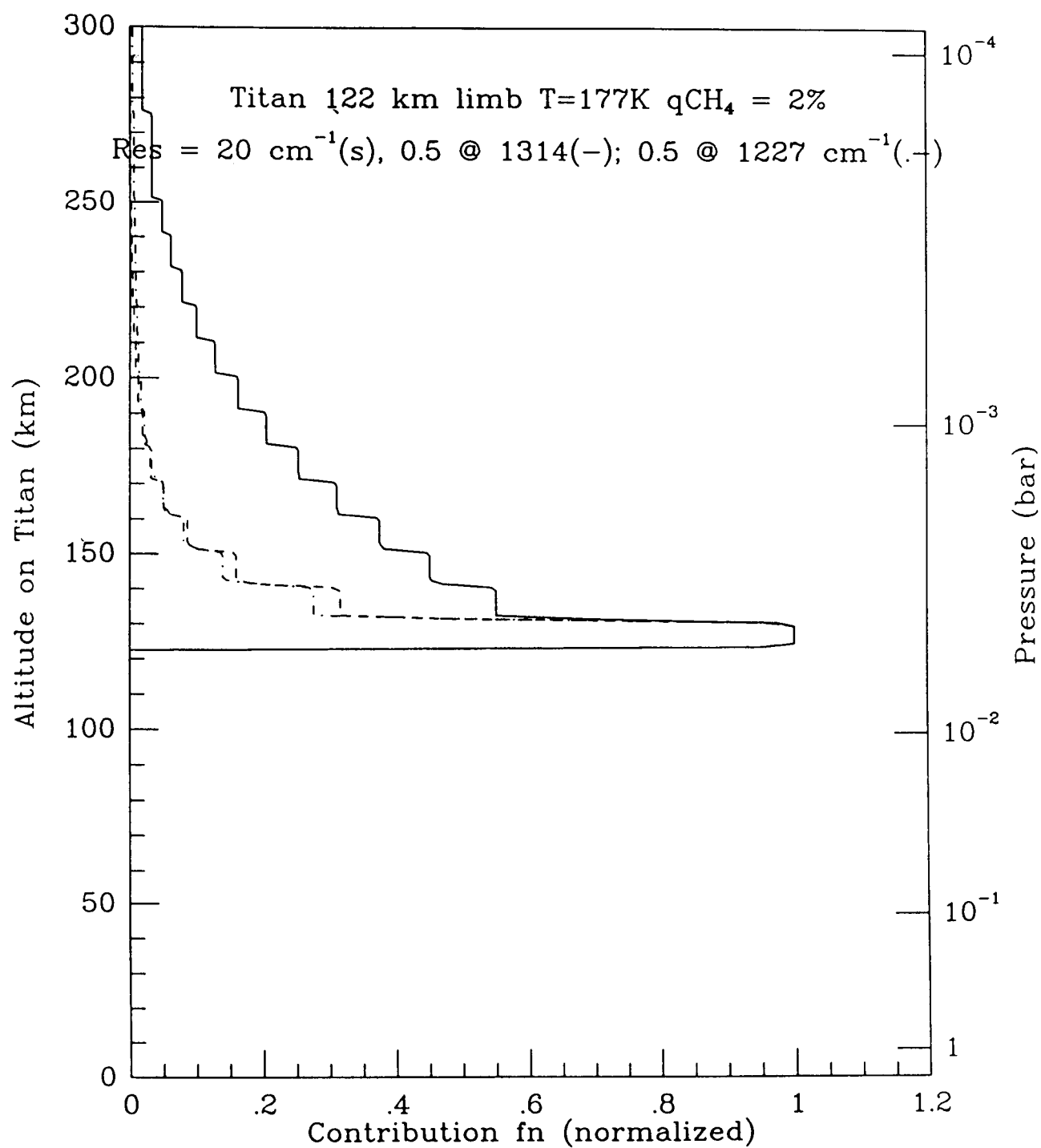


Figure B35 Titan CH_4 contribution function.

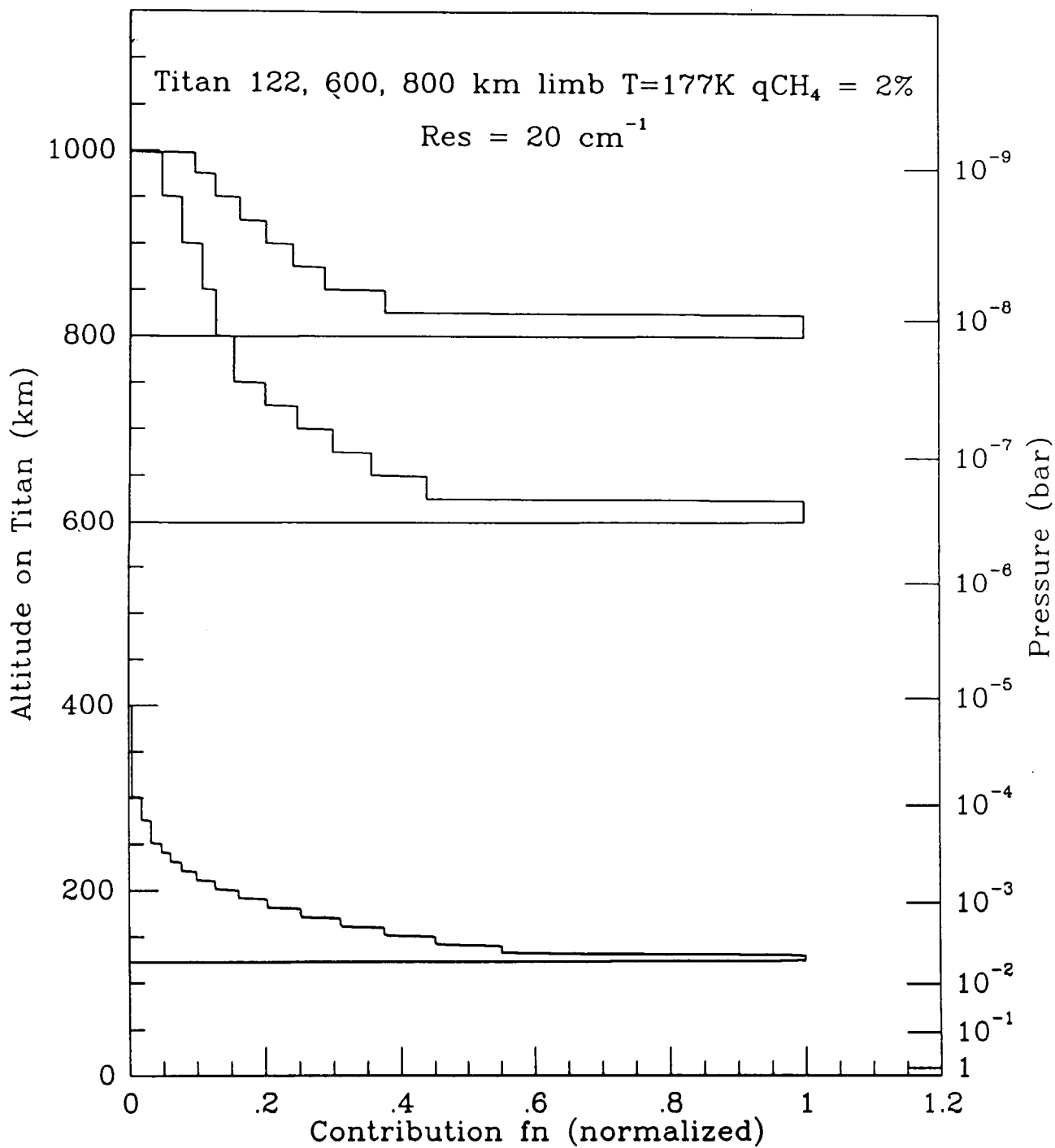


Figure B36 Titan CH_4 contribution function.

APPENDIX C CSS BACKGROUND INFORMATION AND FIGURES

TABLE C1 Estimated CSS instrument and temperature channel performance parameters.

Instrument		
Aperture diameter - cm		40
Detector FOV - μrad		50×1000
$A\Omega$ - $\text{cm}^2 \cdot \text{ster}$		6.2×10^{-5}
Detector D° - $\text{cm} \cdot \text{Hz}^{1/2} \cdot \text{w}^{-1}$		10^{12}
Detector RoA - $\Omega \cdot \text{cm}^2$		>200
Detector size - μm		15×300
Optical Transmission		0.5
Signal Integration time		20 secs
Temperature channel ($1240\text{-}1290 \text{ cm}^{-1}$)		
	Pressure Modulated Signal	Wideband Signal
Energy grasp - cm^{-1}	5.0	50.0
Noise Equivalent Radiance ($\text{w} \cdot \text{cm}^{-2} \cdot \text{ster}^1 / \text{cm}^{-1}$)	1.5×10^{-11}	1.5×10^{-12}
S/N 150K	874	8737
130K	135	1352
110K	11	105
Minimum Detectable Temperature (K)	96	86

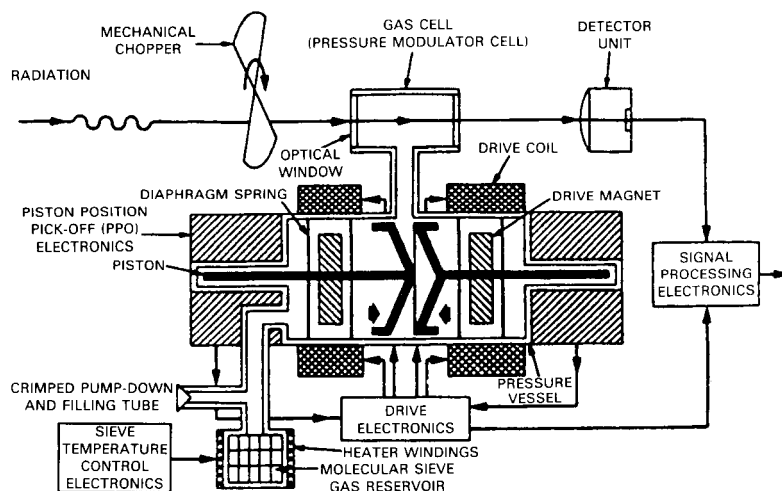


Figure C1 A schematic of a Pressure Modulator Radiometer. Thermal radiation emitted by the atmospheric gas of interest is observed through a cell containing the same gas. The pressure of gas in the cell is modulated by compressing a small trapped volume using two coupled pistons. The use of two pistons minimizes any vibration caused by modulator. The mean pressure of the cell gas is determined by the temperature of a molecular sieve material containing a reservoir of the gas.

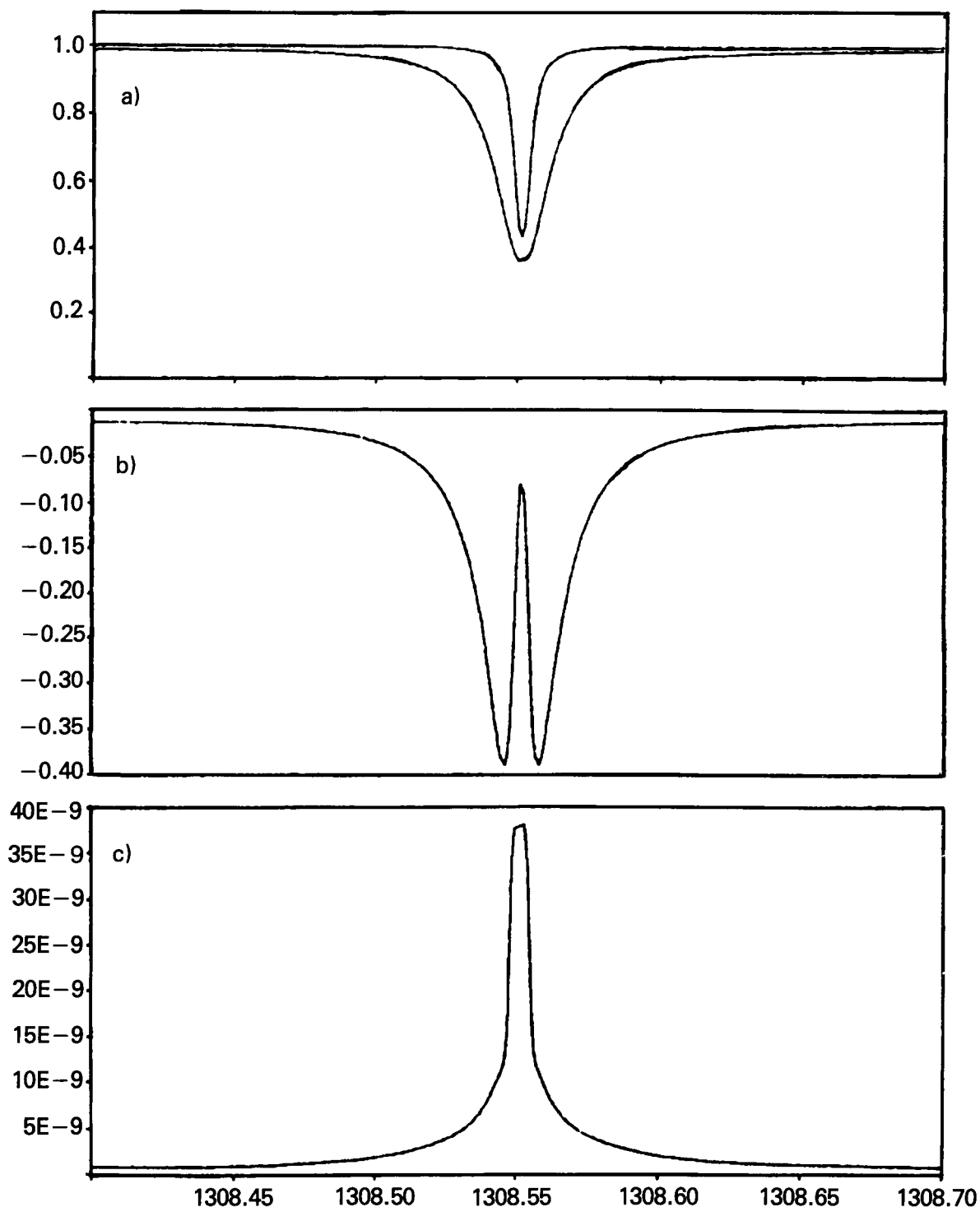


Figure C2 a) The Pressure Modulator cell transmission for extreme pressures of 96 mbar and 24 mbar and b) The difference in transmission, for a small section of the $\text{CH}_4 \nu_4$ band. The difference is the effective spectral response for the modulated signal. The "wideband" signal is that detected at the frequency of the mechanical chopper. Both wideband and modulated signals will detect emission due to aerosols making it possible to discriminate between aerosol and gaseous emission. c) Computer emission spectrum of the ν_4 band of CH_4 for the Saturnian atmosphere as seen by a spectrometer of "infinite" resolution.

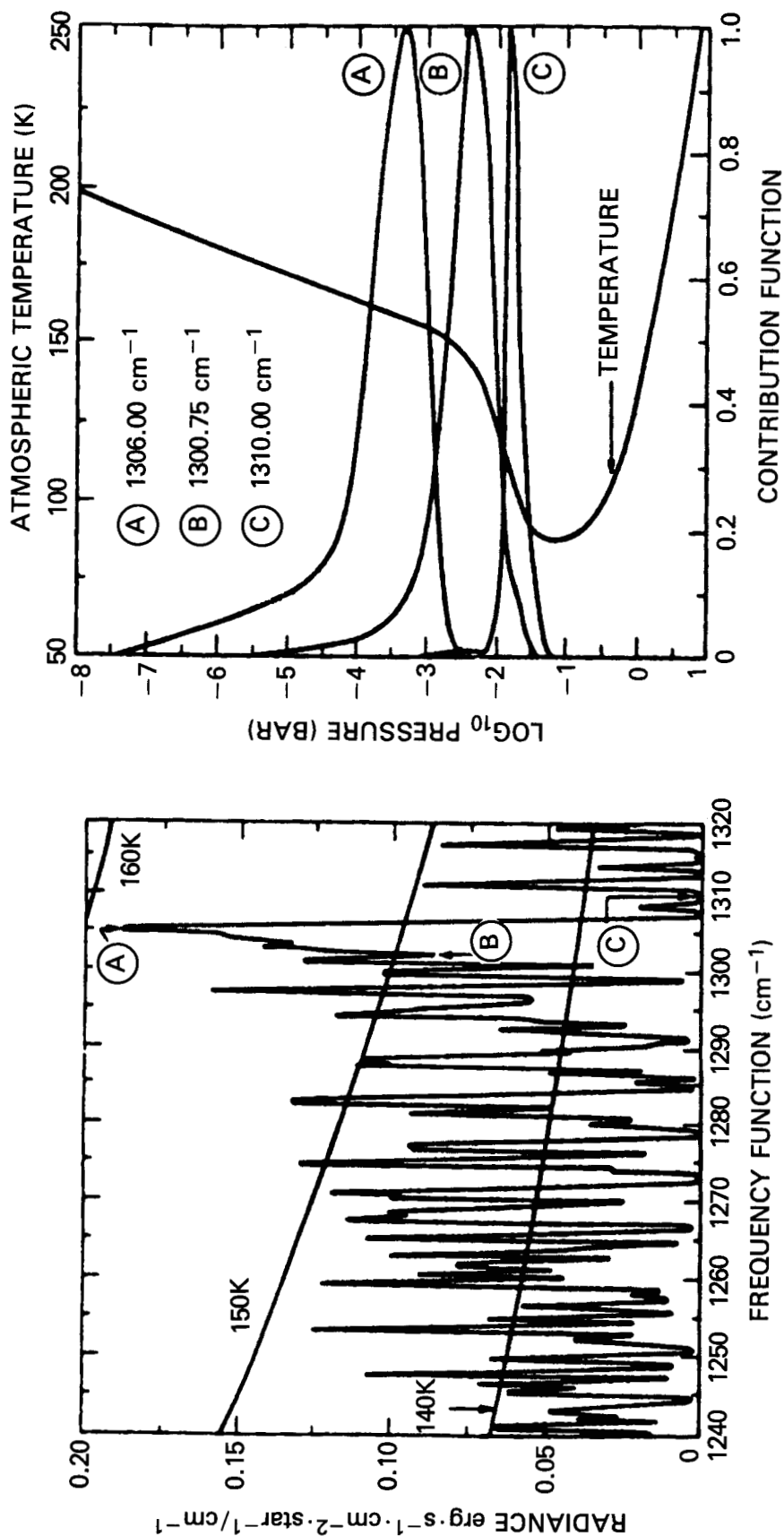


Figure C3 a) Computed spectrum for the ν_4 band of CH_4 in the atmosphere of Saturn as seen by nadir viewing spectrometer with a resolution of 0.5 cm^{-1} . b) Normalised contribution functions $(-B_\nu(y) \frac{dT_\nu(y)}{dy})$ computed for the spectral intervals A, B and C shown in Fig. C3a. The vertical resolution in all three cases is around 130km, or more than two scale heights.

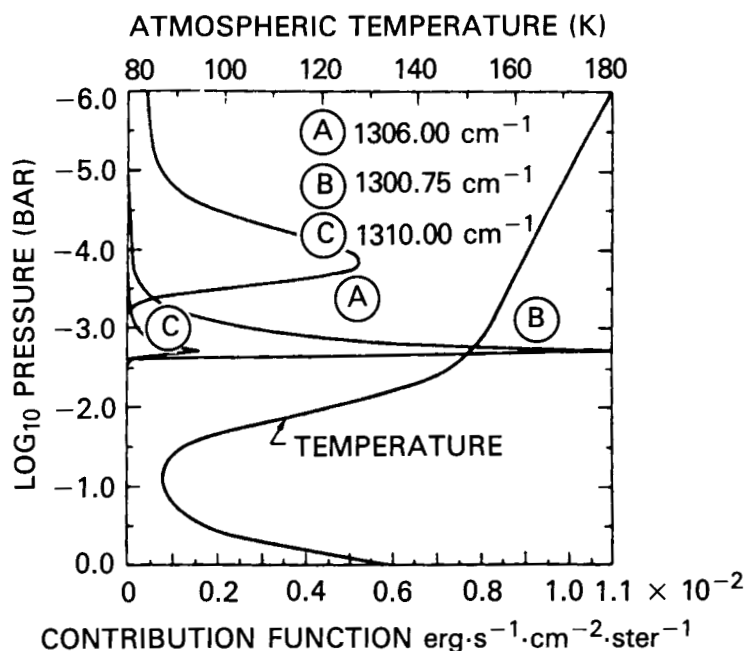


Figure C4 Contribution functions for limb views at the 2 mbar level in the atmosphere of Saturn for a 0.5 cm^{-1} resolution spectrometer for the same frequencies as in Fig C3. Contribution functions including line centres (eg. frequency A) still have high altitude peaks because of the strong temperature dependence of the Planck function at these frequencies. Frequencies can be selected to avoid line centres (b and C) and hence achieve resolution of a scale height or better, but the radiances observed are too small for practical instruments.

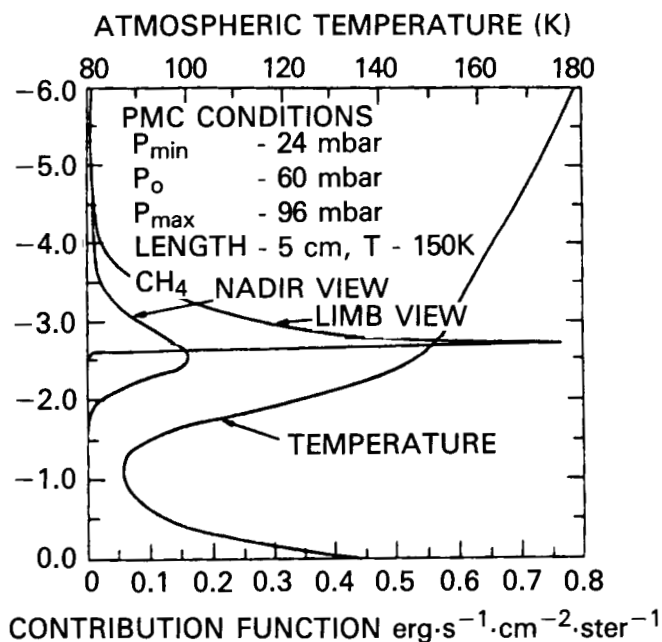


Figure C5 Contribution functions for nadir and 2 mbar limb views of the Saturnian atmosphere for the wide-band signal of a CH_4 pressure modulator radiometer with a $1240\text{-}1290 \text{ cm}^{-1}$ bandpass. The emission from line centres is rejected because of the gas cell, and high vertical resolution limb measurements become practical even at large distances from the planet because the radiometer observes the emission from many line wings.

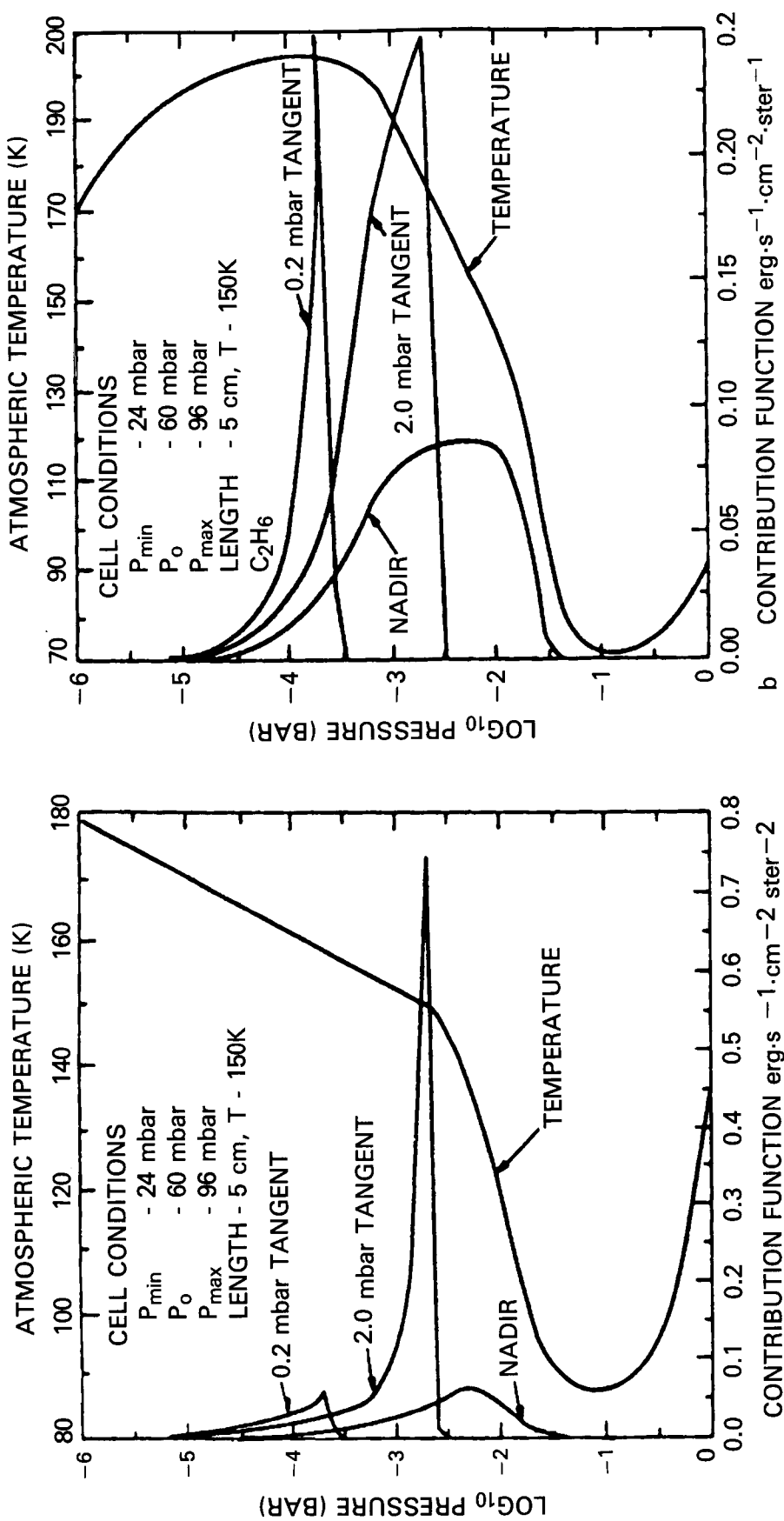


Figure C6 Contribution functions for nadir viewing and a range of limb views for the Saturnian (a) and Titanian (b) atmospheres for the modulated and wideband signals of a CH_4 pressure modulator with a bandpass of $1240\text{-}1290\text{ cm}^{-1}$. A Cassini instrument would employ an array of detectors to measure a number of limb paths simultaneously. (In Fig C6a the 0.2 and 0.02 mbar functions are multiplied by .67, in Fig C6b the 0.02 mbar function is multiplied by 3).

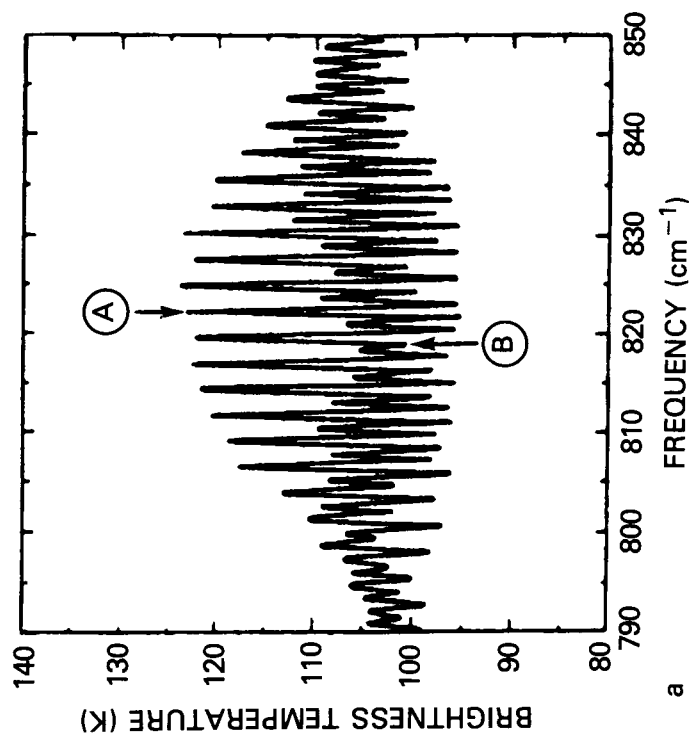
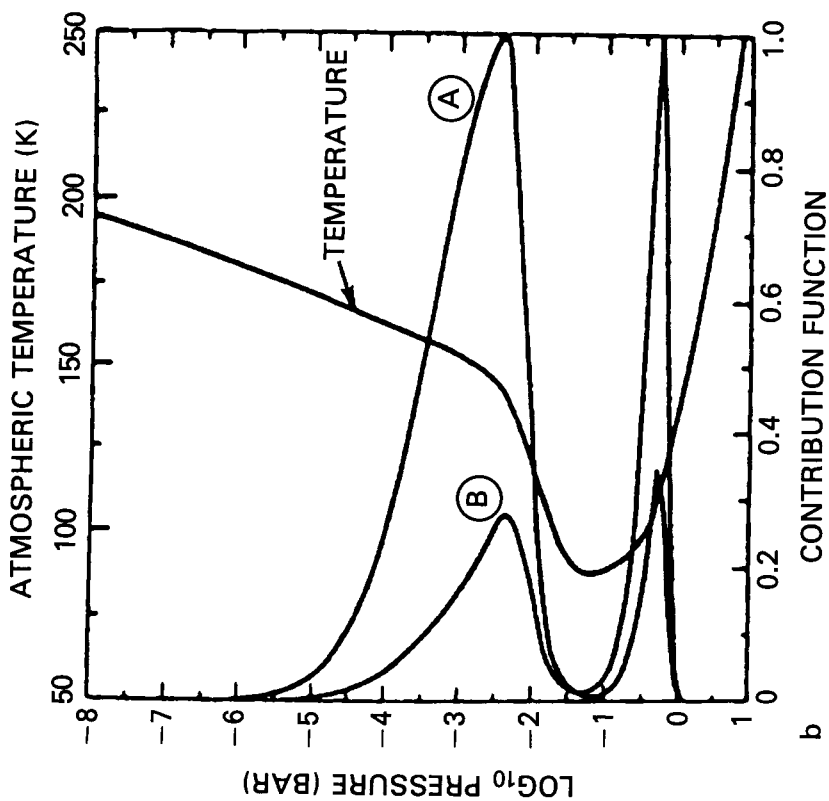


Figure C7 a) Computed emission spectrum for the ν_9 band of C_2H_6 in the Saturn atmosphere as seen by a nadir viewing spectrometer of resolution 0.5 cm^{-1} b) Contribution functions calculated for the spectral intervals A and B in Fig C7a. The contribution functions exhibit the same poor vertical resolution as calculated for CH_4 . In addition there is a lower peak to the contribution functions caused by collision induced H_2 emission which will complicate any interpretation.

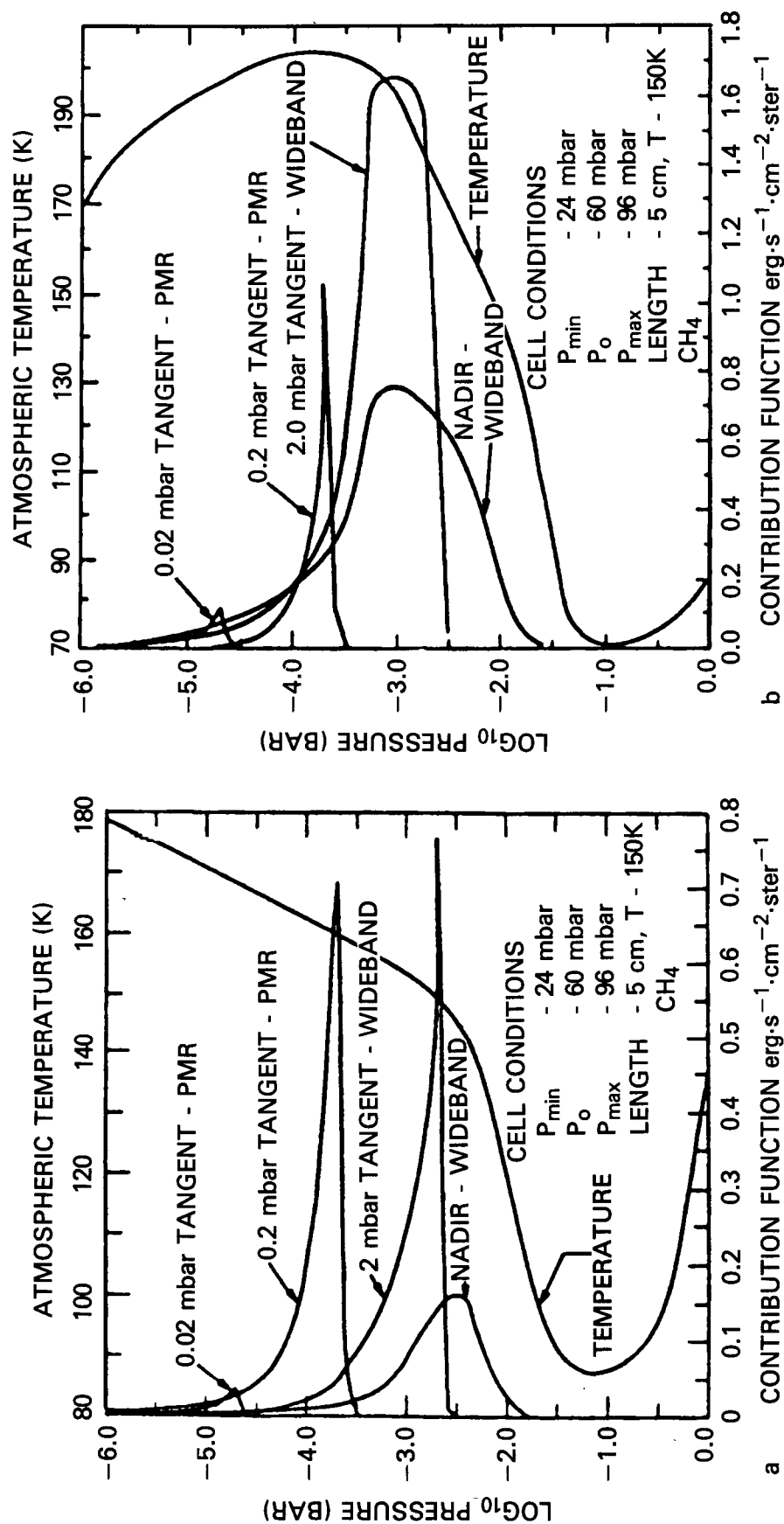


Figure C8 Contribution functions for nadir and limb views of a) the Saturnian and b) the Titanian atmospheres for the modulated signal of a C_2H_6 pressure modulator radiometer with a $805 - 845 \text{ cm}^{-1}$ bandpass, indicating the improved vertical resolution compared to a nadir viewing spectrometer (Fig C7).

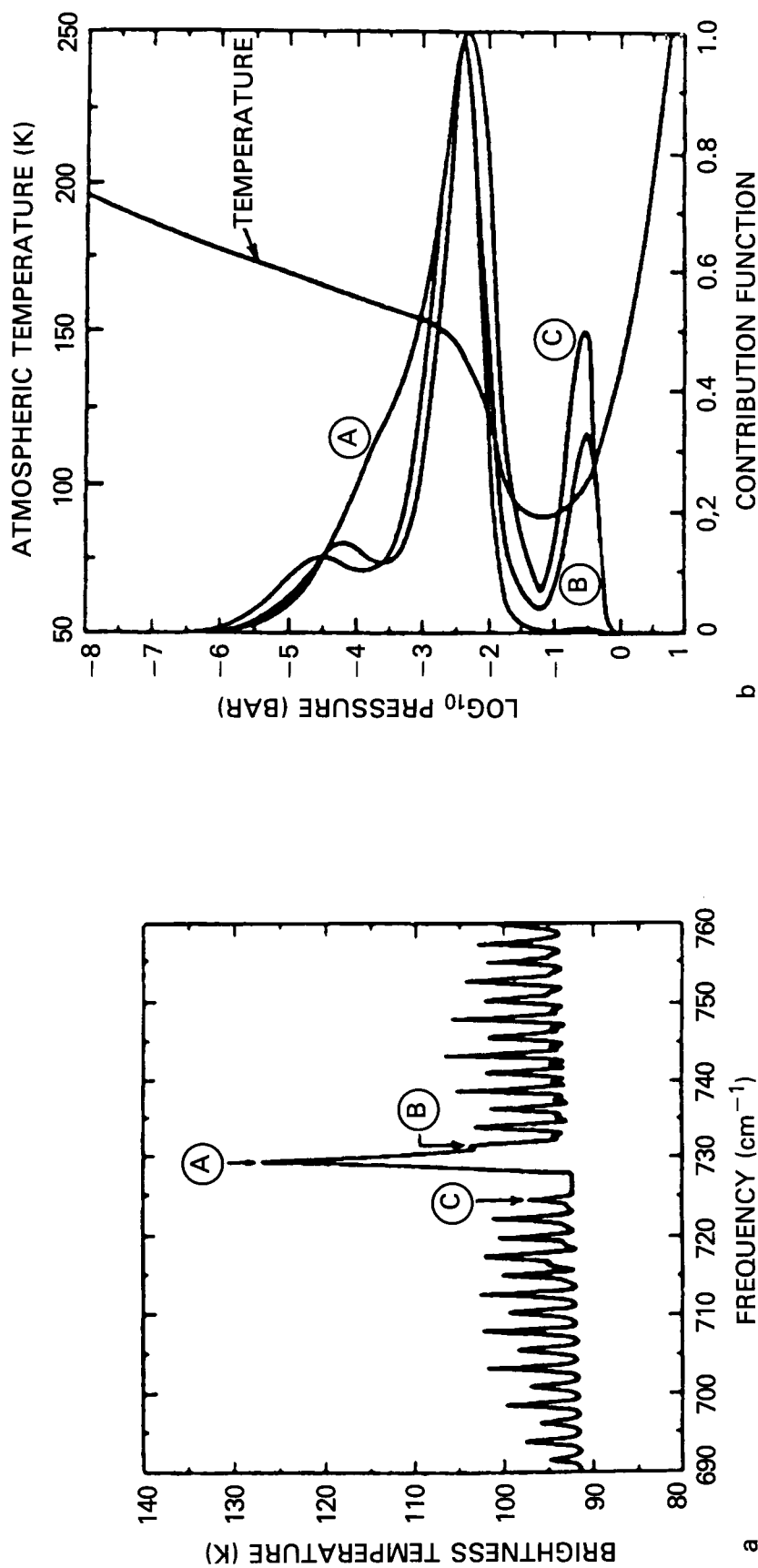


Figure C9 a) Computed emission spectrum for the ν_5 complex of C_2H_2 in the Saturn atmosphere as seen by a nadir viewing spectrometer of resolution 0.5 cm^{-1} b) Contribution functions calculated for the spectral intervals A, B and C in Fig C9a. The shape of the weighting functions shows similar limitations to those of C_2H_6 .

APPENDIX D C-VIMS BACKGROUND INFORMATION AND FIGURES

The Cassini Visible and Near IR Mapping Spectrometer (C-VIMS) is envisioned as a facility instrument whose heritage is the Near-Infrared Mapping Spectrometer (NIMS) on the Galileo mission, and whose characteristics are given as the description of this instrument. Other related instruments include the Visible/Near-Infrared Mapping Spectrometers (VIMS) on Mars Observer and Comet Rendezvous/Asteroid Flyby missions planned for the 1990's.

The C-VIMS experiments uses a grating spectrometer to measure radiances between 0.7 and 5.2 microns with a spectral resolution of 0.025 microns. Images are formed using a line-scan technique. The field-of-view consists of a line of contiguous 0.5 x 0.5 mrad. samples which will be scanned across the target by means of spacecraft and scan platform motion.

C-VIMS science measurements include:

- (1) Global distributions and time-variability of some minor atmospheric constituents.
- (2) Cloud coverage and vertical distribution.
- (3) Scattering characteristics of clouds as a function of solar phase angle and wavelength, and inferences regarding their physical properties and composition.
- (4) Imaging of Saturn and Titan at selected infrared wavelengths on both day and night sides.
- (5) Composition of ring particles and airless satellite surfaces.

The NIRS instrument characteristics are summarized in Table D-1. the instrument (Fig D-1) consists of an f/3.5 Cassegrain reflector telescope with focal length of 800 mm, a grating spectrometer, and a series of detectors in the focal plane. The linear array of detectors has indium antimonide and silicon photodiodes, each of which samples a specific wavelength interval, depending on the order and rotation angle of the grating. Optical filters are used to isolate individual orders. The focal plane assembly is radiatively cooled to 75-80°K.

PRECEDING PAGE BLANK NOT FILMED

TABLE D1 C-VIMS Instrument Characteristics

Parameter	Characteristic
Angular	0.5 mrad \times 0.5 mrad
Angular field	10 mrad (20 pixels) \times 0.5 mrad (1 pixel)
Spectral range	0.7–5.3 μ
Spectral resolution	0.6%; $\Delta\lambda = 0.025 \mu$ ($\lambda > 1 \mu$); 0.013μ ($\lambda < 1 \mu$).
Spectral scan time	4½ seconds (20 pixels, 204 wavelengths).
Telescope	23 cm (9'') diameter $f/3.5$ Ritchey-Chretien, Wobbling secondary for spatial scan, 800 mm equivalent focal length.
Etendue ($A\Omega$)	$1.1 \times 10^{-4} \text{ cm}^2 \text{ sterad}$.
Spectrometer	40 lines/mm plane-grating spectrometer, $F/3.5$ Dall-Kirkham collimator $f = 200 \text{ mm}$.
Detectors	$F/1.75$ wide-angle flat field camera $F = 200 \text{ mm}$ InSb(15), Si(2), discrete elements, Quantum efficiency $\approx 80\%$, Noise Equivalent Power = 10^{-14} Watts , $D^* = 3 \times 10^{13} \text{ cm } \sqrt{\text{Hz}} \text{ Watt}^{-1}$. Radiatively cooled to 80° K .
Noise equiv. radiance	$1.2 \times 10^{-9} \text{ W cm}^{-2} \text{ sterad}^{-1}$ per spectral resolution element (0.025μ) at 3μ .
Signal-to-noise	$\approx 100:1$ (0.075 albedo surface at 3μ)
Mass	18.0 kg
Power	8 W (average), 12 W (peak)
External dimensions	$82.6 \times 36.8 \times 39.1 \text{ cm}$ (optics), $20.3 \times 25.4 \times 12.7 \text{ cm}$ (electronics).
Data rate	11.52 kbps
Date encoding	10 bits

ORIGINAL PAGE IS
OF POOR QUALITY

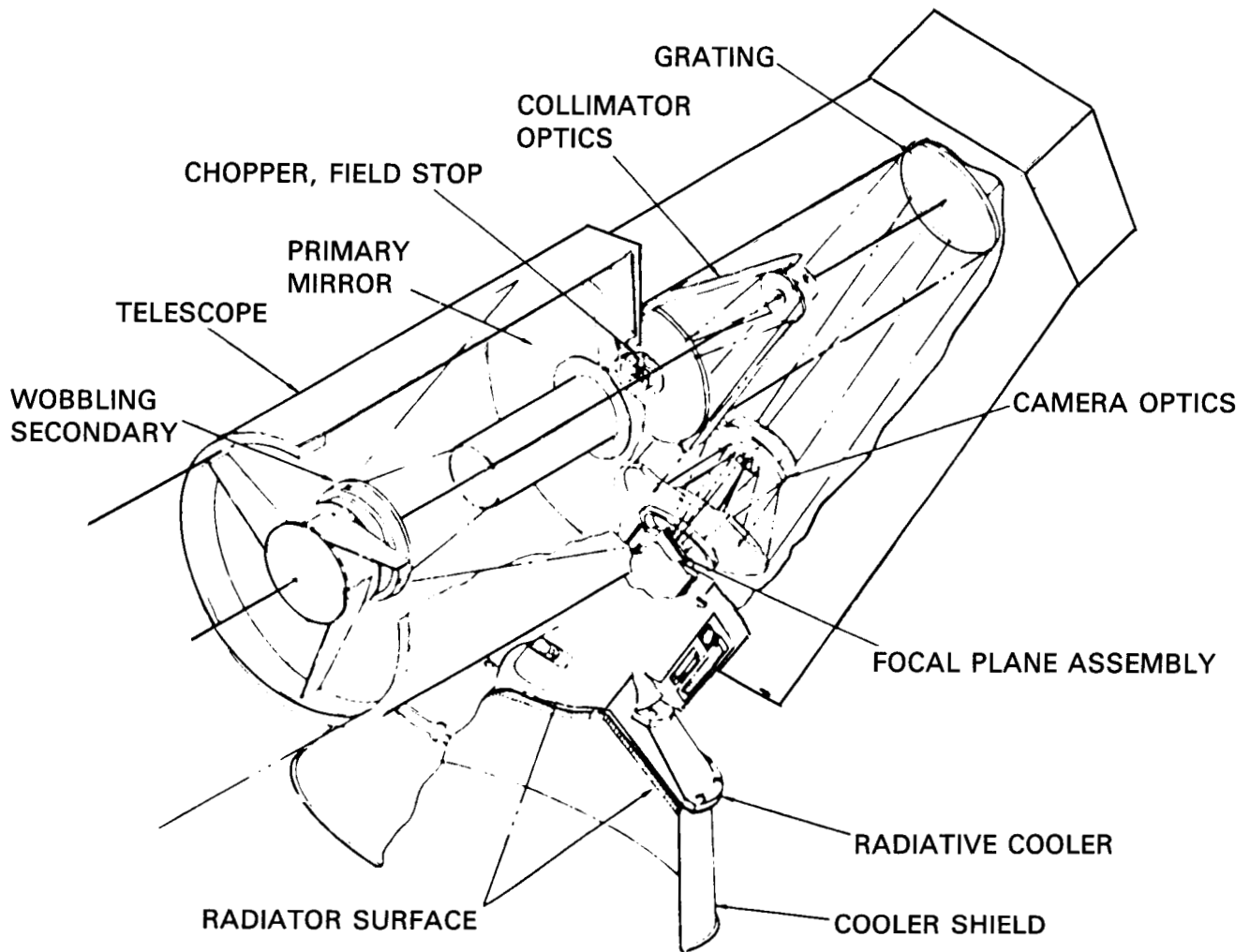


Figure D1 Pictorial view of basic components of C-VIMS.

APPENDIX E DISR BACKGROUND INFORMATION AND FIGURES

PRECEDING PAGE BLANK NOT FILMED

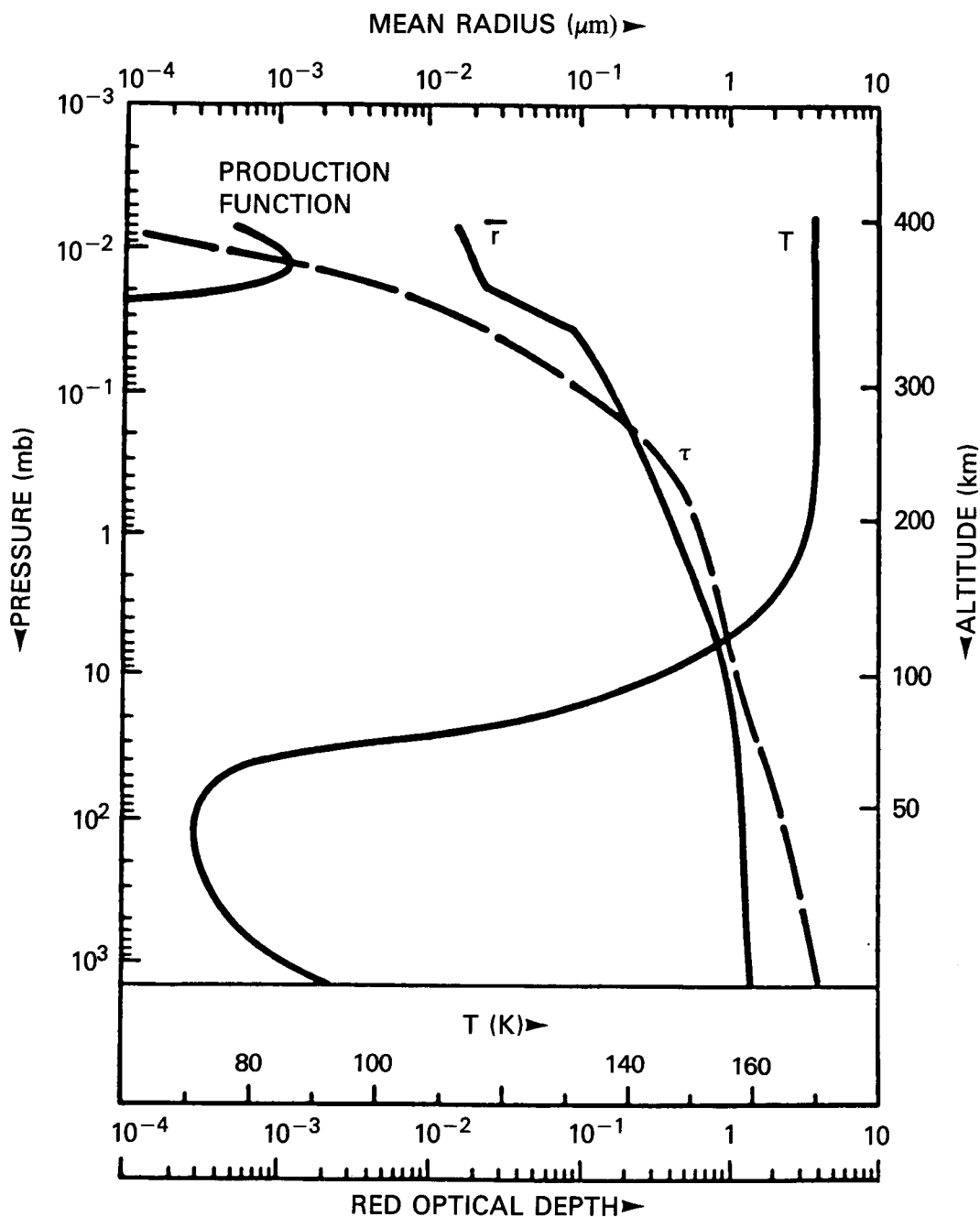


Figure E1 Baseline structure used in calculations of the penetration of sunlight into the atmosphere of Titan (from Tomasko and Pope, 1987). The production of small photochemical aerosols is parameterized at high altitudes with a profile as shown. The run of mean particle size and of the cumulative optical depth at a wavelength of 0.63 microns is also shown as a function of depth into the atmosphere. Electrical charging of the photochemical aerosols and the direct condensation of hydrocarbon particles from the vapor in the lower stratosphere is also briefly considered in some model runs. The spectra of the downward solar radiation at several levels of the models that fit available optical constraints are shown in Figs E2 and E3.

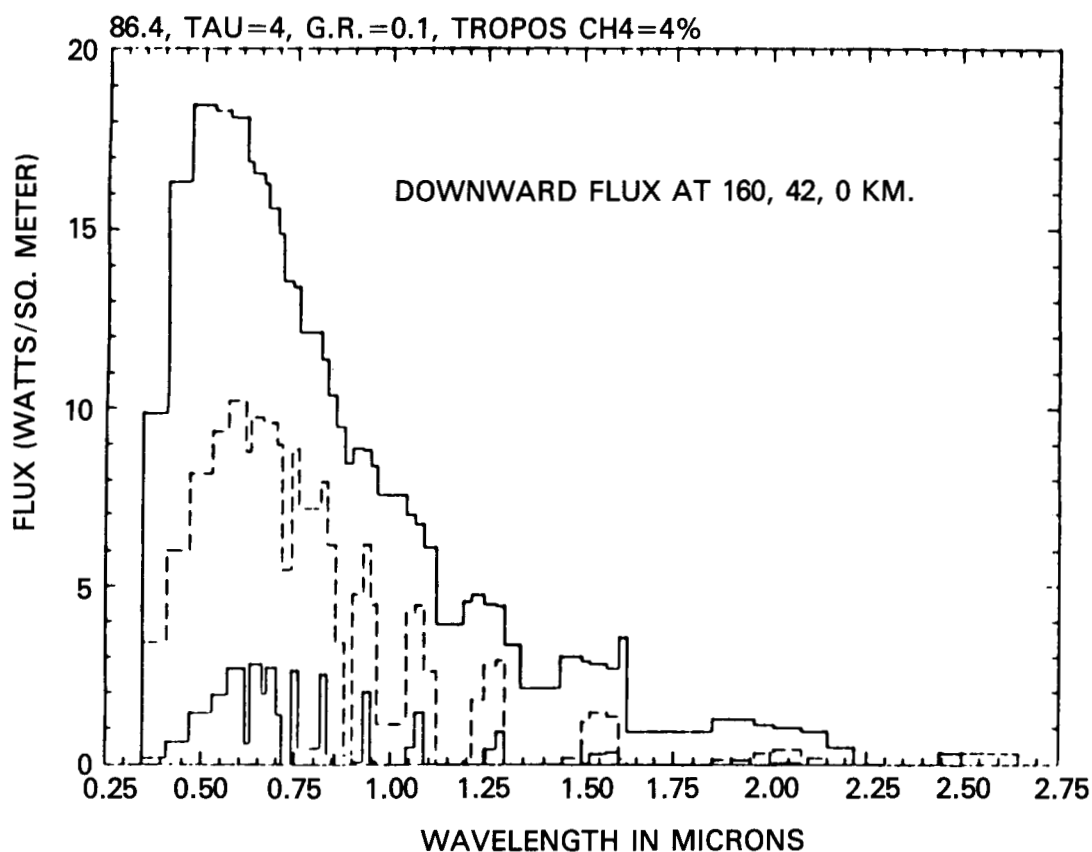


Figure E2 Models of the spectra of the downward solar radiation at several altitudes as labeled from the calculations of Tomasko and Pope (1987) discussed in Fig E1. The entire spectral region from 0.25 to 2.65 microns is spanned in the calculations for the baseline model which contains uncharged photochemical aerosols, a tropospheric methane cloud with an optical depth of 4, a tropospheric methane mixing ratio of 4%, and a ground reflectivity of 10%.

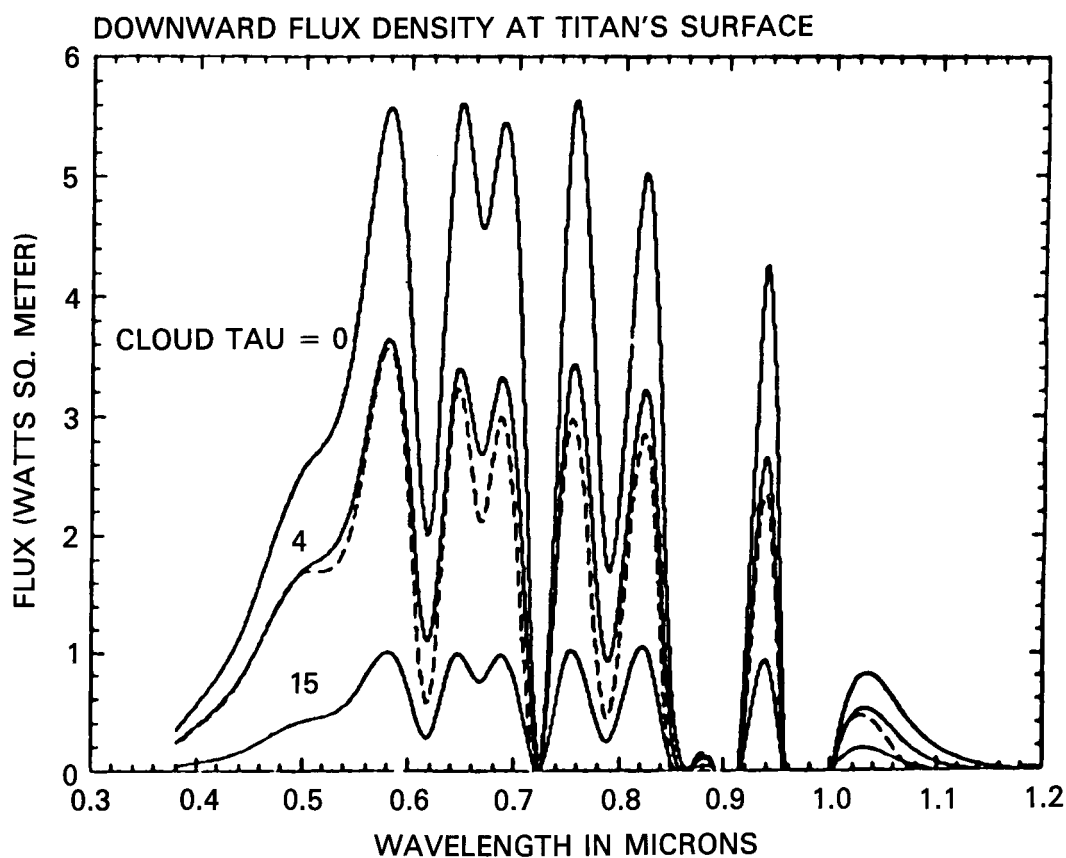


Figure E3 Models of the spectra of the downward solar radiation at several altitudes as labeled from the calculations of Tomasko and Pope (1987) discussed in Fig E1. The variation of the downward solar flux in the region shortward of 1 micron reaching the surface at the subsolar point for several assumed thicknesses of a tropospheric methane condensation cloud as labeled.

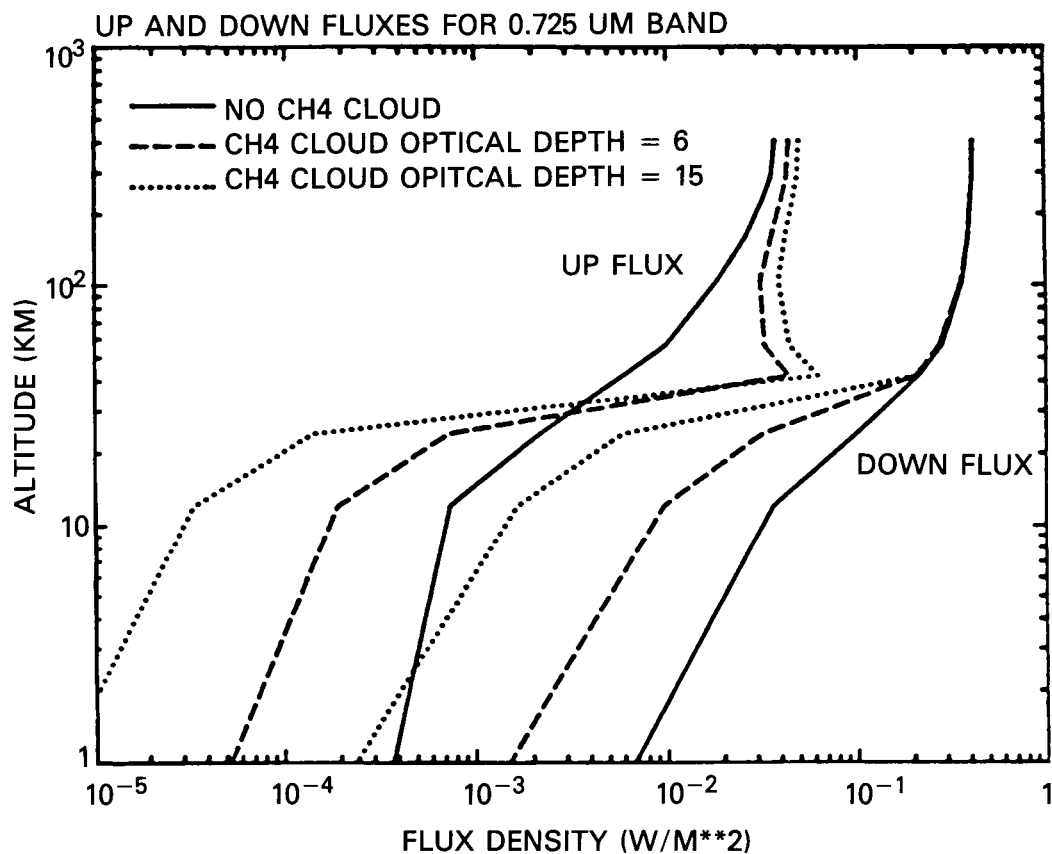


Figure E4 Upward and downward solar fluxes in a narrow spectral region in the 0.725 micron methane band as functions of altitude for three assumed cloud thicknesses. Notice that the upward and downward solar fluxes differ by about an order of magnitude or more throughout the atmosphere. The calculations indicate similar behavior in continuum spectral regions; thus permitting accurate net flux measurements even when separate optics and detectors are used in the upward and downward directions.

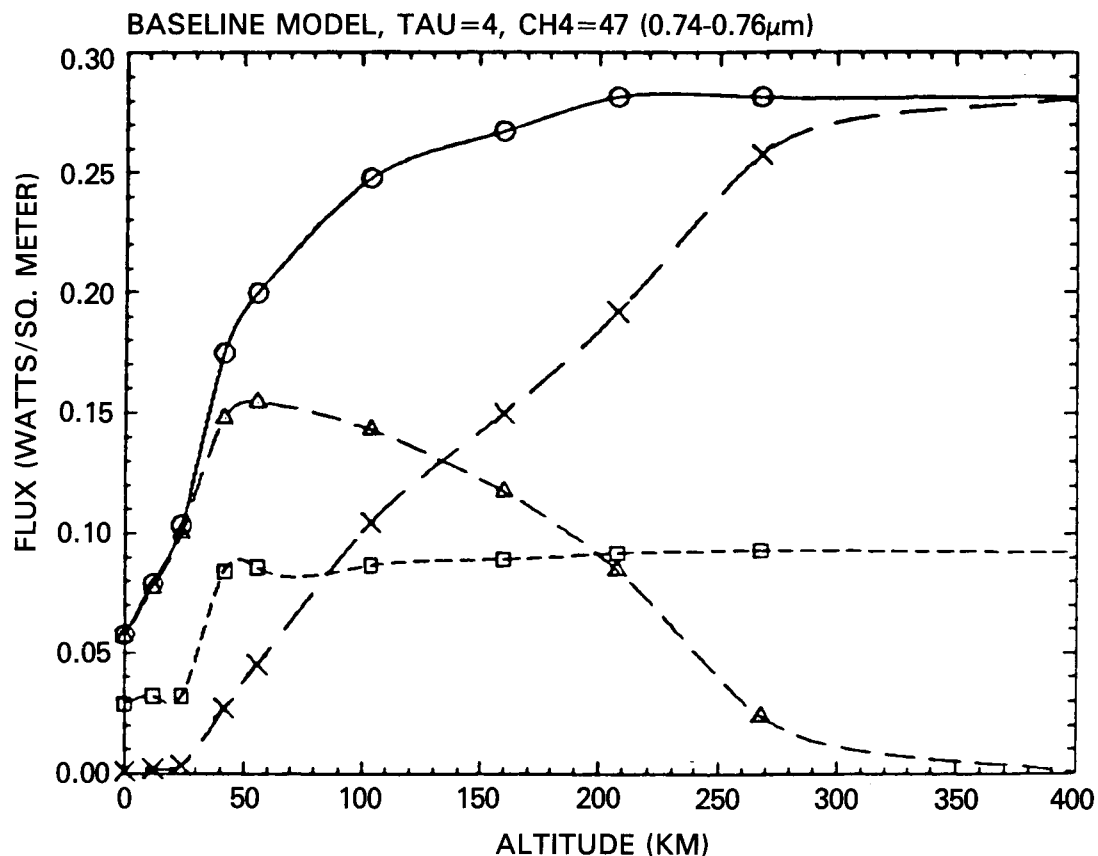


Figure E5 The variation of bolometric solar flux as a function of altitude for the baseline model. The downward direct flux (long dashes), downward diffuse solar flux (medium dashes), total downward solar flux (solid curve), and upward solar flux (short dashes) are shown. Notice that the downward direct flux is greater than the downward diffuse flux above 130 km altitude, and the downward direct flux is a significant component of the total downward flux down to some 30 km altitude.

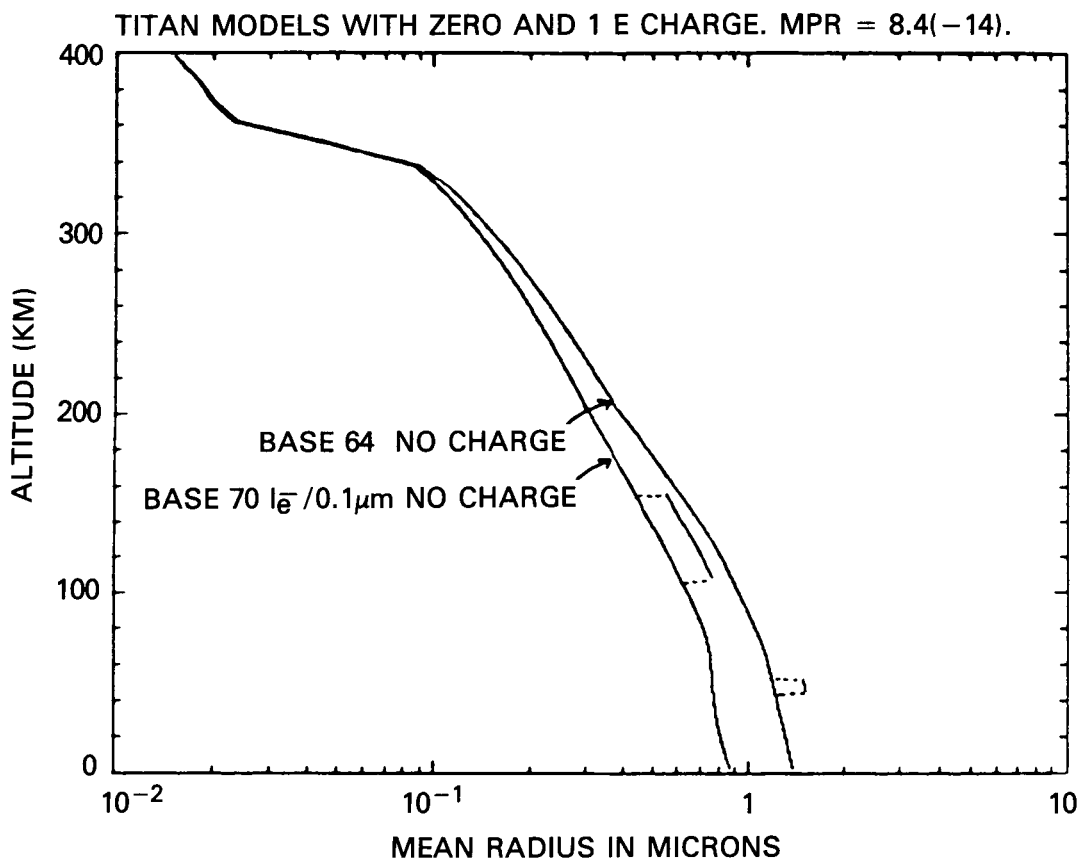


Figure E6 Variations of mean particle radius with altitude in two models of the Titan photochemical aerosols which have different amounts of electrical charge on the particles. The baseline model which contains no charge is also shown with a variation in which the particles in a narrow altitude interval from 42 to 58 are increased in radius by 26%. The effect of this change in particle size on the shape of the solar aureole is illustrated in Fig E7.

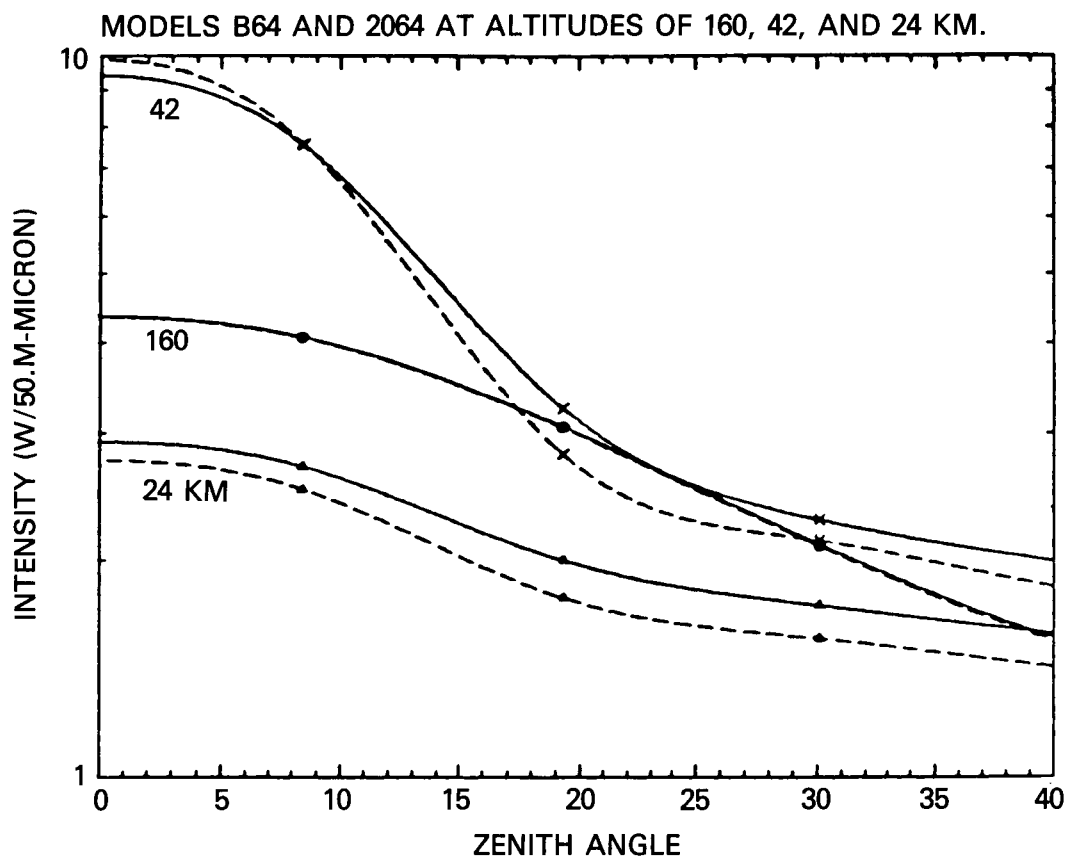


Figure E7 Zenith angle dependence of the downward intensity at three altitudes in the baseline particle models (solid curves) shown in Fig E6 with the particles in one layer increased by 26% (dashed curves). Above the level of the change, as at 160 km, the level and shape of the radiation field is unchanged. At the base of the layer with different sized particles, (42 km) the zenith angle dependence is steeper for the larger particles.

APPENDIX F PIRLS BACKGROUND INFORMATION AND FIGURES

PRECEDING PAGE BLANK NOT FILMED

TITAN PROBE DIODE LASER SPECTROMETER AND NEPHELOMETER

C. R. Webster (JPL), S. P. Sander (JPL), R. Beer (JPL)

J. Ballard (RAL), D. M. Hunten (U. of Arizona), R. G. Knollenberg (PMS, Colorado)

The Probe Infrared Laser Spectrometer (PIRLS) instrument is a tunable diode laser infrared absorption spectrometer and nephelometer designed for the in-situ sensing of Titan's atmosphere on the Saturn Orbiter/ Titan Probe (SOTP) NASA-ESA joint mission.

The PIRLS instrument uses up to ten narrow-bandwidth (0.0001 cm^{-1}) tunable diode lasers operating at 82 degrees Kelvin at selected, mid-infrared wavelengths in the region of 3-20 μm . For the absorption measurements, these sources would be directed over an open pathlength defined by a small reflector located about 20 cm away. Because of the high sensitivity of diode laser harmonic (derivative) detection methods which allow peak absorptances lower than 0.01% to be measured for atmospheric pressures expected on Titan ($<1.5 \text{ bar}$), volume mixing ratios of 10^{-9} should be measurable for several species of interest: vertical profiles of the concentrations of molecules such as CH_4 , CO , CO_2 , HCN , C_2H_2 , C_2N_2 , C_3H_4 , C_3H_8 , C_3HN , C_4H_2 , etc. can therefore be determined simultaneously with a vertical resolution of less than a scale height from 160 km down to the surface. Search for stratospheric NH_3 and H_2O at high sensitivity could also be implemented. For appropriate species present in relatively large concentrations, isotopic ratios such as $^{13}\text{C}/^{12}\text{C}$ and D/H could be determined.

As a nephelometer, the vertical extent of the cloud structure, its physical properties such as the particle size distribution and number density can also be measured using shorter wavelength diode laser sources at 0.78 μm and 0.83 μm returned from the same deployed reflector. As a single particle device, the vertical profile of the particle size distributions from entry down to the surface will be made with a vertical resolution of 100 m. With 32 size classes, particles in the range 0.2-50 μm diameter will be measured. Independent simultaneous forward and back scatter measurements will allow computation of the refractive index.

For both the gas composition and particle size channels, the method of measurement is direct, non-invasive, and, as an all solid-state light source plus detector combination, simple in concept.

PROBE INFRARED LASER SPECTROMETER (PIRLS)

INSTRUMENT SUMMARY

- * High-resolution (0.0001 cm^{-1}) infrared tunable diode laser spectrometer operating at 3-20 microns and 0.7-0.9 microns. Proven techniques.**
- * Atmospheric composition with gas-phase sensitivities at the ppbv (10^{-9}) level. Gas molecules, isotope ratios.**
- * Complementary measurements to mass spectrometer.**
- * Near-IR shadowgraph imaging and nephelometry: vertical profiles of particle size distributions, number densities.**
- * Survey option for the troposphere.**
- * Simple optical configuration integrating gas and particulate measurement capabilities.**
- * Direct, non-invasive technique with wavelength calibration.**
- * Low mass (5.4 kg) and power (12 Watts).**
- * Low data rate of 140 bps. Sub-scale height resolution.**

PROBE INFRARED LASER SPECTROMETER (PIRLS)

SENSITIVITIES

Altitude (km)	Minimum Detectable Mixing-ratio (ppbv)						
	CH ₄	HCN	CO	CO ₂	NH ₃	C ₂ H ₂	H ₂ O
10	1	2	1	0.1	1	1	0.6
50	1	2	1	0.1	1	1	0.5
100	5	4	2	0.2	1	1	2
150	20	15	7	0.7	3	3	5

Sensitivities are for SNR of unity,
and assume linecenter absorptance of 1×10^{-5}
with total pathlength of 2 m.

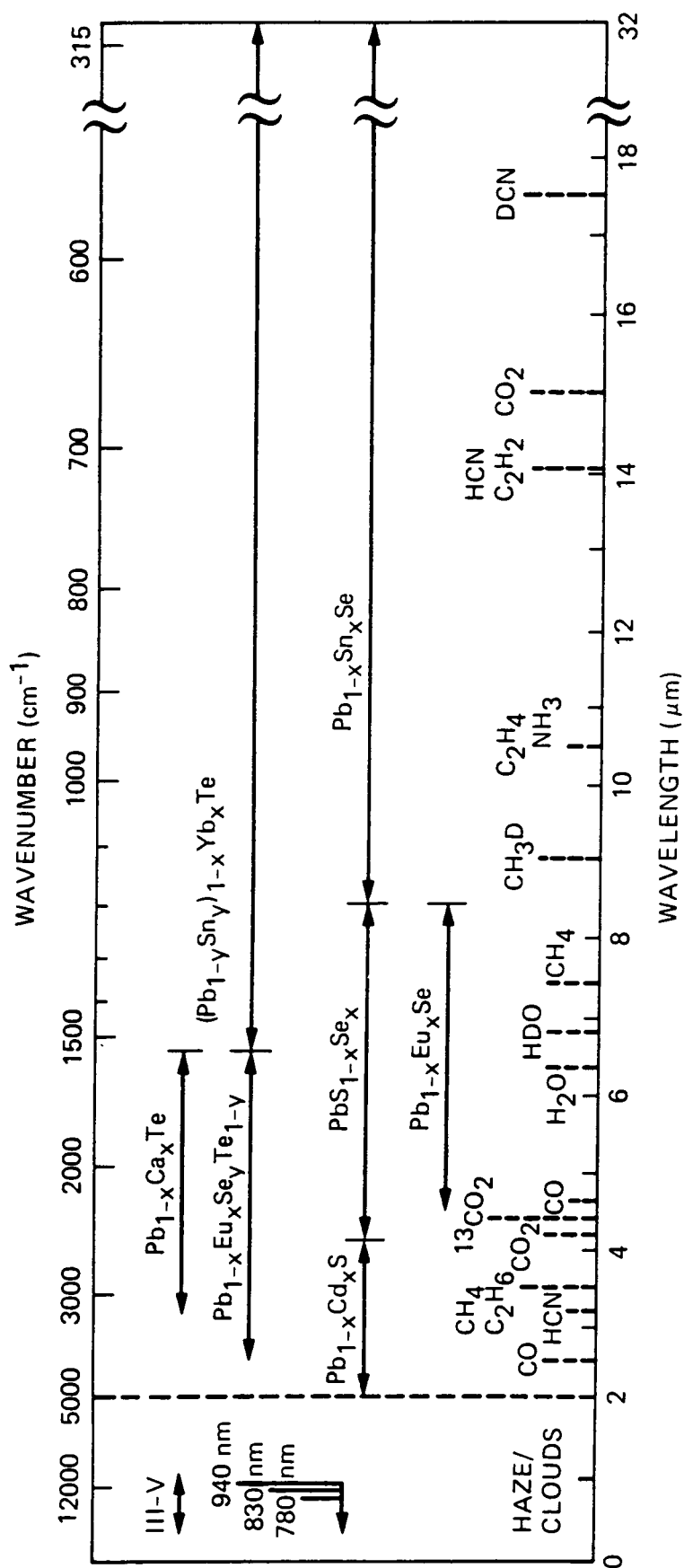


Figure F1 Potential diode laser sources for composition measurements of Titan's atmosphere.

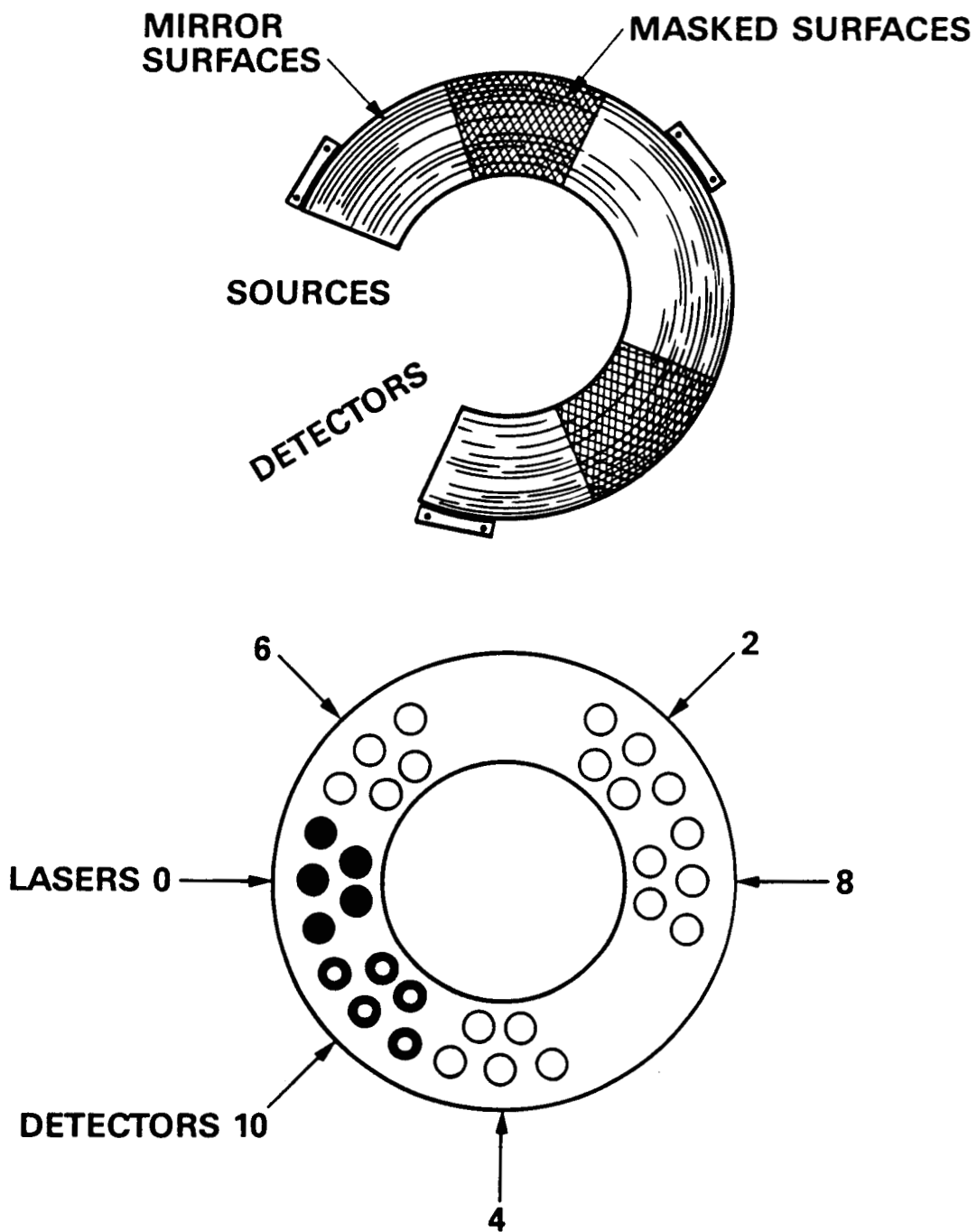


Figure F2 Near mirror for Herriott cell (5 lasers).

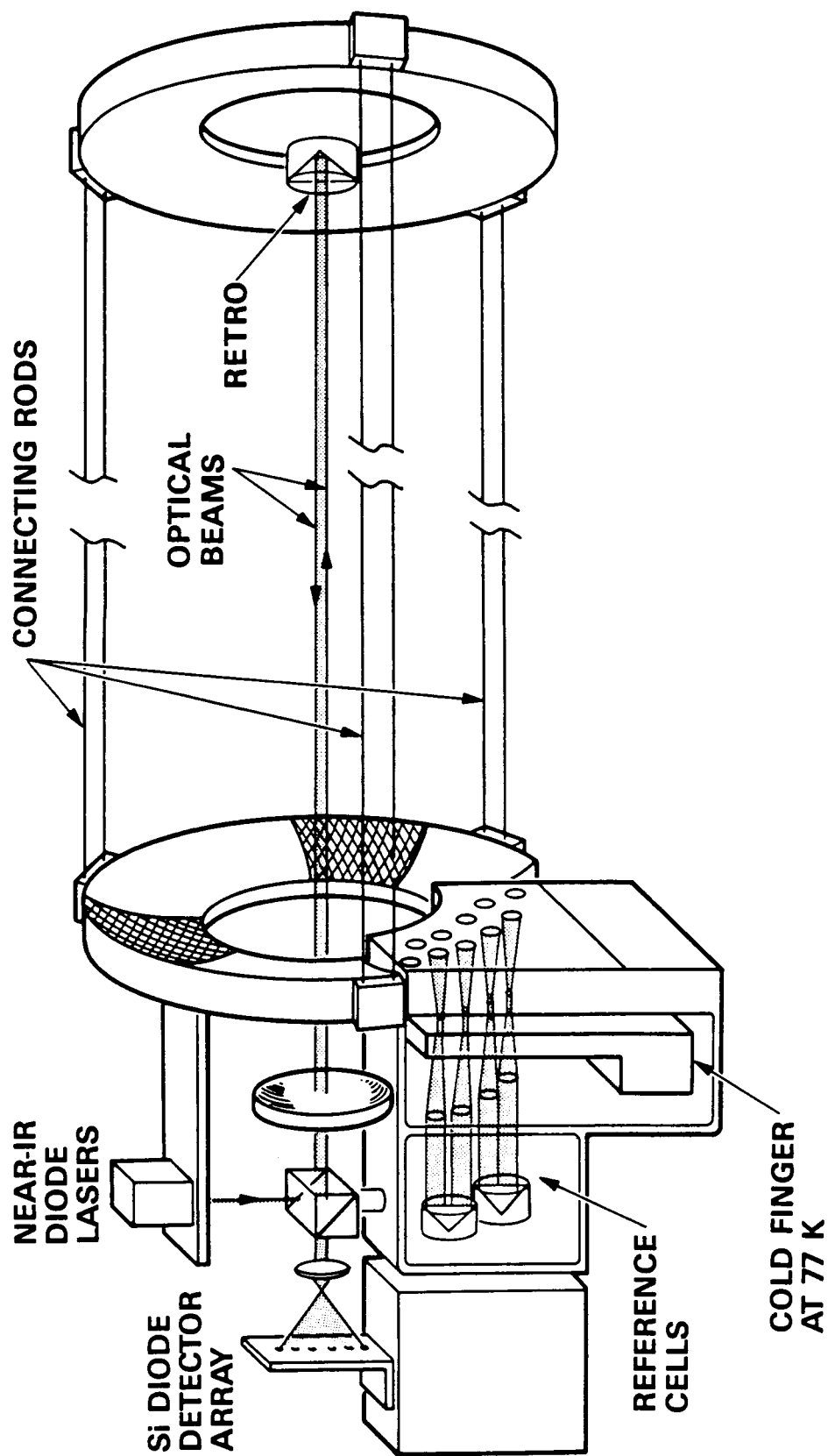


Figure F3 Optical schematic.

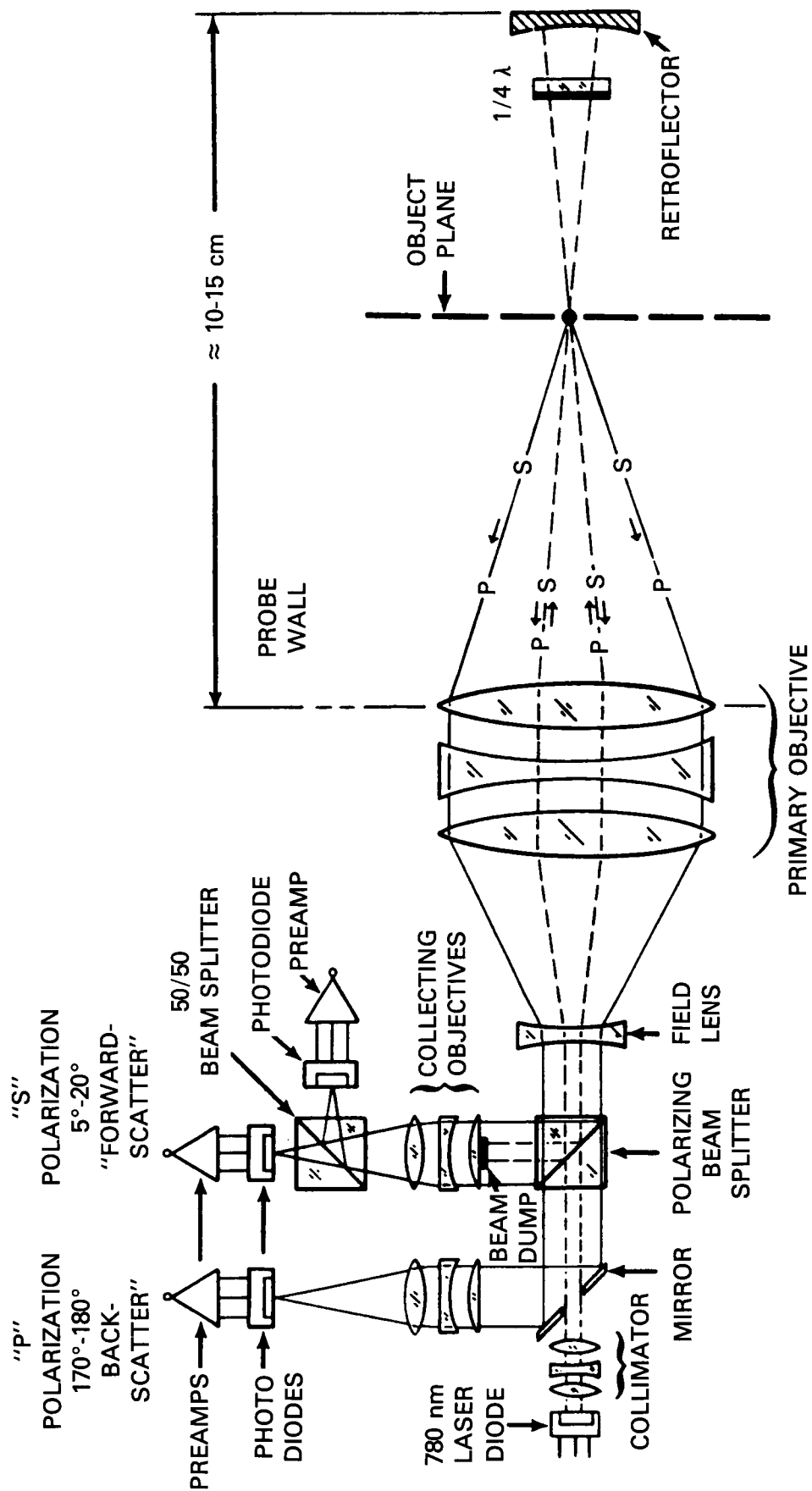


Figure F4 Particle size spectrometer section.

Report Documentation Page

1. Report No. NASA RP-1213		2. Government Accession No.		3. Recipient's Catalog No.	
4. Title and Subtitle The Cassini Mission: Infrared and Microwave Spectroscopic Measurements				5. Report Date January 1989	
				6. Performing Organization Code 693.0	
7. Author(s) V. G. Kunde				8. Performing Organization Report No. 89B0006	
				10. Work Unit No.	
9. Performing Organization Name and Address Goddard Space Flight Center Greenbelt, Maryland 20771				11. Contract or Grant No.	
				13. Type of Report and Period Covered Reference Publication	
12. Sponsoring Agency Name and Address National Aeronautics and Space Administration Washington, D.C. 20546-0001				14. Sponsoring Agency Code	
15. Supplementary Notes					
16. Abstract The Cassini Orbiter and Titan Probe model payloads include a number of infrared and microwave instruments. This document describes 1) the fundamental scientific objectives for Saturn and Titan which can be addressed by infrared and microwave instrumentation, 2) the instrument requirements and the accompanying instruments, and, 3) the synergism resulting from the comprehensive coverage of the total infrared and microwave spectrum by the complement of individual instruments. The baseline consists of four instruments on the orbiter and two on the Titan probe. The orbiter infrared instruments are: 1) a microwave spectrometer and radiometer, 2) a far to mid-infrared spectrometer, 3) a pressure modulation gas correlation spectrometer, and 4) a near-infrared grating spectrometer. The two Titan probe infrared instruments are: 1) a near-infrared instrument, and 2) a tunable diode laser infrared absorption spectrometer and nephelometer.					
17. Key Words (Suggested by Author(s)) Planetary atmospheres, infrared radiation, Cassini, Saturn, Titan, spacecraft instrumentation			18. Distribution Statement Unclassified-Unlimited Subject Category <u>91</u>		
19. Security Classif. (of this report) Unclassified	20. Security Classif. (of this page) Unclassified		21. No. of pages 136	22. Price A07	